Department of Precision and Microsystems Engineering

Stencil Printing of Piezoelectric Vibrational Energy Harvester

Development, fabrication and experimental validation

Sander Kooiman

Report no : 2024.053
Coach : T.W.A Blad
Professor : A. Hunt
Specialisation : Mechatronic System Design
Type of report : Master Thesis
Date : 10 July 2024



TU Delft Delft University of Technology

Challenge the future

Stencil printing of piezoelectric energy harvesters

The development, fabrication and experimental validation

by

S.C. Kooiman

to obtain the degree of Master of Science
at the Delft University of Technology,
to be defended publicly on Thursday July 19, 2024 at 1:00 P.M.

Student number:	-	
Project duration:	September 11, 2023 – July 19, 2024	
Thesis committee:	Dr. A.Hunt,	TU Delft, supervisor
	Dr. S.H. Hossein Nia Kani,	TU Delft
	Dr. ir. T.W.A.Blad,	Memsys B.V.
	S.K. Ammu,	TU Delft

This thesis is confidential and cannot be made public until July 19, 2026.

An electronic version of this thesis is available at `http://repository.tudelft.nl/`.

TU Delft

Preface

As a young boy, I was always interested in technology. In the early beginning, I had the dream of becoming an architect one day, making numerous drawings of fancy houses with all kinds of technological features. Later in life, I found more interest in the art of moving things, with the urge always to take apart electrical or mechanical devices to see how they work. Which guided me towards Mechanical Engineering. Besides gaining a lot of knowledge in this field, I have always had the ambition to become an entrepreneur, with the chance to create something that really impacts other people's lives. However, I always felt I needed to understand the technology before creating value. At MEMSYS, I could combine my technical curiosity with my ambition of creating value and starting a company. In a first-row seat, I could witness how technical value could transform into real-world impact. With the knowledge gained and technical and real-world experience, I enjoyed doing my final mechanical engineering project. I hope my thesis can already contribute to the real-world products MEMSYS is creating.

S.C. Kooiman
Delft, July 2024

Summary

This thesis investigates the feasibility of using stencil printing technology to fabricate piezoelectric vibrational energy harvesters. The primary goal was to develop and improve fabrication techniques for applying a piezoelectric composite material directly onto a stainless steel substrate. The research aimed to determine the power from these fabricated systems by providing a comprehensive analysis that includes theoretical background, fabrication processes and improvements, and experimental validations of the created energy harvester's power output.

Stencil printing is a valuable fabrication method due to its scalability, allowing for the efficient production of both multiple and large systems. This method also offers significant flexibility in optimising the piezoelectric layers' shape, location, and thickness, which are crucial for enhancing the performance and applicability of the energy harvesters. By leveraging stencil printing, this research demonstrates the potential for creating highly customised and efficient energy-harvesting devices.

Multiple influencing fabrication parameters are found with the development of the fabrication method. The effects of these parameters are tested to improve the quality of the samples. This highlights the importance of some steps and the adjustments that need to be made to enhance the end product further.

The stencil-printed piezoelectric energy harvesters demonstrated the capability to harvest up to 0.68 µW of power. However, the power output remains lower than that of the commercial buzzer (PZT patches) samples due to porosity and cracks, which limit the material's density and result in non-uniform properties or broken samples. These defects significantly impact the device's performance, highlighting the need for further refinement in the fabrication process. While other studies have faced similar challenges with piezoelectric composites, mainly due to porosity,

The effect of different thicknesses of fabricated systems has been evaluated. Optimising the piezoelectric layer's global coupling coefficient maximises the mechanical energy converted into the piezoelectric material. However, due to fabrication limitations, no definitive conclusions could be drawn regarding this optimum. Despite the samples showing the highest power outputs at this predicted optimum, no fair comparison can be made due to fabrication inconsistencies.

This research also provides a fabrication manual and identifies necessary improvements to enhance the performance of stencil-printed piezoelectric energy harvesters. Key recommendations include optimising solvent selection, controlling the drying process, and improving the compression during curing. This is to prevent cracks from occurring, achieve high density and thus ensure uniform poling conditions to achieve consistent and high piezoelectric properties.

Overall, this thesis presents a significant step towards implementing stencil-printed piezoelectric energy harvesters. While current limitations must be addressed, the findings provide a solid foundation for future research and development. Continued efforts in refining fabrication techniques and exploring new materials and designs will be essential for advancing the efficiency and reliability of these energy harvesting devices, contributing to sustainable and portable power solutions for a wide range of applications.

Contents

Preface **1**

Summary **2**

1 Introduction **1**
1.1 Energy harvesting . . . 2
1.2 Working principle piezoelectric material . . . 2
1.3 Scalability of energy harvester . . . 3
1.3.1 Size scalability . . . 3
1.3.2 Number scalability . . . 4
1.4 Stencil printing . . . 4
1.4.1 Composites stencil printing . . . 4
1.5 Objective and problem statement . . . 6
1.5.1 Thesis outline . . . 6

2 Size scalability of piezoelectric energy harvesters **7**
2.1 Introduction . . . 8
2.2 Methodology . . . 9
2.2.1 Data selection . . . 9
2.2.2 Classification . . . 9
2.2.3 Data analysis . . . 10
2.2.4 Scaling of current designs . . . 12
2.3 Results . . . 13
2.3.1 Analysis of PEH design . . . 13
2.3.2 Design scores . . . 14
2.3.3 Scaling analysis . . . 15
2.4 Discussion . . . 16
2.4.1 Analysis of PEH designs . . . 17
2.4.2 Design and scaling scores . . . 18
2.4.3 Limitations and state of art research . . . 18
2.5 Conclusion . . . 19

3 Fabrication development of Stencil printing a KNLN3 - epoxy for an energy harvester **20**
3.1 Overview and goal . . . 21
3.1.1 Contribution development . . . 22
3.2 Electroceramic KNLN3 Powder fabrication . . . 24
3.3 Printing process . . . 25
3.3.1 Pre treatment . . . 25
3.3.2 Material and solvent selection . . . 25
3.3.3 Stencil and the way of using . . . 26
3.4 Curing process . . . 28
3.4.1 Drying . . . 28
3.4.2 Compression and curing . . . 28
3.5 Poling process . . . 30
3.5.1 Electrodes and cracks . . . 31
3.5.2 Contact poling conditions . . . 32
3.6 Testing process . . . 33

4 Experimental validation: Stencil printed piezoelectric energy harvesters, a thickness variation **35**
4.1 Introduction . . . 36

4.2 Methodology . . . 37
4.2.1 Theoretical model . . . 37
4.2.2 Fabrication strategy . . . 39
4.2.3 Testing . . . 40
4.3 Results . . . 41
4.3.1 Modelled results . . . 41
4.3.2 Fabricated samples . . . 41
4.3.3 Comparison fabricated samples . . . 42
4.3.4 Visible results . . . 42
4.4 Discussion . . . 44
4.4.1 Feasibility stencil-printing . . . 44
4.4.2 Thickness and power . . . 44
4.4.3 Limitations and further research . . . 46
4.5 Conclusion . . . 46

5 Discussion, conclusion and recommendations **47**
5.1 Overview and discussion of research activities . . . 48
5.1.1 Successes . . . 49
5.1.2 Critical points . . . 49
5.2 Reflection . . . 50
5.3 Conclusions . . . 51
5.4 Recommendations . . . 51
5.4.1 Future research objectives . . . 51
5.4.2 Tips and tricks . . . 52

Acknowledgements **53**

References **54**

A Scalability of Piezoelectric vibrational energy harvesters; Literature review **58**
A.1 Search query . . . 59
A.2 Design score rubrics . . . 60

B Overview fabrication development **62**

C KNLN fabrication manual **68**

D Stencil printing process manual **71**

E Derived and used equations **75**
E.1 Derived stress equation . . . 76
E.2 Coupling equations . . . 77

F Details of fabricated samples **78**
F.1 Thickness measurements . . . 80

G Performance (sub)results per sample **81**
G.1 Sample eigenfrequency analysis . . . 82
G.2 Meausred acceleration data . . . 83
G.3 Interpolation resistance load . . . 84
G.3.1 Apendix F: KNLN3-epoxy D33 (earlier) measurement . . . 84

H Technical drawings **86**
H.1 Technical drawings substrate, stencils and seals . . . 87
H.2 Technical drawings compression units . . . 90

I Models and code **93**
I.1 Comsol frequency model . . . 94
I.2 Effective stiffness model code . . . 94

1

Introduction

This first chapter shows the relevance of energy harvesting with available and promising use cases. At first, a better understanding of piezoelectric energy harvesters is given, explaining the working principle of this smart material and how this material could be applied. As follows, stencil printing is explained, as well as its relevancy to use for piezoelectric energy harvesters. Then, the problem statement states this innovative technology's limitations, introducing the thesis's main objective and research questions. Finally, the thesis outline is provided.

1.1. Energy harvesting

Turning ambient energy into useful electrical energy occurs more and more often, with large-scale systems providing the world with large amounts of energy. On the other hand, we have more and more small, remotely located systems working on batteries. A newer solution is using vibrational energy harvesters, smaller systems that convert ambient vibrations into electrical power. One of the significant advantages of vibrational energy harvesters is their ability to provide power to these small, often remote, systems without relying on traditional batteries. The widespread use of batteries poses significant logistical and environmental challenges. In remote locations, replacing or recharging batteries can be impractical and costly, involving complex supply chains and frequent maintenance trips. Moreover, on a global scale, millions of batteries in use contribute to substantial waste and environmental degradation when they are discarded or improperly recycled.

Piezoelectric vibrational energy harvesters (PVEH) are especially interesting. These systems use a mechanical beam as a resonator, a simple beam which vibrates due to external vibrations. This movement causes a smart material (piezoelectric material) to deform and thereby create an electrical potential. Which can be harvested and used for electricity. These PVEHs offer a sustainable solution to these problems. By harnessing ambient vibrations from sources such as machinery, vehicles, or even natural movements, these devices can generate power locally and reduce the dependence on batteries. This reduces logistical burdens and mitigates the environmental impact of battery disposal and recharging. As we continue to seek innovative ways to power our increasingly digital world, piezoelectric energy harvesting stands out as a promising and eco-friendly technology.

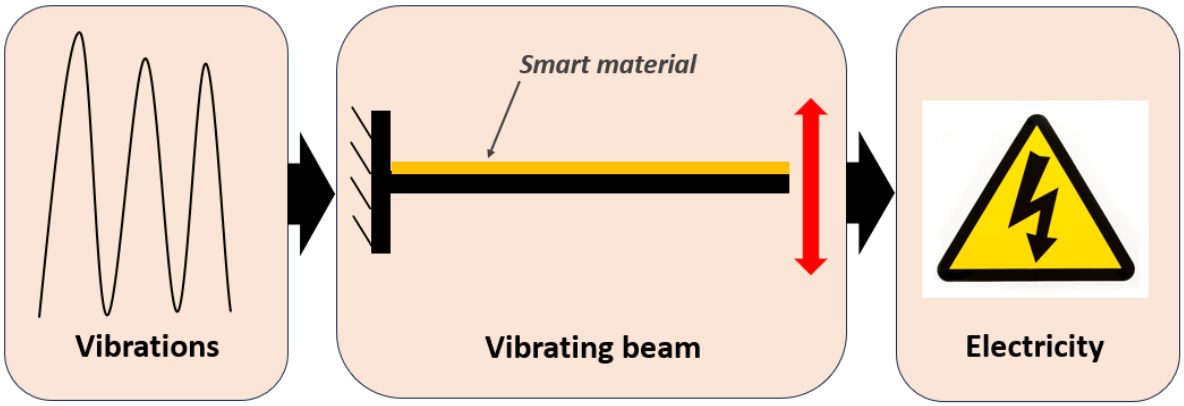


Figure 1.1: The basic effect of a piezoelectric energy harvester, converting input vibrations to electrical energy.

1.2. Working principle piezoelectric material

The piezoelectric effect is a phenomenon where certain materials generate an electric charge in response to mechanical stress. Or by applying an electrical charge, which results in a mechanical deformation, as is shown in figure 1.2. This effect occurs in materials that lack a centre of symmetry in their crystal structure, such as quartz, ceramics, and some polymers. When these materials are subjected to mechanical forces, such as compression, tension, or twisting, their internal dipole structure is disturbed, leading to a separation of electric charges and the creation of an electric field.

This property is harnessed in energy harvesting applications by converting mechanical stresses, such as vibrations, pressure changes, or other kinetic energy forms into electrical energy. Devices designed for this purpose typically incorporate piezoelectric materials that deform under stress, producing an electric charge that can be captured and stored or directly used to power small electronic devices. This technology is particularly valuable for powering sensors, wearable electronics, and other low-power devices in situations where conventional power sources are impractical.

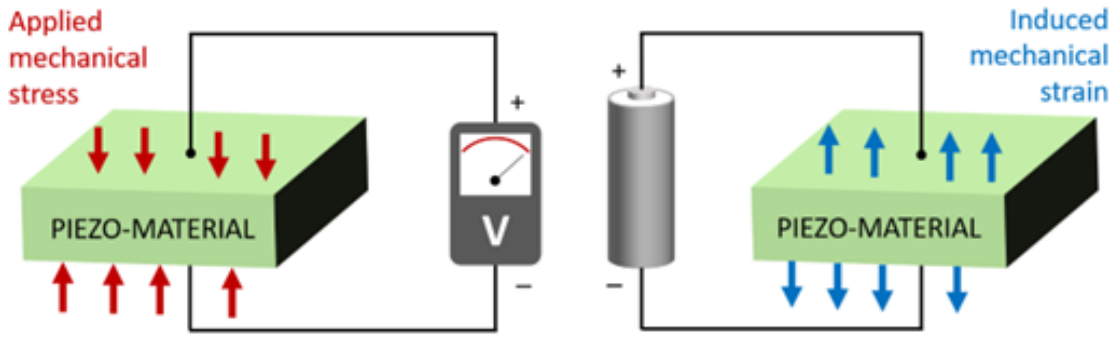


Figure 1.2: The basic effect of a piezoelectric energy harvester, converting input vibrations to electrical energy.

One of the leading coefficients to determine piezoelectric output are the piezoelectric charge coefficients d_{33} and d_{31} are measured in pico coulombs per newton (pC/N) or meters per volt (m/V). These values quantify the material's ability to convert electrical energy into mechanical strain along different axes: d_{33} along the direction of the applied field and d_{31} perpendicular to it. Factors influencing these coefficients include the material's crystal structure, intrinsic piezoelectric properties, domain orientation, and the quality of poling. High d_{33} and d_{31} values indicate better piezoelectric performance for sensors and actuators.

The piezoelectric coupling coefficient is a measure of the efficiency with which a piezoelectric material converts mechanical energy into electrical energy and vice versa. It quantifies the effectiveness of the piezoelectric effect, indicating how well the material can transform energy between mechanical deformation and electrical signals. It is stated as k.

Piezoelectric composites are materials that combine piezoelectric ceramics or polymers with a matrix material to enhance their mechanical or electrical properties. These composites are designed to optimize the piezoelectric effect by improving flexibility, durability, and ease of integration into various applications. Key properties important in a piezoelectric material include a high piezoelectric coefficient, which measures the material's ability to generate an electric charge in response to mechanical stress, and a high dielectric constant, which affects the material's ability to store electrical energy. Additionally, mechanical properties such as flexibility, strength, and stability under different environmental conditions are crucial for practical applications. These composites enhance fabrication feasibility by allowing for easier processing, moulding, and integration into complex structures, making them suitable for a wider range of applications.

1.3. Scalability of energy harvester

These piezoelectric energy harvesters could be the next-generation local power sources for all applications. To get there, these systems need to produce enough power (watts), be widely usable, be manufactured in different sizes, and be mass-producible. Or, in short, it needs to be scalable!

1.3.1. Size scalability

Different sizes of energy harvesters are required for different applications. Generally, a larger system can produce more power, and a small one can be used in more application-dependent environments like the human body. The ratio between power and volume is of great importance for both directions. And could determine if a certain scaled system is well-performing. However, fabrication plays a huge role in making systems bigger or smaller. And the fabrication strategy is often a constraint. Not being able to fabricate certain dimensions or applying piezoelectric material in or on an energy harvester

design is usually a challenge. In Chapter 2, a more detailed analysis of the size scalability of PVEH is displayed. Identifying different design and fabrication strategies to make scalable PVEHs and how they could be scaled further.

1.3.2. Number scalability

The feasibility of making millions of reproducible systems is required. This involves using robust fabrication techniques that ensure consistent quality, reliability, and cost-effectiveness across large production volumes. Achieving number scalability is crucial for the widespread adoption of PEVHs, enabling them to power many devices and systems efficiently and economically.

1.4. Stencil printing

Stencil printing is a widely used fabrication method that involves transferring patterns onto a substrate through a stencil mask. This technique utilises a stencil or screen with a predefined pattern placed over the substrate. Ink or paste is then spread across the stencil, passing through the open areas and depositing material onto the substrate. After the stencil is removed, the desired pattern remains on the surface. Stencil printing is commonly employed in various industries, including electronics for circuit board manufacturing, textiles for fabric designs, and even in arts and crafts. The advantages of stencil printing include its simplicity, cost-effectiveness, and the ability to produce fine, intricate patterns. However, the method also has limitations, such as the difficulty in achieving high resolution for very small features and the required viscosity of the material applied.



Figure 1.3: Stencil printing concept, using a stencil which covers a part of a substrate to print certain shapes.

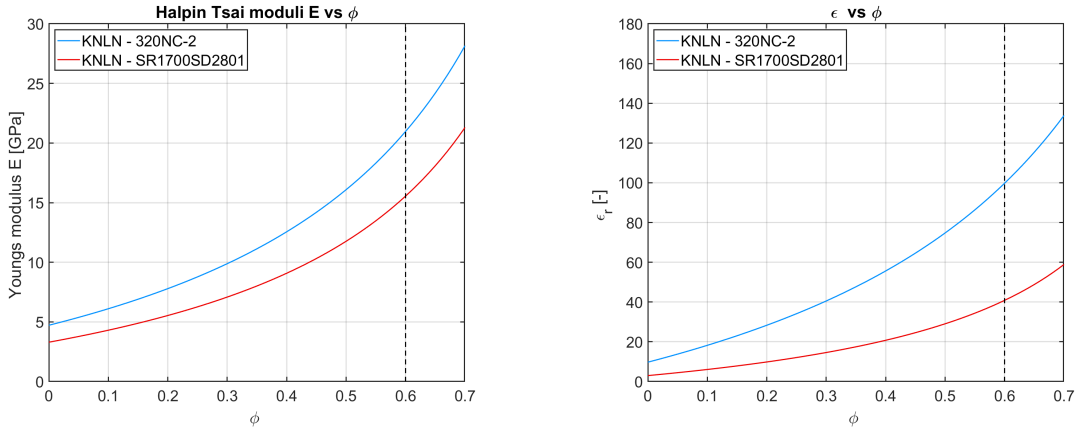
Applying stencil printing to the fabrication of piezoelectric energy harvesters involves printing piezoelectric composites onto a substrate to create patterned energy-harvesting layers. This process can be beneficial due to its scalability and design flexibility. The ability to print patterns of piezoelectric material allows for the adjustment of design parameters, enabling the creation of customized energy-harvesting devices for specific applications. And is still widely usable for multiple systems at once. However, there are also challenges, such as ensuring uniform thickness of the printed layers and applying the piezoelectric properties of the material during or after the printing process. Despite these challenges, stencil printing offers a promising method for creating piezoelectric energy harvesters.

1.4.1. Composites stencil printing

Composite materials are engineered from two or more different substances, combining their properties to create a better-optimised and user-friendly material. Combining epoxy with piezoelectric ceramic infillers gives piezoelectric properties higher than polymer-based piezoelectrics. The high sintering temperatures make working with ceramics difficult; this is not a limitation when used as a filler in an

epoxy matrix. This allows the use of stencil printing of these composites. Thus, the use of composites creates both user-friendly and optimised properties. However, they need more modelling, are less easy to understand, and most final properties are not really well known.

The Elastic modulus and the dielectric constant of a piezoelectric composite material are crucial properties that define its mechanical and electrical performance. The Halpin Tsai model estimates the composite elastic modulus, shown in figure 1.4. A higher filler volume fraction Φ will result in a higher elastic modulus E. An overall higher matrix stiffness is wanted to ensure as much strain is induced in the ceramic filler as possible. The dielectric constant makes piezoelectric materials store an electrical charge. Higher charge storage increases energy storage, resulting in a higher electrical output. The Yamada model is used to see the effect on the dielectric constant by increasing the filler volume fraction [1]. These properties enhance the piezoelectric characteristics and could be varied by different epoxy and fillers. This research uses two different epoxies, with a 60% volume fraction KNLN3 piezoelectric filler. [2]



(a) Elastic modulus E modelling for a KNLN - epoxy composite.

(b) Dielectric constant ϵ modelling for a KNLN - epoxy composite.

Figure 1.4: The Youngs Modulus and Dielectric constant modelled of the KNLN - epoxy composites for different volume fractions Φ.

1.5. Objective and problem statement

Much research is focused on piezoelectric vibrational energy harvesters (PVEH). A promising solution for replacing batteries or other energy sources. Especially with the need for millions of small power sources to guide the new digital era without batteries. With this hurdle, PVEHs also need to be highly scalable, both in size and in the number of reproducible systems.

Different design and fabrication strategies are already used to try to make these systems perform well, be power-dense and still be producible on a large scale. There is still no fully scalable fabrication method that would lift these systems to use worldwide.

This results in the objective of this Thesis:
Develop, fabricate and test a piezoelectric thick-layer stencil printed composite for energy harvesters.

Stencil printing is a widely used, well-known and highly scalable fabrication method. In principle, working in a 2D plane is customisable in terms of thickness and surface patterns. Therefore, stencil printing allows the design to be optimised for energy harvesting.

With the research question:
How does introducing a stencil-printed thick-layer piezoelectric energy harvester affect the total harvested power?

With the analysis of multiple subquestions, this research will provide a good base to understand the feasibility, limitations and performance of the stencil printing method

- What are the limitations of stencil printing?
- What are potential process optimisations?
- What is the effect on power by changing the layer thickness?

1.5.1. Thesis outline

In this research, the main focus is on developing a stencil printing method and coupling it towards performance in terms of power. **In Chapter 2,** the literature report is presented on the topic of the size scalability of piezoelectric energy harvesters. The design and fabrication methods of out-of-plane scaled harvesters are analysed and further evaluated on further size scaling. This concluded with a status quo of what design and fabrication methods can be used to scale certain systems. What works, what doesn't, and what are the limiting factors in terms of design and fabrication? **Chapter 3** describes the development of the stencil printing fabrication method. Divided into 5 main steps, the major parameter changes and limitations are discussed. **In Chapter 4,** experimental research is conducted, looking at the fabrication of different layer thicknesses of stencil-printed piezoelectric material and evaluating the effect on harvested power. **In Chapter 5,** a complete overview and reflection of the research is stated with the answers given to the research question. Also, the main conclusions are drawn, and further research recommendations are given.

2

Size scalability of piezoelectric energy harvesters

Size scaling of Piezoelectric Vibrational Energy Harvesters: Exploring Non-flat Design and Fabrication Strategies

S.C. Kooiman

Abstract — **Piezoelectric vibration energy harvesters (PVEH or PEH) are a potential solution to power the increasing amount of IoT applications. Currently, most research is focused on validating the principle of PEHs. Not meeting all requirements to be used in real-world applications. This research focuses on the design and fabrication strategies to make non-flat PEH's, which are a solution to make PEHs better size scalable systems. By analysing the current harvesters, it can be seen that simpler designs are now better performing and easier to fabricate. The systems are only good scalable by stacking multiple individual systems. The lack of research on good size scalable systems highlights the opportunity to improve the current status quo. And thereby optimize the power over volume ratio.**

Keywords: Piezoelectric, vibration, energy harvesters, size scaling, design strategies, fabrication methods, non-flat

2.1. Introduction

In today's rapidly evolving technological landscape, efficient and sustainable power sources are more critical than ever. More and more sensors are used to monitor all types of data. In remote locations where sensors and devices play a role in data collection and communication, a common challenge persists in the reliance on traditional batteries. These batteries demand frequent replacements and recharging, presenting logistical and environmental challenges. Estimates say that in 2025, more than 78 million batteries are being discarded daily.[3]

Amid this challenge, piezoelectric energy harvesters (PEHs) have emerged as a potential solution for generating electricity. These devices harness ambient vibrations to produce power, offering a possible solution to replace battery-dependent systems. While the field of PEHs has seen extensive research and development, a notable gap remains in their practical, scalable, real-world applications.[4]

The existing landscape of PEHs is primarily based on flat unimorph and bimorph cantilever beams, as can be seen in figure 2.1. These systems are planar, which is stated as a flat design during this research. These systems work in a D31 operation mode (material deflection occurs perpendicular to the poling direction).[4] Although these designs have shown promise, their efficiency in using volume efficiency is limited. The efficient use of space is one of the factors that enhance the system's total performance. Increasing the power-to-volume ratio, resulting in better real-world applicable systems. The potential size increase of PEHs is stated as the system's scalability. The limitation to scaling a system is possibly due to the design and fabrication methods used.

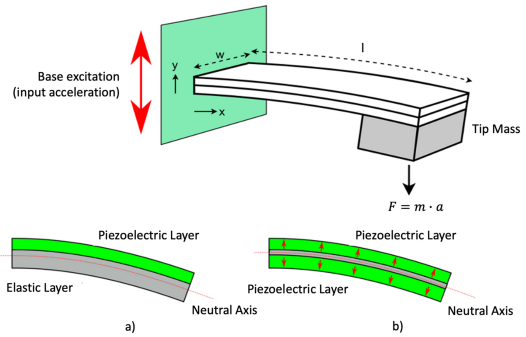


Figure 2.1: Cantilever (flat) structure of piezoelectric generators with (a) unimorph and (b) bimorph construction. These are simple, flat design examples.[5]

Recognizing this limitation, the focus of this study is to address the question: **"What design and fabrication strategies are used to make piezoelectric vibrational energy harvesters more scalable by using a non-flat design? And how to scale further?"**. These non-flat designs aim to enhance scalability by effectively utilizing the 3-dimensional space. The primary objective of this research is to comprehensively map and analyse the current field of non-flat PEHs and evaluate the impact of scaling on different design and fabrication strategies. This study is the foundation for a forthcoming thesis project, aiming to contribute to well-working real-world applicable piezoelectric energy harvesting.

First, in section 2.2, the paper presents the method

used, explaining how to address the research objective. Then, this method will deliver results presented in section 2.3. These results are further elaborated and reflected in the discussion in section 4.4, also providing further research objectives. Finally, in section 2.5, a conclusive response to the research question is provided.

2.2. Methodology

This section provides insights into the methods used to find, analyse, and reflect on size-scaled non-flat PEHs. A schematic overview of the methodology is presented in figure 2.2 on the next page. First, we search for literature creating a dataset with used filters and keywords. Next, a classification is made into 4 different design groups, which deviate the dataset in the strategy used to make the designs non-flat. Then its fabrication techniques and design parameters are analysed, providing an overview of the current situation. Thereafter, scores are given based on the analysed parameters to concisely compare the different designs. Finally, further analyses of scaling of the non-flat designs have been done to get a better understanding of what scaling possibilities are used.

2.2.1. Data selection

The approach to finding the most relevant papers in the field of structured PEHs starts with defining the criteria each paper needs to fulfil. Papers of PEH designs are required, which try to use the 3-dimensional space. Instead of the widely used cantilever beam PEHs which are flat, the aim is to find so-called 'non-flat designs'. However, due to the difference in the definition of 3-dimensional space and non-flat designs a lot of different keyword searches are conducted, see table A.1 in section A.1 for the used search terms. Scopus has been used as the scientific database to conduct this research because of its reliability and diverse filter options. After gathering 95 papers a manual selection procedure is made to filter the still present flat design out of the data-set. The selection is based on images present in the paper which resulted in 3 options: flat designs, non-flat designs and others. Taking only non-flat designs into the dataset. When fabrication details were not provided the paper got deselected for further review. This resulted in **23 papers** to proceed in total analysis.

2.2.2. Classification

To provide a general study, a classification of the design strategies is made. 4 categories are drafted which together cover the whole field of non-flat designs but in a more concise way. With the overview shown in figure 2.3. The categories are more elaborated in figures 2.4, 2.5, 2.6 & 2.7.

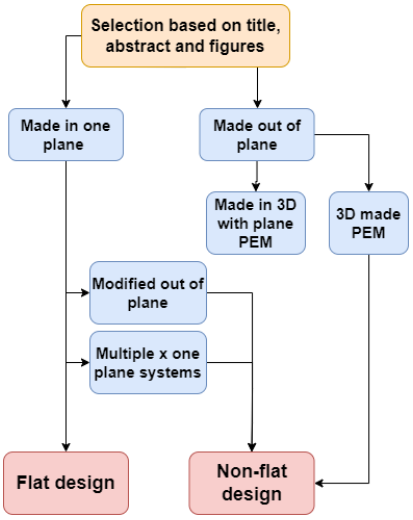


Figure 2.3: Overview of selection tree of the 4 different categories, resulting in non-flat designs.

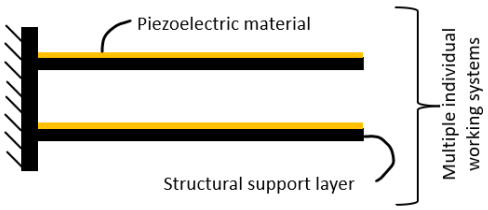


Figure 2.4: Stacked 2D PEHs: Multiple flat systems are placed next to or on top of each other, such that the overall system makes use of a 3-dimensional space. - *Criteria*: More than one individual flat working system.

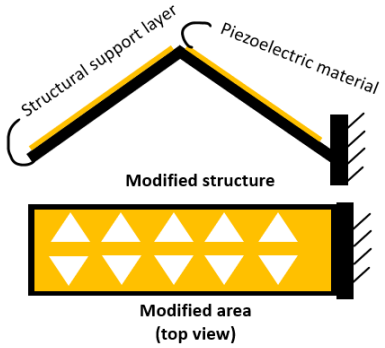


Figure 2.5: 2D structures modified PEH's: 2-dimensional flat structures are used, and are shaped into a 3D structured design by use of modifications. - *Criteria*: Sheet or beam with at least 1 bend or removal of beam material to change its topology.

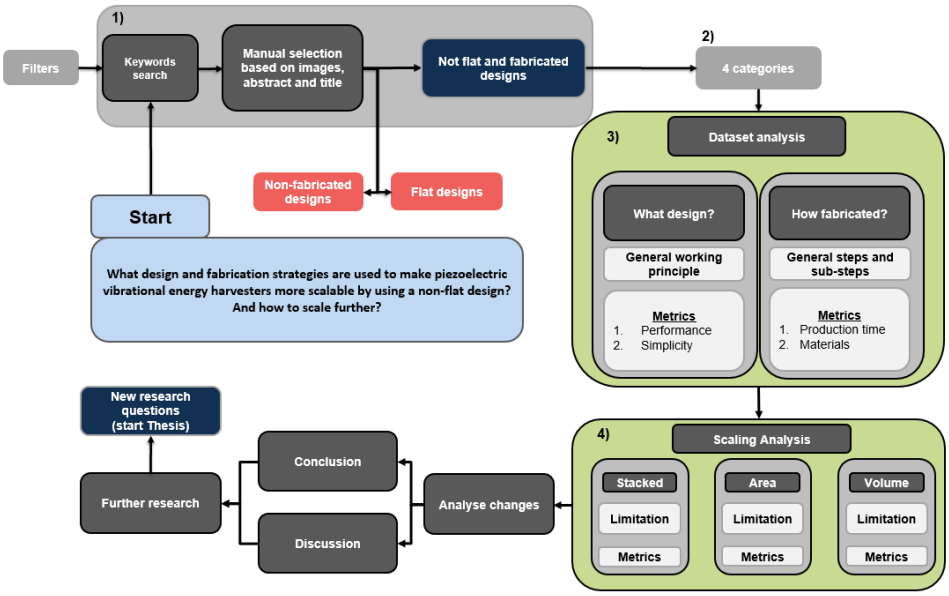


Figure 2.2: Structure of methodology; 1) Data selection, 2) Classification, 3) Design score from general and metrical information, 4) Analyse the effect of scaling.

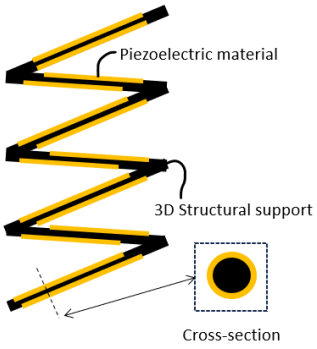


Figure 2.6: 3D structured support for piezoelectric material (PEM): A 3D substrate that shapes the overall system and allows certain movements, with applied piezoelectric material on specific or all areas. - *Criteria*: 3D support structure/substrate on which the PEM is applied.

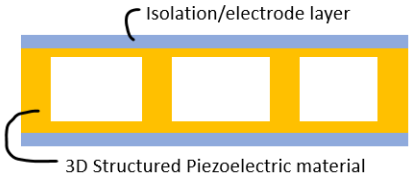


Figure 2.7: 3D structured piezoelectric material PEM: The piezoelectric is formed in a 3-dimensional way, to alter overall mechanical properties. - *Criteria*: No substrate is needed to support PEM structure, supported by PEM itself. Mostly metamaterial structures.

2.2.3. Data analysis

From the collected designs, the design and fabrication strategies are identified. This leads to a better understanding of the relation between the defined fabrication techniques and design metrics. The 3 different design scores are used to comprehensively analyse the current status. Making use of the simplicity, performance and production time scores.

Fabrication techniques

To identify the design's fabrication techniques, first multiple papers about fabrication of PEHs are consulted. Some papers specifically focused on new innovative ways to process PEM into a design others to make the PEM itself [6], [7]. The commonly used fabrication techniques are discussed in the following subsections.

Layer deposition techniques the most common technique for PEHs makes use of piezoelectric ceramic layers on a substrate layer. The overall thickness of the layers can differ a lot with different processes, between $0.1\mu m - 1mm$. The layer deposition can be done in different ways with different sub-processes, such as Chemical vapor/solution deposition, SOL-Gel, solid state synthesis, sputter deposition, tape casting, sintering and annealing. [8]

Bulk fabrication techniques This process involves creating piezoelectric materials in large, bulk

forms, typically through high-temperature sintering of piezoelectric ceramic powders. The powders are pressed into moulds to form desired shapes and then heated at high temperatures to create a dense, polycrystalline structure. Bulk fabrication is suitable for producing larger and multiple identical piezoelectric elements.

Additive manufacturing of PEH's is a promising technique, and makes use of current AM techniques with a specific method to add or implement PEM. To make custom shapes different AM techniques can be used. 2D AM integrated PEM, based on a single-layer fabrication method of polymers with nanoparticles of piezoelectric material (mostly ceramics) integrated into the layer. Used methods are; inkjet or screen printing. 3D AM integrated PEM combining multiple layers submerged on top of each other, based on fused deposition modelling (FDM). With PEM integrated between layers of printed polymer. Poling-assisted AM, a voltage applied on the printed material before, during or after the AM process. Done by putting a potential difference in the material resulting in piezoelectric properties. This poling treatment can be done before, during or after the AM process. [9], [10], [11]

Micro-machining refers to precise and miniature fabrication techniques. It involves processes like photolithography, etching, and laser machining to create tiny, intricate structures on substrates.

Assembly is needed after forming PEM or implementing it into a support structure, these steps are needed to connect different parts. Which are a substantial part of the fabrication of PEH.

Material choice of the piezoelectric used, reported into 4 categories; Ceramics, polymers, composite or crystal based. To see possible correlation between fabrication methods and material. Ceramics and crystals have overall higher piezoelectric coefficients compared with polymers. However, polymers are more flexible. Composites could combine these properties. [7]

Design scores

To create an overview of the current designs and analyse the effect of different fabrication techniques the overall design parameters need to be examined. To evaluate different designs multiple criteria have been set up. With these criteria, 3 scores could be provided. The design simplicity score, performance score and process time score. Which can be compared to see how each is related to a certain fabrication or design category, and are further elaborated in coming subsections. Because of the limited detailed information in most papers, the metrics must be related to information commonly available and still be measurable. A rubric is used to efficiently go through the process of individually ranking the designs. A higher score means better.

Simplicity score: The overall practical implementation of a design, and the reproducibility of a system depend on how well-understood the system is. Criteria like general size scale, fit into and be applicable as commercial product will contribute to simplicity. Namely, in the current stage further research is always beneficial, the more complex the design the harder this is. In section A.2 the ranking rubric for simplicity score can be seen in table A.2.

- *The total size* is the order of scale of the system. Volume based measured categorized in; nano (1-100nm), micro(100nm-1mm), milli(1mm-1cm), macro(1cm – 1m) and large scale(>1m). A bigger scale is easier to see, feel, fabricate and use so is less complex.
- *The number of components* of the whole system, will contribute to the simplicity metric. Compare repeated components with individual used components. When information is not clearly stated in the paper components are estimated based on the figures.
- *The degrees of freedom* into what direction energy can be harvested. Multiple directions result in a wider range of power harvesting but make the system more complex. Different direction calculations, assumptions and simulations are needed.
- *Use of PEM* in the design gives a better understanding of the working principle. See if it is integrated into the system or added to the system. Integration of PEM is more complex due to combination of electrical and mechanical properties in the same material.

Performance score: Indicates the use in a real-life environment. Performance in this context refers to the adaptability and efficiency of a piezoelectric system, determined by its frequency operating range, the diversity of its eigenfrequencies, the operating modes (d31 and d33), and its total PEM coverage percentage. In the section A.2 table A.3 the ranking rubric for the performance score can be seen.

- *The frequency operating bandwidth* is an indication of application purposes and what bandwidth the design can be used. It says

something about the usability of the overall design. A broader ranged system can harvest in a more stochastic world. Be able to harvest more energy in a broader range.

- The real-life use of PEH depends on harvested energy frequencies compared to the most common vibration frequencies in machines. A range of 10 to 40 Hz is stated as a preliminary good frequency to harvest energy from machines. [12]
- *The number of eigenmodes* of a design contributes to the overall power output in more real-life applications. Multiple modes indicate there are multiple working ranges. The counted modes are defined as and required to get a (local) maximum of voltage or movement in the fabricated or modelled design by a particular frequency. Specific modes can be designed for specific frequencies, wider modes contribute to broader energy harvesting.
- *PEM operation mode* can be in 2 different directions. The D31 mode is loading the material perpendicular to the poling direction. The D33 mode occurs during compression or extension in the same direction as the poled material. D33 does provide higher power outputs. When both modes are available the performance increases.
- *The total coverage of PEM* regarding the total system indicates how much power can be generated. Higher coverage means more PEM to harvest energy from. However, the way the PEM is applied does matter this is neglected for this metric. The parameter is measured in volume or area percentage of the whole system.

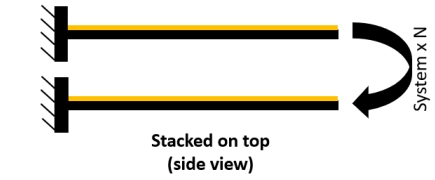
Production time score is a result of the number of steps necessary, the possibility of making it automated and the overall difficulty of making the total system. Often the real time needed to fabricate a design is not stated a relative score is given based on measurable metrics. In section A.2 table A.4 the ranking rubric for production time can be seen. A higher score means better production time.

- *The number of steps* needed to make custom-sized components or combine/assemble the components. Assembling the final components is seen as a single step.
- *Post processing*, is sometimes necessary after the completion of the assembly, requires more work and results in a longer production time.
- *Fabrication procedure* says something about the required labour to make the systems. Is the system made manually or is automation possible/applied?
- *Assembly complexity*, the more variation in steps compared to multiple the same steps needed. Also, are the steps done together or separate from each other?

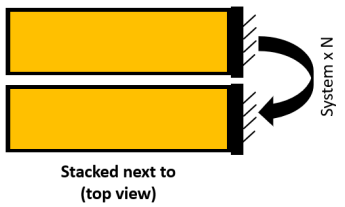
2.2.4. Scaling of current designs

To evaluate the effect of size scaling on the created dataset, an analysis of the change of measured parameters is conducted. This will result in a scaling score. Total size scaling is defined in 3 possible ways and all results are reported. By the basic rules of scaling and intuitive physics a comprehended result on what designs are still producible and usable after scaling. And what would be the effect on the different metrics. *Further scaling of PEHs can be defined by;*

- Repeated systems xN (figure 2.8)
- Area scaled system x$N^2[m^2]$ (figure 2.9)
- Volume scaled systems x$N^3[m^3]$ (figure 2.10)



(a) Stacked systems on top.



(b) Stacked systems next to

Figure 2.8: Stacked scaling of individual working systems (x N)

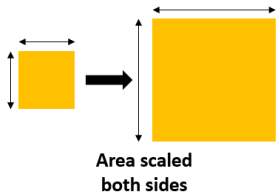


Figure 2.9: Area scaling of 1 individual system (x N^2)

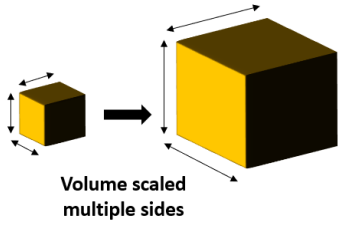


Figure 2.10: Area scaling of 1 individual system (x N^3)

To analyse each design, 2 limiting factors are analysed.

1. Is the system still operational/usable if scaled?
2. Can the system still be fabricated with the same technique if scaled?

If one of the answers is 'no', no further scaling analysis is needed because the limitation factor is the fabrication or working principle. Thereafter, the change of multiple parameters is evaluated, to see the rate of change after the size scaling. The following possible outcomes are measured; no change, sub-linear increase, (linear) increase, exponential increase and decrease. The analysed metrics with weight scores are provided in the section A.2 table A.5. With these, the total scalability score could be calculated. Which would give a score 3 if all design parameters are not affected by scaling. A higher score results in overall better-performing size scalability.

2.3. Results

In this section the results of the method described in section 2.2 are shown. Firstly, an overview of the analysed papers of each category in table 2.1 is given. Followed by the analysis of the different designs, looking at the design strategies and materials used. Then the fabrication methods of PEHs are given. Thereafter the 3 design scores are provided. Lastly elaborating on the scaling score results.

2.3.1. Analysis of PEH design

More than a dozen papers are found for the 'Stacked' and '2D modified' categories. Supporting a wide range of designs. The '3D PEM' and 'Supported' categories, on the other hand, are limited, and a lot of found design papers didn't manage to get a fabricated working energy harvester. The 'Stacked' and '2D modified' designs, most often are made out of ceramics or polymer-based piezoelectric materials. The '3D PEM' and 'Supported' designs are also made out of piezoelectric composites. Which contain small strips or particles of PEM combined with a more flexible or durable material to enhance the total performance of the material. In Figure 2.11 the material type per category is shown.

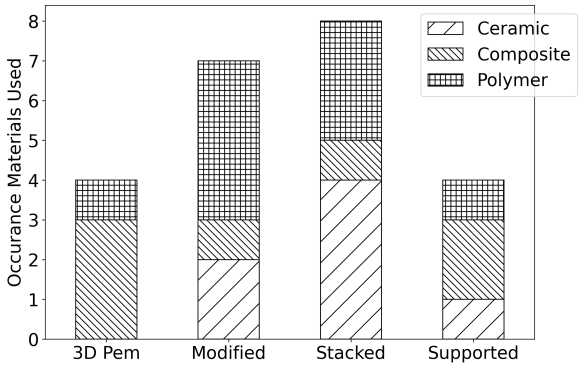


Figure 2.11: PEM per design category

The frequency operating range is for most designs in the range of 2 – 50 Hz. Designs with higher frequency ranges consist of 4 different non-cantilever beam PEH designs. The 'Stacked' designs, often have the objective to use multiple systems in series or parallel to increase the overall bandwidth. Which resulted in multiple eigenmodes of different sub-systems. The '2D Modified' designs have the objective of using increased DOFs to harvest multi-direction vibrations. And thereby increase the range of operation. In figure 2.12, the bandwidths of the designs are shown.

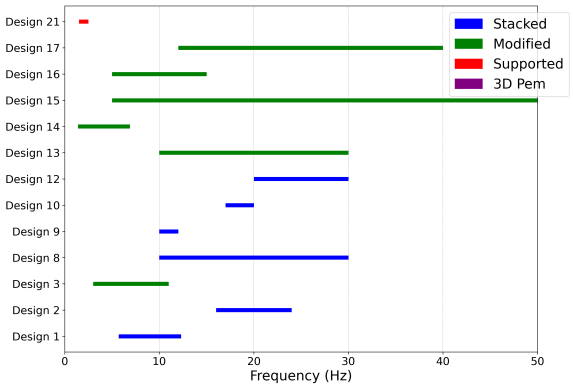


Figure 2.12: Frequency operating bandwidth of all designs between 0 - 50hz. Higher operating frequencies are omitted for clarity.

Fabrication

The most used methods are layer deposition methods and bulk fabrication based on powder sintering. These methods are used in 17 designs. For the 'Supported' and '3D PEM' categories, additive

manufacturing methods have been used as well.

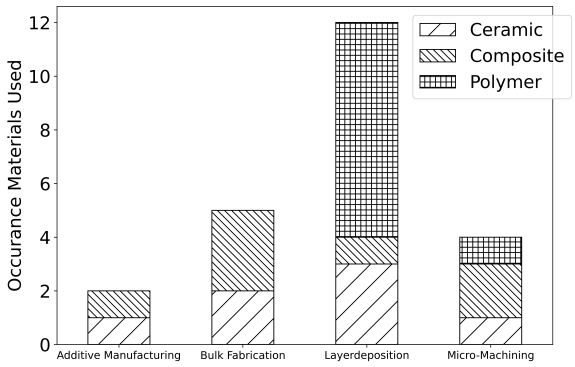


Figure 2.13: Material usage for each fabrication method.

As shown in Figure 2.15, assembly is used the most to integrate the PEM into the design (13 times). Both the '2D modified' and in 'stacked' categories make use of this method. Glueing, mounting or clamping are methods used. Some processes make it possible to fully integrate the PEM into the design, by combining the PEM manufacturing with the system fabrication. Commonly done in the '3D PEM' and 'Supported' categories. Sol-gel methods, porous layer deposition and additive manufacturing methods with filament containing PEM nano-particles have been done. The PEM used for different fabrication methods differs, as can be seen in Figure 2.14. For layer deposition methods mostly polymers PEM are used. For the other methods primarily composites and ceramics are used.

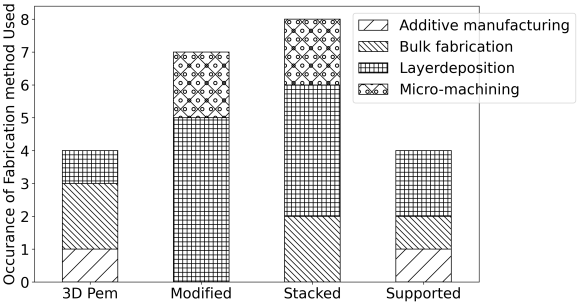


Figure 2.14: Fabrication approach for PEM per design categories.

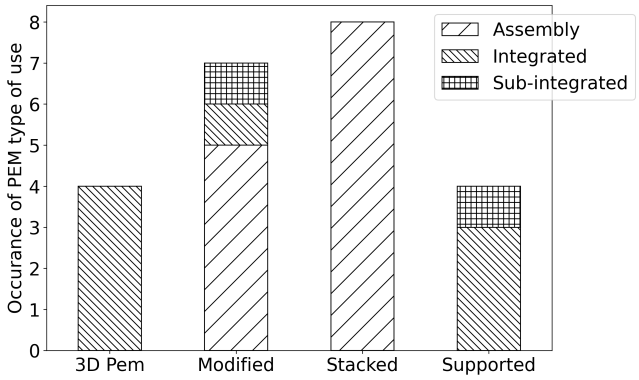


Figure 2.15: Used PEM integration method per design category.

2.3.2. Design scores

With the design metrics subtracted from the papers and the weight of the metrics, the total scores of each design are plotted in Figure. For the simplicity score and the production time score, all data could be gathered from the papers.

Simplicity score: The higher this score the simpler the design, so a higher score means less complex. It can be seen that 'Stacked' and '2D modified' systems are in general complex. Mainly because the use of assembly of subsystems compared with the more advanced fabrication methods to integrate the PEM with the use of more complicated materials (composites).

Performance score: The higher this score the better the performance of the design and the better applicable in a real life situation. The results of the performance are more scattered and no clear trends are visible. '2D modified' designs score the highest on performance. Due to their wider bandwidth and PEM system coverage.

Production time score: The higher this score the easier and faster the system can be made. All 4 categories have a wide variation of production time, with the more simple 'Stacked' designs also having the lowest-scoring designs based on production. In general '3D-PEM and 'Supported' are not hard(er) to produce compared to the more available 'Stacked' and '2D-modified' designs. With the '2D-modified' systems scoring more in the mid-range.

Score comparison; Shown in Figure 2.16 are the results of the 3 scores plotted against each other. Showing that a higher simplicity score does not always result in easier producible designs. The

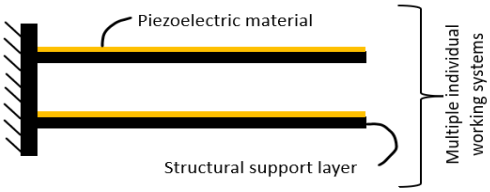
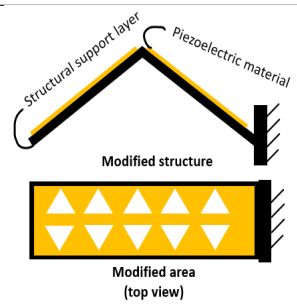
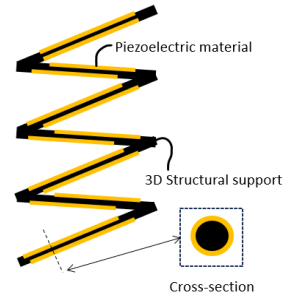
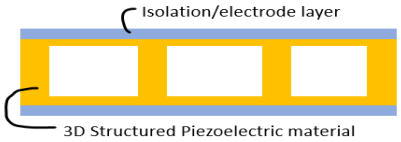
Category	Representative figure	Design ID	Reference
Stacked 2D PEH's ('Stacked')		1 2 7 8 9 10 11 12	[10] [13] [14] [15] [12] [16] [17] [18]
2D structures modified PEH's ('2D-modified')		3 13 14 15 16 17 23	[19] [20] [21] [22] [23] [24] [25]
3D structured support for PEM ('Supported')		4 6 18 21	[26] [27] [28] [29]
3D structured PEM ('3D-PEM')		5 19 20 22	[30] [31] [32] [33]

Table 2.1: The 4 different design strategy categories.

simplest designs score relatively lower at production compared to less simple designs. As small degrading trend is visible. With seeing a degrading trend with higher performance resulting in a lower production time score. Indicating that a broader bandwidth and increased PEM usage go hand in hand with increased production time. With the score comparison of the simplicity and performance. A clear order trend in categories can be seen. With a higher simplicity score will have a greater performance. With '2D-modified', 'Stacked', 'Supported' and '3D-PEM degrading in both scores in spoken order.

2.3.3. Scaling analysis

With the scaling analysis, multiple designs became not producible anymore or did not function anymore. If a system is already not producible it becomes automatically not functional. The results displayed in table 2.2 give the limiting factor of scaling for different design categories. With bulk manufacturing, layer deposition and micro machining could be limiting factors at area scaling. At volume scaling the layer deposition method is least favourable. Additive manufacturing methods is not reported as a limiting factor.

The scalability score for stacked, area and volume scaling compared to the production time score,

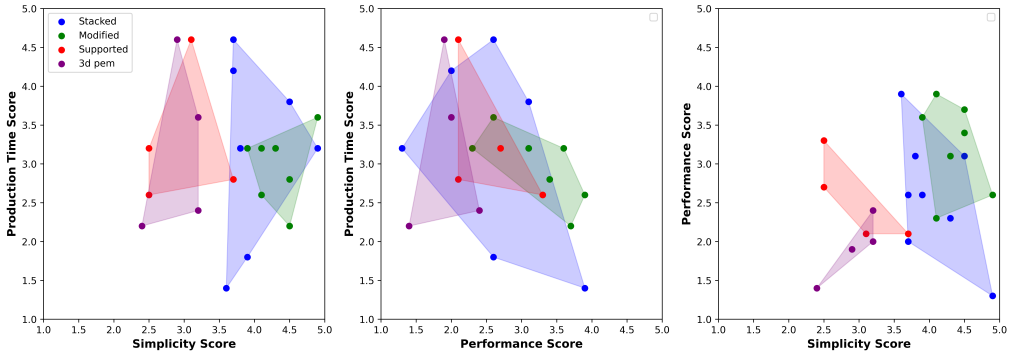


Figure 2.16: Simplicity, performance and production time scores plotted against eachother

	Stacked scaling		Area scaling		Volume scaling	
	Not producible	**Not functional**	**Not producible**	**Not functional**	**Not producible**	**Not functional**
Stacked	-	1	3	1	4	2
2D modified	-	-	-	-	1	4
Supported	-	-	1	-	-	-
3D PEM	-	-	-	-	1	-
Total	**0**	**1**	**4**	**1**	**6**	**6**

Table 2.2: The limitation factor of scaling with a certain method. Displays the number designs which or not producible or non-functional for different design categories.

performance score and simplicity score are seen in figures: 2.17a, 2.17b and 2.17c. The 3-score line indicates a non changed system, and thus equally as before scaling.

Stacking of designs can always be done, and gives overall a better score than just one individual system. Often the productions steps can be done simultaneously, reducing the average number of production steps required for each individual system. There is no correlation visible in the production time vs stacked scaling. A rising trend in the performance vs stacked scaling score can be seen. There is no trend seen between the simplicity of a design and its possible stacked scaling score.

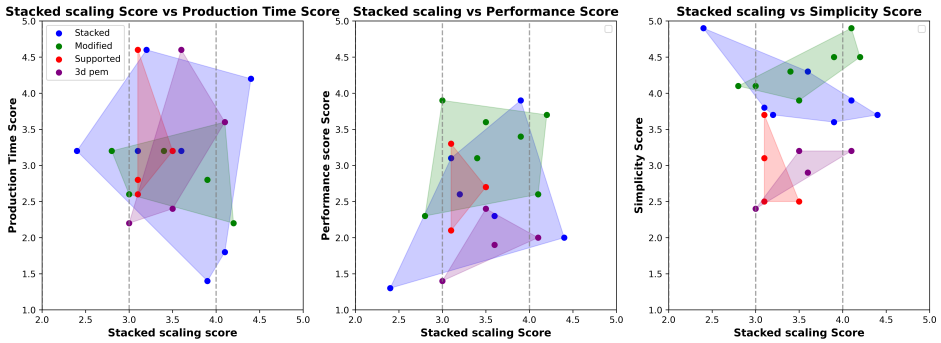
For area scaling the overall scores are downgraded, and only 4 designs are still at or above the 3-line. A rising trend can be seen in the area scaling score vs the production time score. Downgrading trends can be spotted with the area scaling score vs the performance and simplicity score.

Volume scalable designs are mostly 'Supported' or '3D PEM' systems. They hover just below the 3-score mark. Looking only at 'Supported' or '3D PEM' designs (red and purple) a rising trend in performance vs volume scaling score can be seen, as well as a downgrading trend of 'supported' designs in simplicity compared with volume scaling score. Furthermore, no clear trends can be seen in the volume scaling, and a high variation in the categories is realized.

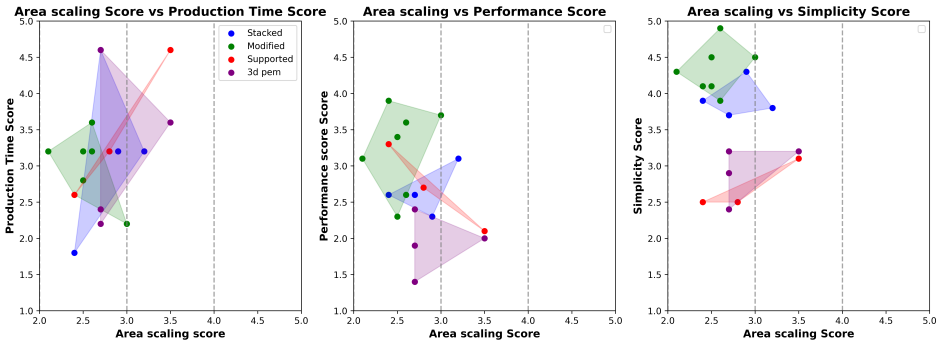
The best scoring design on stacked and volume scaling methods is a Bulk-fabricated stacked design making use of a D33 operating mode. For area scaling, both a '3D-PEM' and 'Supported' have a high-scoring design. Both make use of the out-of-plane structured principle but are fabricated in a 2D-scalable manner.

2.4. Discussion

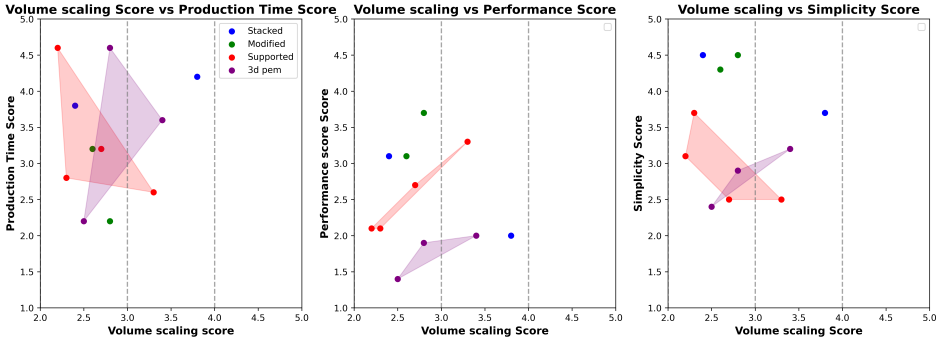
In this section, a discussion based on the results will be provided. This will create the answer to the research question and show what is done and what can be done to create non-flat, size-scaled PEHs. First, a reflection on the analysed status quo has been made, to see why design strategies and fabrication methods are used. Then a deeper look into their design scores will be provided. Concluding what possible ways to further scale the size of the analysed systems can be used by diving further into



(a) Stacked scaling scores



(b) Area scaling scores.



(c) Volume scaling scores.

Figure 2.17: Scaling scores compared with the Production time score, Performance score, Simplicity score.

the scaling scores. As last the limitations of this study and its results are discussed, and compared with other literature about scaling.

2.4.1. Analysis of PEH designs

The most common 'stacked' designs confirm that these designs are best researched in a wide range of the PEHs field. With the additional benefit of higher performance and simplicity. These systems are made with ceramics or polymer-based PEM. Fabrication of ceramic PEM is well known, but because of the brittleness harder to work with. Polymers are user-friendly and a cheap solution [34]. However, polymer-based PEM has way lower electric coefficients and therefore has less potential to work as a high-power-generating energy harvester. The need for assembly, makes the designs overall less complex, explaining why there is being done more research on these types of designs. However, this requires more manual labour and thus higher production time, which is acceptable for unique and experimental design production. Assembly is on the other hand less applicable for larger or more of the same units. The layer deposition and bulk manufacturing of PEM are commonly used, these methods are also more conventional and used in other applications. They have more use cases besides making PEM [35]. However, better integration of these fabrication methods with the total system would decrease the production time. The more advanced micromachining or additive manufacturing, need real specific requirements or sub-processes to eventually make the PEM. This

makes them harder to use, but easier to automate because less manual assembly is necessary.

Materials: Composites are a less used but promising piezoelectric material consisting of a ceramic PEM, often PZT or BCZT, combined with a more flexible polymer. Which are more commonly used in 3D-PEM and Supported systems. This material can make it possible to integrate the PEM within the overall system. This causes the designs to be more complex, and require the need for different fabrication methods, but enhances the total performance of the PEM and makes it better for fabricating automation. The combination of harder-to-integrate PEM, relatively new fabrication processes and the lack of operational bandwidth knowledge, makes composite PEM a less researched but thereby an interesting opportunity to make PEHs. Especially when these materials are used in the more researched 'Stacked' or '2D-modified' designs. This would improve their production time and still have a high performance score.

2.4.2. Design and scaling scores

The design scores help to understand the design and fabrication concisely. The more researched systems scored higher on simplicity and could explain why more research was initially done on these types of designs. On the contrary, only a few papers are found regarding the scaling of these 'simple' systems, which would suggest more potential can still be discovered.

The objective of a design paper often influences the performance of the system. Papers more focused on wider bandwidth will therefore score higher. On the other hand, papers focused on implementing a completely new fabrication method, new material or new working principle don't provide much information about their performance. The '3D-PEM' and 'Supported' category papers don't cover all the required performance score information, and make use of more innovative fabrication methods.

Comparison of the different design scores, the correlation between higher performance and worse production time requires the consideration of what is more important, performance or manufacturing. Making higher performance systems better producible would be even more beneficial. With the additional benefit of increased stacked and area scalability. This goes hand in hand with our expectations, if production is easier and automatable it becomes 'easier' to make multiple or bigger of the same system. With volume scaling of '3D-PEM' and 'Supported' designs, we see the same opportunity, but they first require to improve on their simplicity. If the system stays as easy to produce, these categories will outperform the current designs regarding volume scaling. However, the lack of quantitative research for these categories and their performance is limiting and could be the cause of wrong conclusions.

Looking at the scaling results of different scaling methods, we can say stacked scaling has the most effect. Requiring less coarse changes in the design and fabrication methods, and is usable in every situation. However, looking at the efficiency of the volume occupied, with stacked scaling only a linear increase is possible. With area and volume scaling theoretically able to be scaled more volume efficiently compared with stacked scaling. Area and volume scaling theoretically allow the system power-to-volume ratio to scale with a to the power 2 or 3. However, current literature doesn't support this claim. To be able to produce a scalable system, the consideration of different fabrication methods is needed. The same step multiple times is more convenient regarding production time.

2.4.3. Limitations and state of art research

Taking a qualitative look at the gathered data from the design papers, the input is mainly derived from graphs and images. Despite not providing 100% accurate metrical data, a general trend of design and fabrication strategies could be determined. Especially with the scaling scores, which are based on intuitive physics and scaling laws [36]. However, these scores give a better understanding of the effect of different kinds of scaling and provide promising opportunities combined with the other scores.

The lack of some particular data changes the scores. The missing operating range data for the '3D-PEM' and 'Supported' categories cause the performance score not to represent its real state of the art. However, performance papers on these designs are something for further research. Also, the production scores are influenced by some simplifications, like the fabrication automation and assembly complexity. If fabrication is done following the paper this would be assumed the same approach for a scaled system. With this in mind, a scaled system would automatically perform worse (longer fabrication time), but when scaling of a system would be an objective, the fabrication time

could most likely be reduced.

Compared with existing literature about scaling of PEHs, so far never an absolute result could be given. The five factors that influence the power generated by a harvester are the Scaling, Composition, Inertial, Material, and Power factors, see figure 2.18. Which are mostly interconnected variables and make power scaling a big optimization challenge. This study mainly focused on size and inertial scaling. With also taking composition, material and fabrication into account. Therefore the study itself lacks the in-depth conversion towards total power output. But analyses 4 out of 5 factors contributing to total power output and the effect on fabrication is analysed. To get a more complete study the power factor can be reported, making this a power–volume ratio optimization and see how it would be affected by size scaling. This would be advised as further research to get a more comprehensive result.

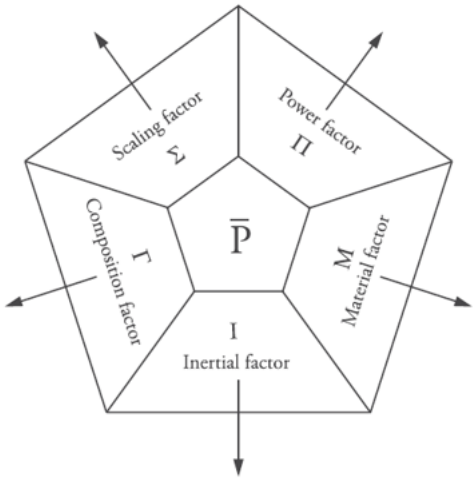


Figure 2.18: Representation of power generated by a piezoelectric energy harvester. The portrait indicates the five key performance factors for Scaling, Composition, Inertial, Material and Power factors. The arrows indicate that increase in each factor increases the normalized power $\overline{P}$ [37]

2.5. Conclusion

This research describes the design and fabrication methods used to make non-flat vibrational piezoelectric energy harvesters. And analysed how they would react after different size scaling methods. With the use of a classification and scoring method, an overall current status regarding; the performance, simplicity and production time of the designs has been created. Indicating that more researched, simpler designs perform better. Making use of more widely available parts by use of already well-known fabrication methods. Not seeing a clear trend in size scaling performance between the categories.
But, with area and volume scaling, fabrication and operationality become a limiting factor. These types of scaling would theoretically be more efficient regarding the power-to-volume ratio. But currently, the opposite occurs, area and volume scaling perform worse compared with stacked scaling. Indicating the gap of possible improvement in the use of these scaling methods. As well as the use of better suitable design and fabrication strategies concerning size scaling.

With this research, a better understanding of the effect of size scaling is created. Despite the design scores not being 100% based on measurable data. The scores give an idea of the performance, simplicity and fabrication of different designs and their approaches. The lack of performance data in the less researched categories results in downgraded scores. However, this indicates the necessity for further research to fully understand their capabilities. Compared with existing scaling research, this paper mainly focuses on the size, material and fabrication of PEH excluding the total power output. Giving a good basis to define potential and limitations. In further research, total power output could be included to completely define the performance.

Good performing and good-sized scalable systems would be beneficial for real-life applications. Making it possible to increase total power output or decrease the used volume for the same application. With the lack of papers fully focused on size and performance scaling, this paper contributes to an overall view of what is done, what works and what doesn't work. **But empirical research is still needed to completely validate promising strategies and make PEHs better applicable in the real world.**

3

Fabrication development of Stencil printing a KNLN3 - epoxy for an energy harvester

This chapter elaborates on developing a fabrication method for creating piezoelectric energy harvesters through stencil printing. Stencil printing, widely used across various other industries, is known for its simplicity, high scalability, and cost-effectiveness. It allows for multiple design parameter adjustments, including shape, location and thickness. Applying piezoelectric material with this approach allows for a potential large-scale production of integrated and optimised systems.

3.1. Overview and goal

In this chapter, the objective, the development of the total fabrication strategy together with all smaller sub-steps, is elaborated.

The development of the method is done by fabricating multiple batches, each time looking at different steps, changing certain parameters or trying different equipment and approaches. A trial-based approach is established each time, anticipating possible outcomes, noting what has been done and looking back to analyse key learnings and possible improvements. Eventually, a systematic approach is developed, allowing for the fabrication of piezoelectric energy harvesters using stencil printing. With a lot of learnings, this section provides a basis for further development of this method. This provides the guidelines for further research.

The fabrication development was picked up from existing work on the fabrication of piezoelectric composites, consisting of piezoelectric particles inside an epoxy or polymer matrix. Showing the practical approach of producing piezoelectric composites based on theoretical models and experimental validation. [38] [39] [40]
Objective: Develop a stencil printing fabrication strategy to make piezoelectric energy harvesters by directly integrating the material onto a resonator substrate.

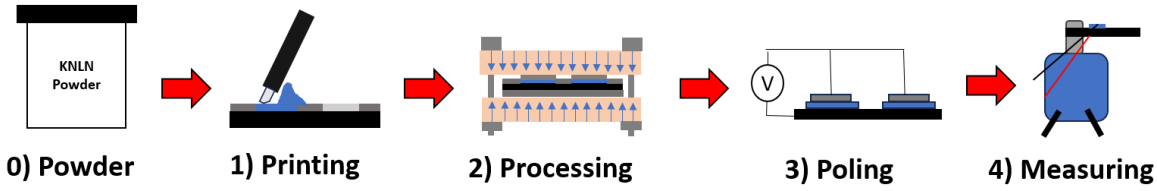


Figure 3.1: The total fabrication process contains 5 major steps

Each major step has its own sub-objective:

0. Creating electroceramic piezoelectric powder.
1. Make and apply a paste-like substance in certain shapes, thicknesses and locations on a substrate.
2. Dry, cure and process the material.
3. Give the material piezoelectric properties by applying an electrical field.
4. Measure and validate the properties and performance.

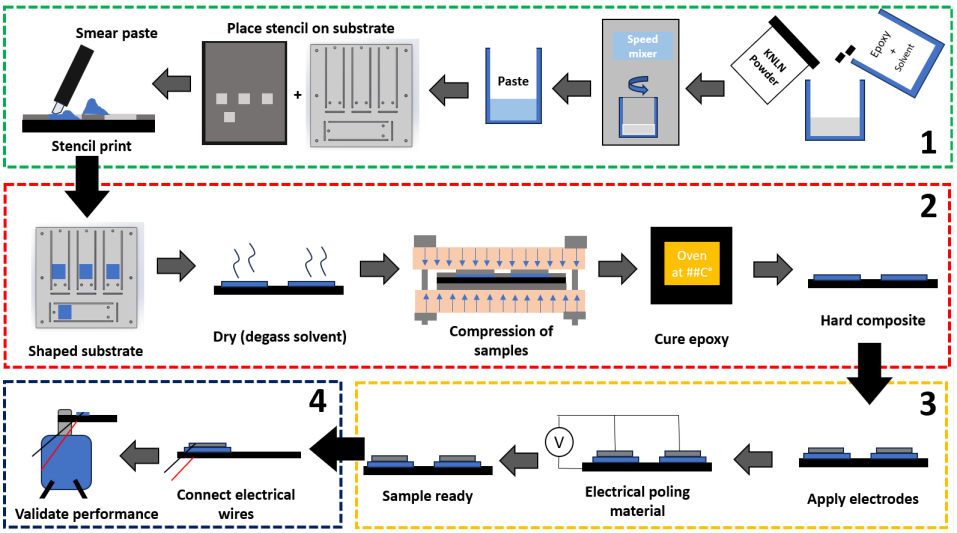


Figure 3.2: Stencil printing fabrication overview.

The development of the 5 major steps are explained in the coming sections. Appendix B shows an overview of all altered steps.

3.1.1. Contribution development

The development of the stencil-printing method for piezoelectric energy harvesters presents several significant contributions. Firstly, it shows the entire cycle, from material selection and integration to giving piezoelectric properties to the system, altering dimensions and parameters, and testing and validating the power output. Thereby integrating piezoelectric material directly with a resonator beam. Additionally, the development delves into the various fabrication factors, including the impacts of solvents, compression, curing, and adhesion, which are crucial for optimising the performance and reliability of energy harvesters. Finalising as a fabrication manual with detailed steps for fabricating these harvesters shown in appendix D.

This allows for more concrete follow-up studies, picking up parts of the fabrication to study how different factors actually play a role in the final product. Basically, find a mix of all parameters to establish a smooth, uniform and highly dense sample in a more controlled way. This leads to recommendations shown in section 5.4.

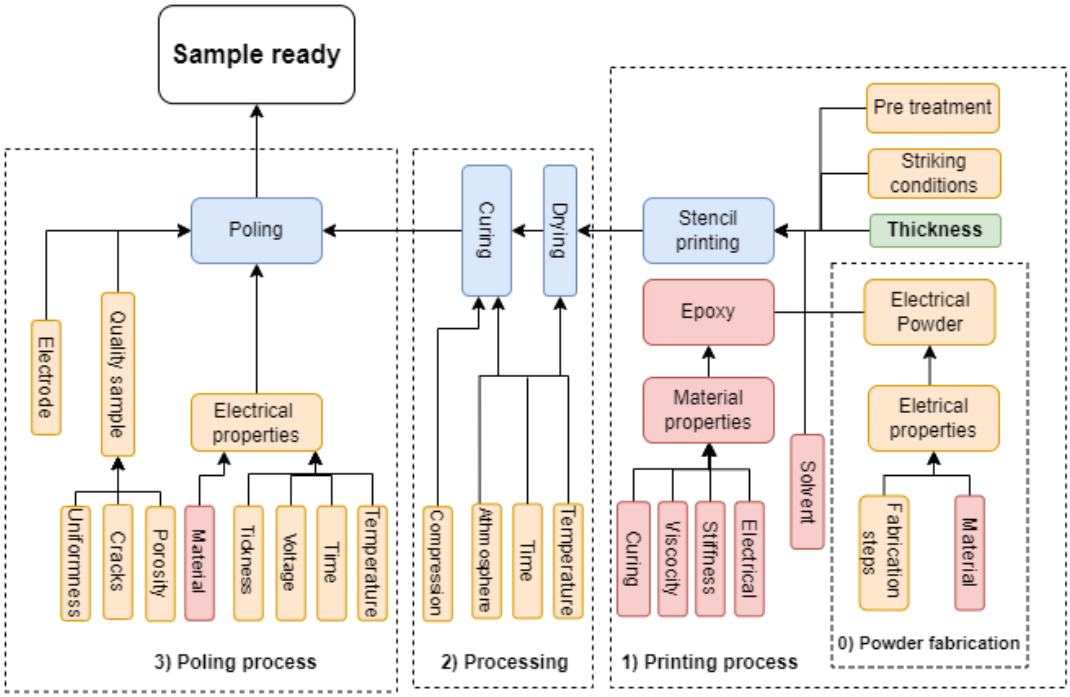


Figure 3.3: All parameters displayed that influence the final sample. The material influence is in red, and the fabrication steps influence is in orange. In blue the main fabrication steps are shown. Green is the parameter changed in the experimental validation study in chapter 4

The main findings from the development of the fabrication substeps process are outlined and further elaborated in this chapter.

Printing Process - section 3.3

- Established guidelines for selecting solvent and epoxy, emphasizing the importance of their material properties for optimal printing outcomes.
- Developed a customizable sealing method to better control the printed shapes and the quantity of material deposited, enhancing precision and uniformity.
- Identified the critical impact of substance deposition technique and striking direction on the uniformity of the samples, suggesting targeted improvements for consistency.

Curing Process - section 3.4

- Highlighting the importance of surface treatment before printing.
- Explored using a low-pressure atmosphere to reduce drying time, noting its potential benefits in highly controlled environments.
- Emphasized the necessity of all-side compression to prevent material leakage during curing.
- Demonstrated that higher top-down pressure can partially heal surface cracks, although deeper cracks remain unaffected.
- Found that kinematically constrained pressure yields more uniform thickness but is insufficient for adequately restoring cracks.
- Highlighted that individually compressed samples allow for greater control over pressure application, leading to improved crack restoration and sample integrity.

Poling Process - section 3.5

- Underlined the importance of preventing cracks to achieve higher poling voltages and enhanced piezoelectric properties.
- Determined that temperatures below 100°C adversely affect the poling efficiency.
- Concluded that uniform samples result in consistent piezoelectric properties.
- Noted that cracks or pores in the samples cause non-damaging dielectric breakdowns, which limit the effective electric field during poling.

Testing - section 3.6

- Validate the voltage output of a fabricated sample as soon as possible. Also, besides measuring D_{33} values, due to inaccurate measurements.
- In the piezometer, apply a conducting plate on top of the sample to equally compress the whole sample.

3.2. Electroceramic KNLN3 Powder fabrication

The basis for the piezoelectric properties in the composite are piezoelectric ceramic particles. The fabrication method of these powders is well-researched, and all different materials are available. The most commonly known is PZT, a piezoelectric material known for its high coupling factor and high electric output. However, his material contains lead, which is very toxic and bad for the environment. An alternative material, KNLN3 powder, is a sintered material of 4 different minerals combined, creating piezoelectric particles. [2][39]

Figure 3.4 shows a schematic overview of these particles' fabrication. Appendix C provides a more elaborated description and manual.

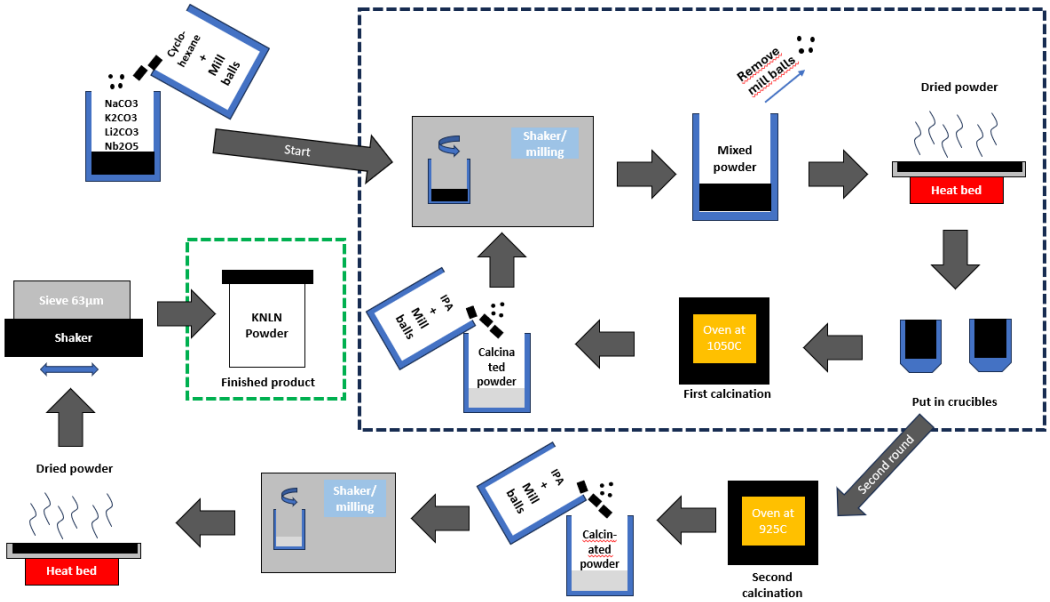


Figure 3.4: Fabrication process of KNLN3 particles.

3.3. Printing process

The printing process describes the steps from selecting to adding different materials and striking the material substance along a stencil to apply the material on a substrate.

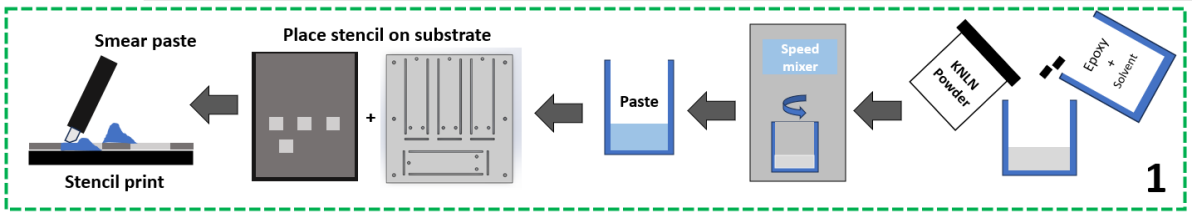


Figure 3.5: A schematic overview of the printing process.

3.3.1. Pre treatment

Surface treatment of the substrate before printing improves adhesion. Cleaning with acetone to remove lubricant residues of the stainless steel substrate. Grinding the surface in 4 directions (vertical, horizontal, 2x diagonal) with 80-grid paper increases the surface roughness and surface area. A second round of acetone cleaning is required to remove the grinding debris. In Figure 3.6, a treated surface can be seen right before the assembly of the printing setup.

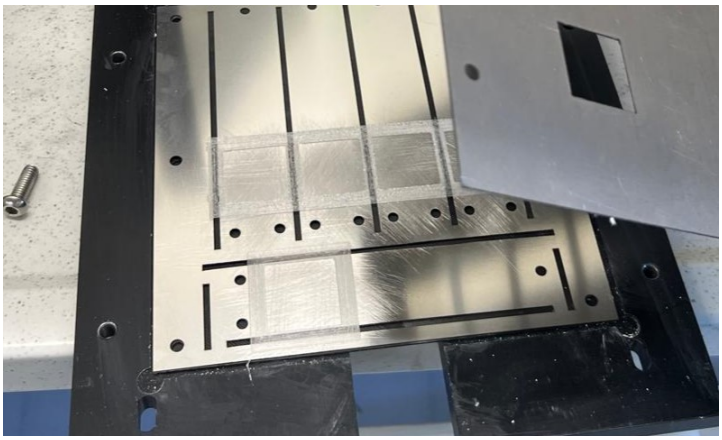


Figure 3.6: Before printing setup with treated surface and applied seal explained in section 3.3.3.

Especially with thicker layers, the mechanical stresses at the boundary layer increase, causing earlier delamination. Cracks and small holes in the sample allow silicon oil to enter underneath the sample during poling, seeing earlier delamination with untreated surfaces.

3.3.2. Material and solvent selection

Multiple material properties are of great importance when creating piezoelectric materials. The created substance consists of 3 major ingredients: an electroceramic powder, an epoxy and a solvent. Providing the right quantity mix to get a liquid enough substance is well mixed and, when cured, has high piezoelectric properties. The solvent must solve the used epoxy, evaporate after application, and preferably not be toxic. The tried combinations are shown in table 3.1. The effect of solvents is further elaborated in section 3.4.

The main influence epoxy has on the created piezoelectric material is its electrical resistivity, strength, and operation limits, such as temperature. Also, the curing conditions and time required to cure depend on the epoxy. The Simicon SR1700+SD2801 and Epotek 320NC-2 epoxies are used; Epotek H77 is not used but has some potential and is recommended for further research. This epoxy provides a higher young modulus and operating temperature, which might benefit the material's piezoelectric coupling coefficient and poling condition (because of higher poling temperatures).

Solvent	Simicon SR1700 + SD2801	Epotek 320NC-2-SDS
Hexane	Non-solvent	-
Isopropanol	Solvent	-
Ethanol	Solvent + quick drying	Solvent + quick drying

Table 3.1: Solvents compatibility with different types of epoxies

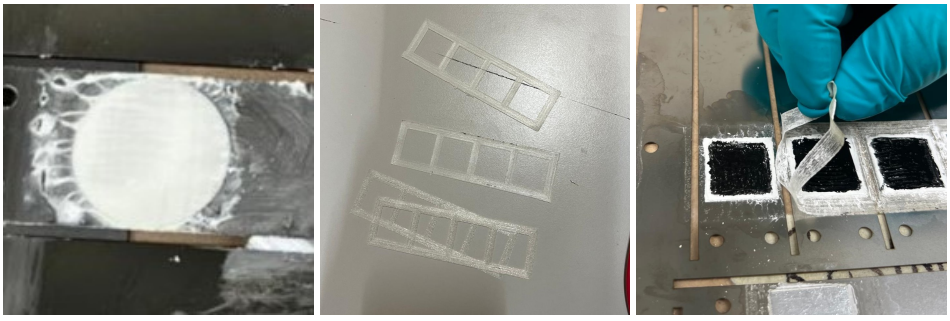
Property	SR1700 + SD2801	320NC-2-SDS	H77
Dielectric Constant (1kHz)	4.0	9.75	5.64
Resistivity ($\Omega \cdot cm$)	1×10^{13}	1×10^{13}	1×10^{13}
Young's Modulus (GPa)	3.05 - 3.20 (depending on curing)	4.7 (684,864 psi)	6.55 (950,693 psi)
Strength (Tensile) (N/mm^2)	65 - 80 (depending on curing)	24.4 (3,556 psi)	12.2 (1,778 psi)
Thermal Conditions (Operating Temp)	-40°C to 120°C	< 275°C (intermittent)	< 350°C (intermittent)
Glass transition temp (T_g)	97°C	50°C	80°C
Curing Requirements	24h 23°C + 24h 40°C or 24h 23°C + 16h 60°C or 24h 23°C + 8h 80°C	70°C for 1 hour or 23°C for 24 hours	150°C for 1 hour or 100°C for 1 hour + 120°C for 2 hours

Table 3.2: Properties of SR1700 + SD2801, 320NC-2-SDS, and H77 Epoxies [41], [42] & [43]

3.3.3. Stencil and the way of using

With the created substance, the material can be printed onto a substrate; by covering an area, the material will only be deposited in certain places. The influence of the stencil, the thickness of the stencil and how the stencil is used have a direct influence on the end product.

The varying thicknesses of different stencils allow for thinner or thicker printed layers. The amount of material needed must be calculated based on the required volume, with solvent volume fraction influencing the left-behind material. The connection between the stencil and substrate must be closed, preventing substance leakage underneath the stencil and thus better-placed shapes on the substrate. A TPU98 3D printed thin layer seal has been designed to prevent substance leakage, shown in figure 3.8. These seals must be $1 - 2mm$ bigger than the stencil printing area to prevent sticking under the printing area, creating a gap causing delamination. Different thicknesses of stencils and seals used are summed in table 3.3. In appendix H.1, the technical drawings of the substrate, stencil and seals are shown.



(a) Before the use of a seal. **(b)** TPU98 seal used. **(c)** After using the seals.

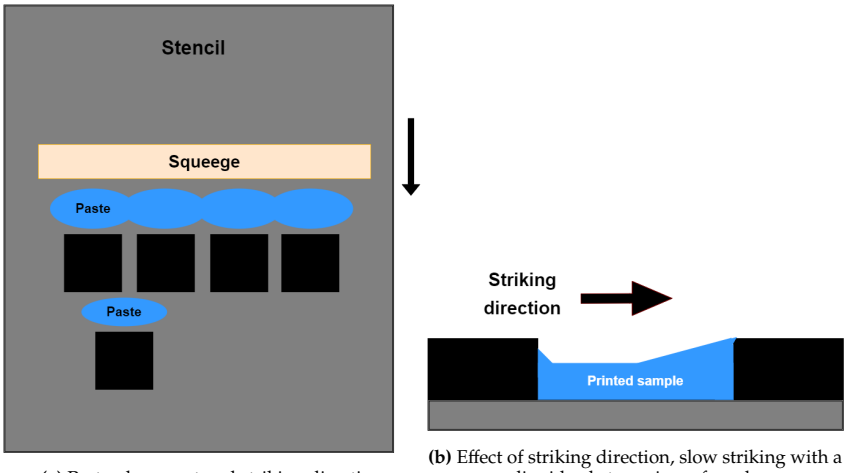
Figure 3.7: A TPU98 seal used to prevent substance leakage and better-shaped layers.

The amount of paste, the striking direction, and the number of strikes have a major influence on the surface structure of the end product. Due to the drying of the substance between strikes, some harder

Thickness of stencils used	0.1 ; 0.25 ; 0.5 ; 0.75 ; 1.0 ; 1.5 ; 2.0mm
Thickness of seals used	[no seal]; 0.15 ; 0.30 ; 0.45mm

Table 3.3: Stencil and seal thicknesses used

pieces may scrape the material. Only one strike is preferred. However, due to the scarce material, the placement of the substance on the stencil is important. See recommended substance positioning in figure 3.8a. Ensure one strike is enough to fill the area to be printed completely. Simultaneously, the paste must still be liquid enough to move slowly in all corners of the printed area. Less liquid paste also results in even more inclined samples shown in figure 3.8b



(a) Paste placement and striking direction

(b) Effect of striking direction, slow striking with a liquid substance is preferred.

Figure 3.8: The effect of striking direction and inclined samples. This is also affected by the viscosity of the substance/paste applied.

3.4. Curing process

The curing process describes the steps from having printed material on a substrate to drying the solvent and curing the epoxy. Basically, it is the process of removing the solvent and transforming the epoxy to its final rigid state.

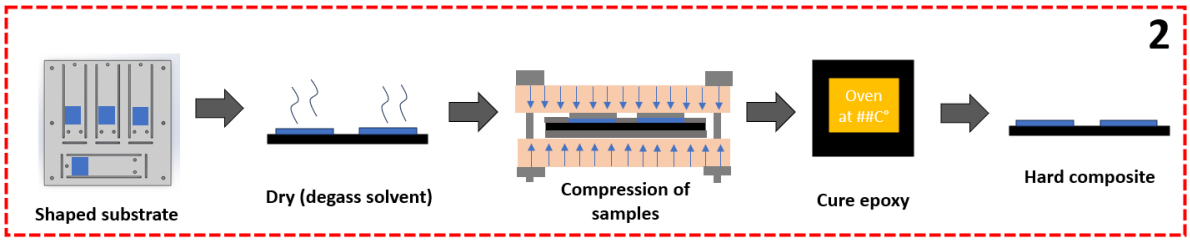


Figure 3.9: A schematic overview of the curing process.

3.4.1. Drying

One of the major effects on sample quality is the quantity and type of solvent used. Drying too slowly makes the epoxy cure already at room temperature; drying too quickly causes quicker sample contraction, resulting in cracks in the samples.

A way to quicken the drying period can be done by decreasing the environmental pressure. Make sure the solvent is not boiling and not drying too quickly. The change in boiling temperature under different pressures can be described using the Clausius-Clapeyron equation. Rearranged to solve for the new boiling temperature T_2:

$$T_2 = \left(\frac{1}{T_1} - \frac{R \ln\left(\frac{P_2}{P_1}\right)}{\Delta H_{vap}} \right)^{-1} \tag{3.1}$$

Where T_1 is the initial boiling temperature (in Kelvin), P_1 is the initial pressure, P_2 is the new pressure, R is the universal gas constant (8.314 J/(mol·K)), and ΔH_{vap} is the enthalpy of vaporization (in J/mol). [44]

Using a quicker drying solvent instead of lower pressure is a more recommended solution. The drying process is smoother, and fewer cracks occur. Both variations are possible for thinner layers. Using less solvent and a slower drying solvent for thicker layers can improve their sample quality.

		Stencil+seal: 0.1 - 0.40mm	**Stencil+seal: 0.5 - 0.75mm**	**Stencil+seal: 0.75-1.20mm**	**Stencil+seal: 1.25mm+**
Isopropanol	1 bar	0.5h drying time No cracks	1.5h drying small cracks	2h+ drying time Small Cracks	3h+ drying time Large cracks
	0.5 bar	Not needed	x	1h drying time Small cracks	x
	0.3-0.4 bar	Not needed	1h drying time small cracks	1h drying time Exploded cracks	x
Ethanol	1 bar	0.5h drying time No cracks	1h drying time Small cracks	1.5h drying time Large cracks	x

Table 3.4: Drying times and crack formation for different stencil+seal thicknesses and pressures using Isopropanol and Ethanol

3.4.2. Compression and curing

The epoxy is the leading factor for the required curing conditions, as seen in section 3.3 table 3.2. For final piezoelectric properties, 2 major points are important: the porosity, defined as relative density and the surface roughness. [40]

Sample compression during curing makes denser samples and can restore small cracks. The surface roughness of the sample is improved by increasing the pressure, but inclined samples occur more often due to non-equal pressure. Single beam compression improves these results. However, non-uniform

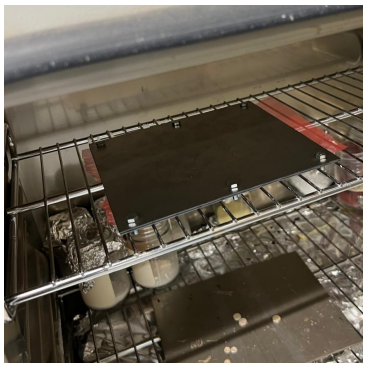
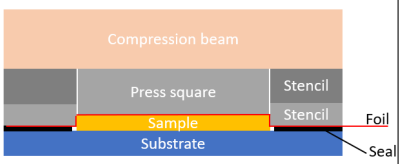
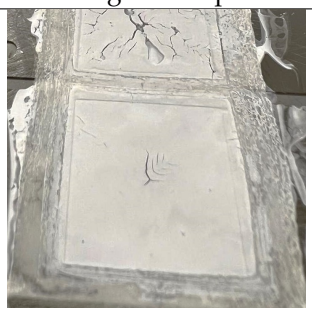
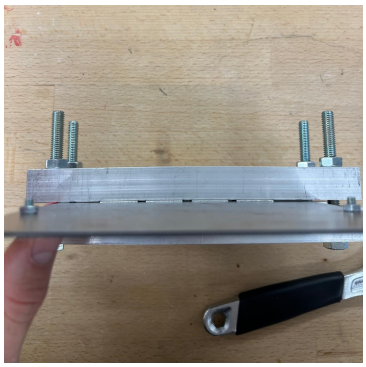
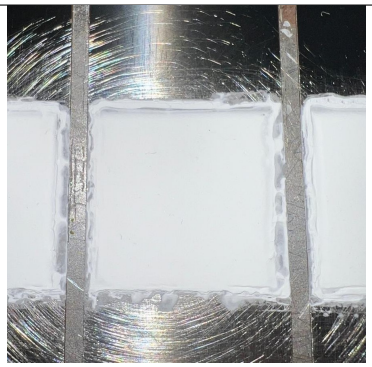
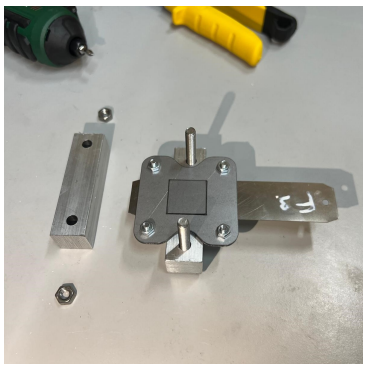
	Compression Principle	Compression Figure	Result Sample
Only plates	**Compression of sample between two plates** simple compression from top to bottom.		 Leakage of the paste
Beams + stencil (kinematic constraint)	**Kinematically constraint:** The compression beam and square equalize to same height getting more equal thickness		 Smooth and uniform sample, no cracks restored
Beams + stencil	**Higher compression:** Thicker press square so more pressure on sample because not constraint.		 Extra compression possible, less uniform thickness
Single Beam + border	**1 beam compression:** to apply higher pressure and better uniform layers per individual sample.		 Smoother samples under higher pressure

Table 3.5: Compression principles and results for different configurations

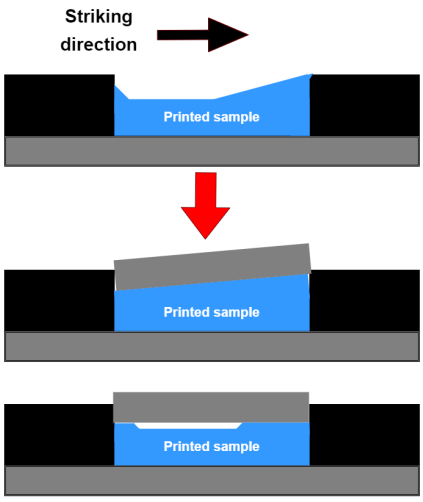


Figure 3.10: Liquidity of printing substance and direction cause inclined samples

samples still occur. Kinematic constraint compression works best for uniform layers, but if cracks occur, this method cannot restore these. In the next section 3.5, it becomes clear that cracks are the worst thing and need to be prevented as much as possible. In table 3.5, the 4 different compression types are displayed with the resulting samples. A cause of non-uniform layers is the paste sticking to the sides more during printing, as shown in figure 3.10. The technical drawings of the compression systems can be seen in appendix H.2

The thickness of all samples is measured with a micrometer Mahr 40ER to know the exact thickness and what voltage needs to be applied during the poling process.

3.5. Poling process

The poling process describes the steps of preparing the samples with electrodes to put them in a heated silicon oil bath under a high-voltage field to give the material piezoelectric properties.

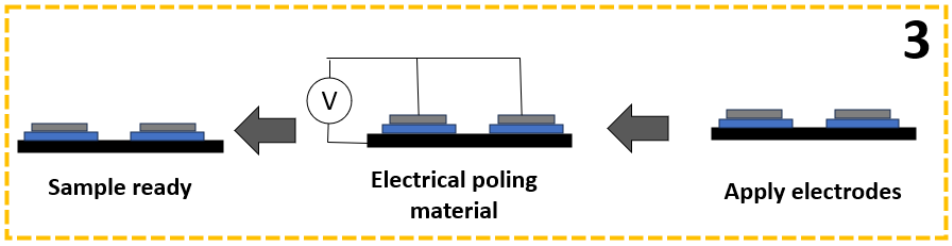


Figure 3.11: A schematic overview of the poling process.

Poling piezoelectric composite samples consisting of randomly oriented particles in an epoxy matrix involves aligning these particles to achieve desired piezoelectric properties. This process includes applying an electric field to the composite at elevated temperatures. The electric field reorients the dipoles within the piezoelectric particles, aligning them along the field direction. In figure 3.12, the effect of poling can be seen aligning the poles of the particles inside the epoxy. The elevated temperature makes the epoxy soft to more easily rotate the particles. The sample needs to cool off with the electric field still applied to keep the orientation of the particles in line. This alignment enhances the overall piezoelectric response of the sample. The applied electric field is dependent on the distance between the 2 electrodes, as can be seen in equation 3.2, E represents the electric field measured in volts per meter (V/m), V denotes the applied voltage in volts (V), and d indicates the thickness of the sample in meters (m).

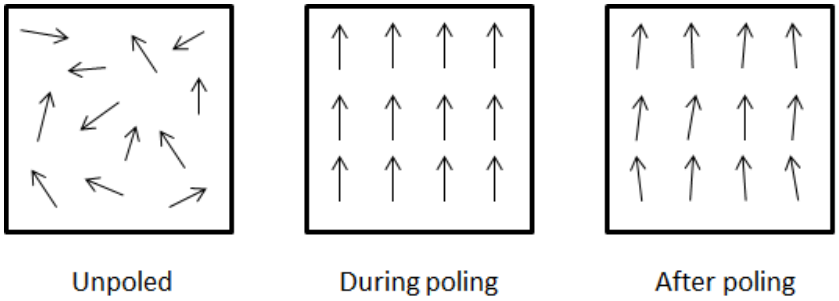
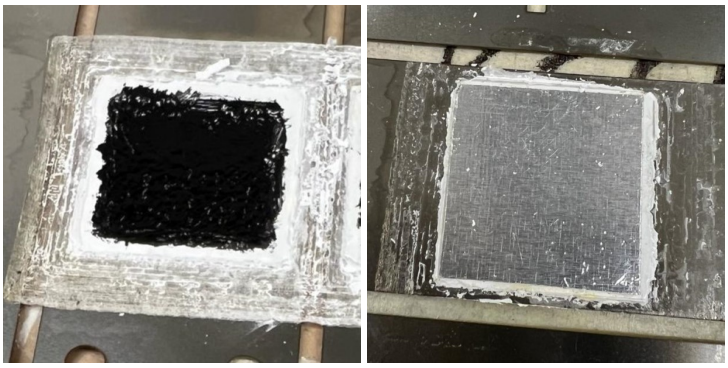


Figure 3.12: A schematic overview of the poling principle, aligning the poles of the particles.[45]

$$E = \frac{V}{d} \tag{3.2}$$

3.5.1. Electrodes and cracks

The electrode type influences the poling conditions, the fabrication time, and the effort required. As the bottom electrode, the stainless steel substrate is used. This directly integrates it into the PVEH design but gives some extra points to consider. The adhesion of the layer to the substrate must be good. Underneath surface cracks or delamination decreases the electrode function. Also, the climbing of the substrate needs to be electrically isolated, preventing the current from leaking directly to the ground. Carbon electrode paint is an easy approach to applying a custom-sized electrode; some drying time and precision are needed to ensure no short circuit occurs. With cracked or porose samples, the carbon paste managed to suck in the holes. The distance between the top and bottom electrode decreased, causing earlier voltage breakdown. With cracks completely through from top to bottom, carbon paint could already cause direct short circuits. Using aluminium tape as an electrode prevents this from happening and could be applied before or after curing. Done after curing makes it possible to better visually inspect the samples and measure the thickness. The addition of aluminium tape will influence the stiffness of the total structure a bit; however, with thicker layers $0.15mm+$, this can be neglected. In creating thinner samples, it is recommended that the electrode choice be reconsidered.



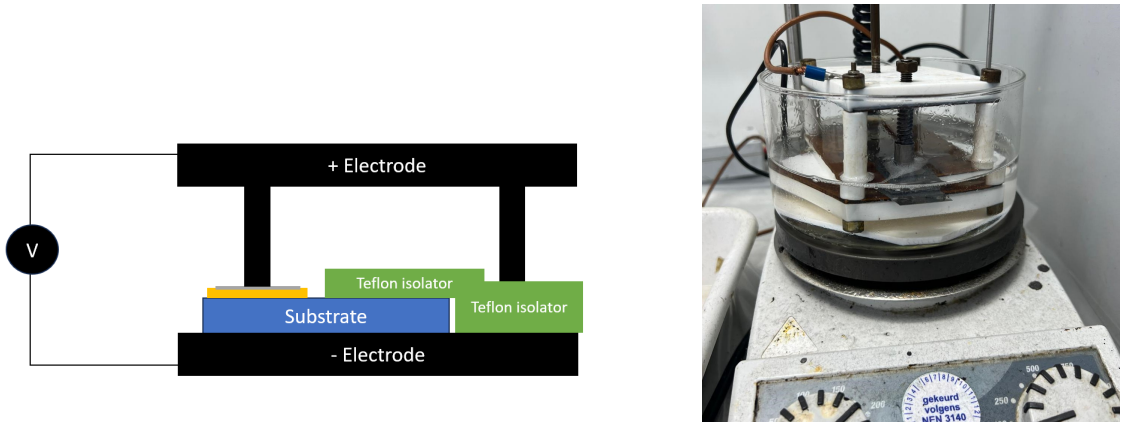
(a) Carbon electrode **(b)** Aluminium electrode

(c) Schematic overview, carbon and aluminium electrode effect on cavities.

Figure 3.13: Two different used electrodes.

3.5.2. Contact poling conditions

To get the highest piezoelectric charge coefficient D_{33}, 3 major poling conditions play a role. The temperature ($^{\circ}C$), electric field strength (kV/mm) and poling time (min) influence the piezoelectric charge coefficient. Because we are poling a stainless steel substrate, the contact or close distance between the top electrode and the substrate needs to be prevented or extra isolated. The environment also needs to be considered because the amount of kV/mm that can be applied is limited by the breakdown resistance of the environment. A poling bath of silicon oil prevents this breakdown. Porosity and cracks of a sample contain air, which breaks down already at 2 kV/mm and thus prevents higher poling voltages. Also, the contact resistance plays a role, making sure the contact between a substrate and the lower electrode or the top electrode with the contact pin is low. Corrosion of the pin and lower electrode prevents the electric field from crossing the whole area of the sample electrode. To prevent this issue, grind the poling setup and ensure good contact is established before poling by doing a trial run without a sample to see if a current starts flowing.



(a) schematic poling setup, with extra teflon isolation to protect against unwanted short circuits.

(b) Contact poling setup inside a silicon oil bath with controlled temperature.

Figure 3.14: Contact poling setup.

All different effects of the conditions have already been well studied, but they differ for each material used. [39] [38] Some things are tested to see their influence. However, complete empirical studies have not been performed on the KNLN-epoxy combinations that were used. This is recommended for optimal uses. Some key findings after trial and error are:

- Poling voltages below, 0,3-0.5kV, are very sensitive to contact resistance.
- Too fast voltage increase (seconds) increases the chance of partial breakdown.
- Higher temperature 130°C+ results in earlier breakdown.
- Time under poling after 5 min doesn't influence D_{33} value for both epoxies.
- Current leakages occur more with thicker and/or cracked samples.
- Extra isolation prevents short circuits with the substrate.
- Temperature below 100°C limits the D_{33} value.

3.6. Testing process

The testing process describes the steps of analysing sample properties to evaluate the performance of the energy harvester.

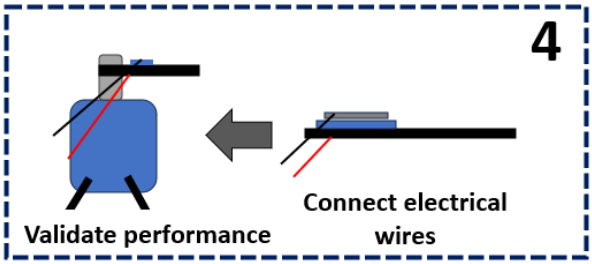


Figure 3.15: A schematic overview of the testing process.

It is time to validate the systems after cleaning all oil residues from the polling process. Starting with measuring all properties like capacitance C_p, resistance R, impedance X with an Agilent 4263B LCR and piezoelectric charge coefficient d_{33} by using the PiezoMeter System PM300. In operation, the d_{33} is not used but gives a good comparison between all the samples; in operation, the d_{31} coefficient is leading. The relation is stated in equation 3.3, and derived by using the poison ratio of 0.3.

$$d_{31} = \frac{1}{3} * d_{33} \tag{3.3}$$

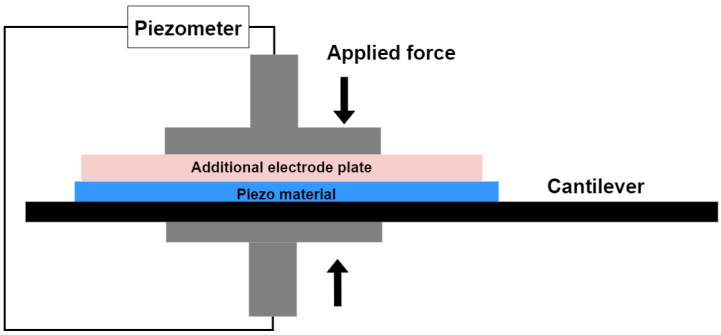


Figure 3.16: PiezoMeter setup, requiring an extra electrode plate to completely coffer the piezoelectric sample.

After measuring all properties, the samples are wired with aluminium tape. Soldering has been tried, but melting the epoxy sample thus is not an option. A better integration method of the electrode and wire would further improve the system. With a multimeter, check if the wires and electrodes are connected properly.

The dynamic testing setup involves a Tira shaker TV51140 setup and an accelerometer PCB356B21 measuring the input acceleration. The voltages are measured with a NIDAQ-USB6002 and stored with NIDAQ software. The voltages U created by the energy harvester is measured across the load resistance R and are used to calculate the power [watt], with the test setup shown in figure 3.17. It is recommended after each fabrication batch to validate if the sample produces a voltage output (done by simply tapping on the sample is sufficient) besides only measuring the d_{33} value. Multiple performance tests need to be performed to properly compare different fabricated samples. This is dependent on the type of energy harvester. The main points to consider are the optimal resistance load, the operating bandwidth of the system and the input frequency and acceleration. A voltage divider may be used with very high (exceeding $10V$) to prevent damage to the NIDAQ.

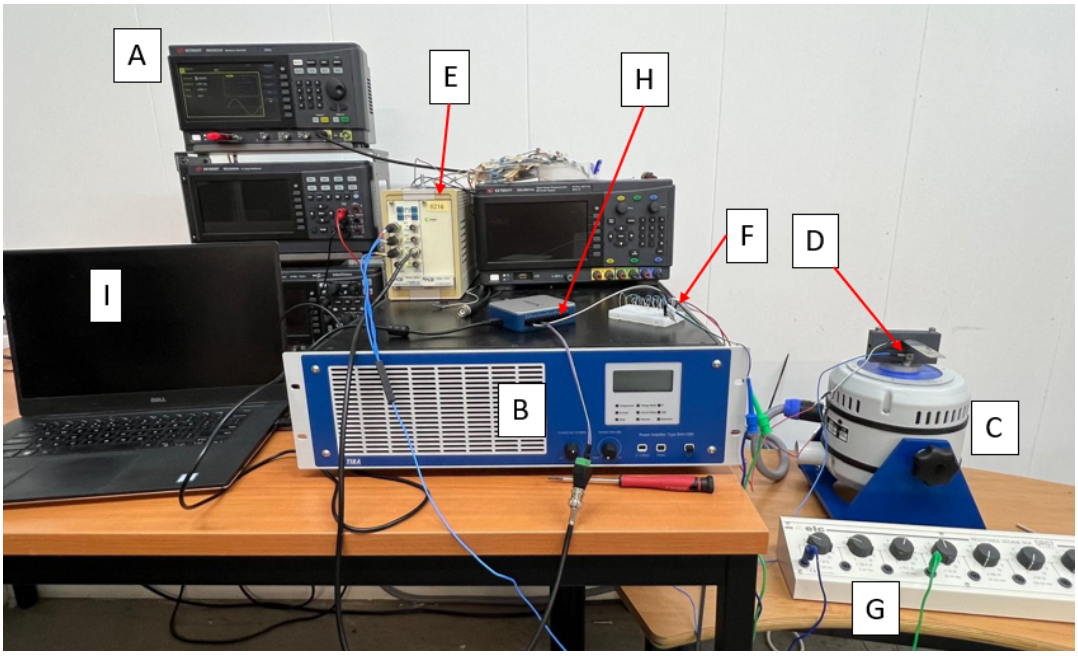


Figure 3.17: Overview of the test setup. A) Signal generator, B) Amplifier, C) Shaker with cantilever mount, D)Accelerometer, E) Accelerometer voltage amplifier, F)Breadboard, G)Decade resistance box, H)NIDAQ express, I) Laptop.

4

Experimental validation: Stencil printed piezoelectric energy harvesters, a thickness variation

This chapter presents an experimental study analyzing the impact of varying piezoelectric layer thicknesses on power output using stencil printing. It outlines the methodology for fabricating and evaluating these harvesters, assessing their performance in terms of power generation. Together with the potential fabrication constraints and findings after putting the harvesters in operation.

"Nothing is real unless it is observed"

John Gribbin

Stencil printing piezoelectric KNLN-epoxy layer for energy harvesting, an experimental thickness to power validation

S.C. Kooiman S.c.kooiman@student.tudelft.nl

Abstract — **Piezoelectric vibrational energy harvesters (PVEHs) provide a sustainable alternative for powering small devices by converting ambient vibrations into electricity. Despite their potential, commercial applications remain limited due to scalability and reliability challenges. This study investigates stencil printing to fabricate piezoelectric composite layers, focusing on how layer thickness affects power output. Experiments show that thinner layers (up to 0.25 mm) generate significantly more power than thicker layers, likely due to better mechanical impedance and fewer defects like cracks and delamination. The highest-performing samples produced power an order of magnitude lower than conventional piezoelectric buzzers. However, this method shows promise for optimising design parameters like thickness and shape, with further research needed to enhance material properties and better-controlled fabrication techniques. The conclusion highlights stencil printing as a feasible method for creating PVEHs, directly integrating the piezoelectric material (PEM) with a resonator, with current limitations mainly due to fabrication inconsistencies.**

4.1. Introduction

Energy harvesting involves converting ambient energy into electrical energy, utilizing sources like solar power, wind, and hydro. Piezoelectric energy harvesters (PVEHs) represent a method of transforming ambient vibrations into electricity. Ideal for powering small, remote, or numerous devices. Devices which currently require batteries. Millions of batteries pose logistical and environmental challenges in a digital era where the demand for data and sensors is rapidly growing. PVEHs offer a sustainable alternative, harvesting energy from low-frequency vibrating environments (1-100hz) such as trains, motors, and pumps. Using this electricity to power sensors and devices eliminates the need for batteries and enables continuous data collection. Piezoelectric materials are an alternative solution to commonly used energy harvesters. Using the piezoelectric effect, a phenomenon that creates an electric charge under mechanical stress or deformation. This makes them effective in vibrational energy harvesting applications, due to the size needed to make these systems work.

Currently, many PVEH are made and tested producing energy in the micro- to milli-watt range.[46] With current sensor applications requiring the same amount of energy. But still, no systems powered by these harvesters are commercially available. Highlighting, multiple steps still need to be taken to get these devices from promising to actual power sources. One of these steps is making the fabrication of these harvesters better optimised for large-scale production, remaining high in power output and making it possible to apply certain design parameter optimisations. One of the often-used solutions is a design covered with pre-made piezoelectric transducers. Mostly cheap and widely available transducers called buzzers, used for creating sounds, shown in Figure 4.1 are used. These harvesters consist of a substrate glued together with a buzzer, which includes top and bottom electrodes. These buzzers produce sufficient power but are hard to work with, difficult to change in dimensions and contain lead, which is very toxic and bad for the environment. They are produced in high-tech facilities under enormous pressures, a controlled environment and high temperatures.

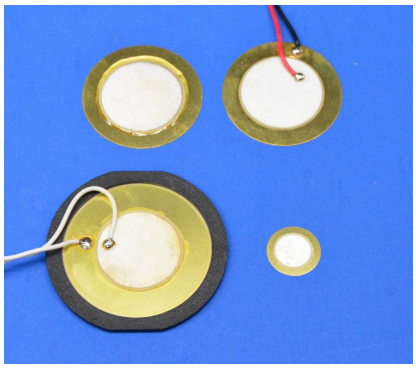


Figure 4.1: Piezoelectric transducers, commonly used for buzzer/speakers. Being a cheap and widely available source of piezoelectric material for energy harvesters.[47]

A promising fabrication strategy is stencil printing, a planar fabrication method to print piezoelectric material in certain shapes, thicknesses and locations. A stencil covers certain areas of a substrate, followed by striking a viscous substance over the stencil and covering only certain spots to be covered with material, as shown in figure 4.2. Stencil printing is a widely used technology in a lot of industries. It is highly reproducible, can cover large areas, and provides multiple changeable design parameters such as thickness, shape, and location. Also, it is a faster and easier method to test certain design optimisations because parameters are easier to adjust. [48]

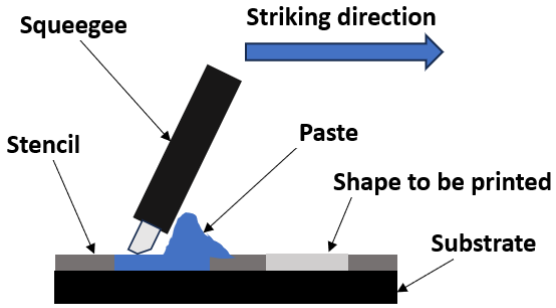


Figure 4.2: Stencil printing working principle.

To use stencil printing for piezoelectric material, it is not preferred to use high curing and brittle piezoelectric ceramics. These materials are hard to work with and are difficult to make liquid. Combining piezoelectric ceramic particles with a polymer creates a more easy-to-work-with material, and piezoelectric properties remain high compared to the use of piezoelectric polymers. Creating a piezoelectric composite containing KNLN3 particles inside an epoxy or polymer matrix combines these 2 wanted properties and already has some proven methods [40], [39]. The remaining challenges arise in applying stencil printing onto energy harvesters, thereby integrating the two separate systems. The effect on the total producible power of this composite applied on energy harvesters is still unknown; the method's limitations need to be discovered, and the influence of layer thickness on the output can be discovered.

Seeing stencil printing as a promising and feasible fabrication strategy, the focus of this study is: **Analysing the influence of layer thickness of a stencil-printed piezoelectric layer on the total power harvested by a piezoelectric vibrational energy harvester**

In section 4.2, the method used to develop, fabricate and experimental validate the piezoelectric energy harvester performance. Then, in section 4.3, the results of the theoretical model and experiments are given. As follows, in section 4.4 the results, main findings and limitations of this study are discussed. The conclusion is drawn in section 4.5.

4.2. Methodology

This section elaborates on the methods used to develop, fabricate, test and analyse different thicknesses of stencil-printed layers on cantilever substrates. And how this influences the power of a linear energy harvester. This is also compared with a linear harvester with a piezoelectric buzzer. First, a theoretical model of the mechanical and electrical optimal thickness is explained. As follows, the detailed fabrication method to produce the different sizes is given. As follows, the test setup to experimentally validate the performance is presented. The total structure is seen in figure 4.3.

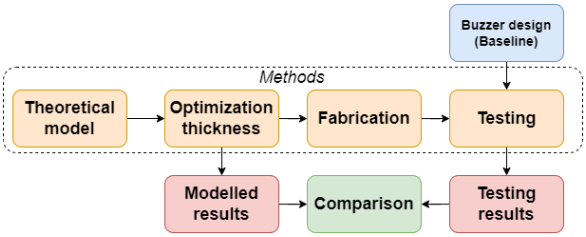


Figure 4.3: The methodology structure; combining theoretical modelling, fabrication strategy and testing of the produced energy harvesters to analyse the effect on power harvested.

4.2.1. Theoretical model

The developed theoretical model allowed for a better understanding of the effect of different design parameters on the generated power. Also, theoretical constraints and boundary conditions are taken into account. This makes it possible to see the correlation between the applied piezoelectric material, mechanical resonance system and the power output. Starting with the input constraint and the piezoelectric energy harvester coupling factor, including converting mechanical input towards work into the PEM, As follows, the electrical circuit and the required electrical impedance will be discussed.

The total system is modelled as an unimorph cantilever beam, on which piezoelectric material is applied and which is excited at the same force input. The total input force needs to be equal to get an equal representation for the different sizes of harvesters. The force is the product of the accelera-

tion input and total mass. With the feedback of the known input acceleration, the input force can be held steady for alternating frequencies. Considering the change in layer thickness does not influence the cantilever's weight much.

The input vibrations cause the cantilever beam to deform, resulting in mechanical strain. The piezoelectric layer converts some of this strain into electrical charge output. The amount of converted energy is called the coupling factor. This coupling factor depends on the substrate and PEM stiffness K_{st} and K_m, respectively, capacitance C_{el} and piezoelectric charge coefficient D. The stiffness determines the total mechanical energy converted towards the piezoelectric material. The capacitance allows for temporary electrical energy storage, with the piezoelectric coefficients defining the size of the created charge. In equation 4.1, the global coupling coefficient is shown, which influences the generated electrical energy $W_{el,gen}$ regarding the input energy $W_{m,in}$ shown in equation 4.2.

$$k^2 = \frac{D^2 k_m}{C_{el}} \tag{4.1}$$

$$W_{el,gen} = (1 - (1 - k^2)^2) \cdot W_{m,in} \tag{4.2}$$

In the unimorph cantilever, the substrate and the piezoelectric material absorb the mechanical input energy. The work applied to the piezoelectric material needs to be maximised to get the most energy out of the piezoelectric material. The cantilever beam and its printed layer can be modelled as a spring-mass system, with the two layers modelled as 2 parallel springs. In figure 4.4, the modelled spring system is shown, with the maximal work in k_m occurring when $K_{st} = K_m$. The rest of the cantilever is modelled in series and is an additional constant regarding the change of the piezoelectric layer thickness. This is in further modelling not taken into account, and in the model, the beam is completely covered with PEM. When the stiffness of the PEM becomes bigger, the neutral axis of bending will be shifted in this layer, which causes internal cancellation of the electric field. With this mechanical effect, the effective coupling coefficient depends on this stiffness ratio α seen in equations 4.3 and 4.4. [49]

$$\alpha = \frac{k_m}{k_m + k_{st}} \tag{4.3}$$

$$k_{eff}^2 = \alpha \cdot k^2 = \frac{k_m}{k_m + k_{st}} \cdot \frac{D^2 k_m}{C_{el}} \tag{4.4}$$

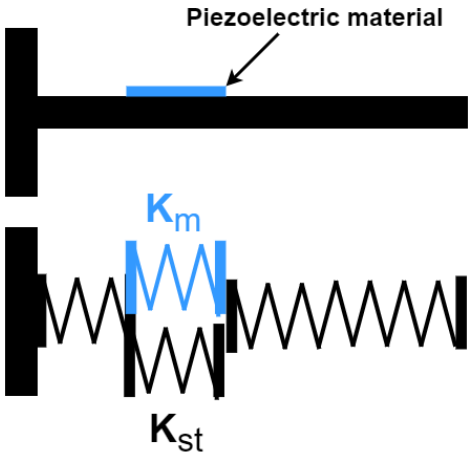


Figure 4.4: Parrelel spring work real situation; however, for modelling, it is assumed the whole beam is covered with PEM.

An optimal printed layer stiffness relative to the substrate layer must be achieved to maximise mechanical impedance. This maximises the conversion of mechanical energy into the piezoelectric material, resulting in the highest possible coupling factor. Influential parameters on the effective layer stiffness are the young modulus, dimensions, and neutral axis location. In this paper, only the thickness t will be altered. With a known substrate, the optimal thickness of the printed layer can be derived by plotting the substrate's effective stiffness and the printed layer's effective stiffness dependent on thickness t. In equations 4.5, 4.6, and 4.7, the effective stiffness calculations dependent on thickness are shown. Making use of the neutral axis theorem.[50] With the Neutral-axis Y_{NA} and the centre line of the two layers as y_1 and y_2, A_1 the area of the substrate, b the width and t the thickness of the PEM. E_1 and E_2 being the Youngs moduli of the substrate and PEM. The Halpin Tsai model approaches the Youngs modulus of the used piezoelectric composite, resulting in $21GPa$. [51]

$$y_{\text{NA}} = \frac{(E_1 A_1 y_1) + (E_2 b t y_2)}{(E_1 A_1) + (E_2 b t)} \tag{4.5}$$

$$I_{NA} = \frac{bt^3}{12} + A|y_c - y_{\text{NA}}|^2 \tag{4.6}$$

$$K = \frac{3EI}{L^3} \tag{4.7}$$

This correlation states no limitation of converting mechanical energy towards power. An infinitely stiff substrate would require an infinitely thick layer on top and still follow the thickness optimum regarding the coupling factor. However, there are two boundary conditions. First, the maximum

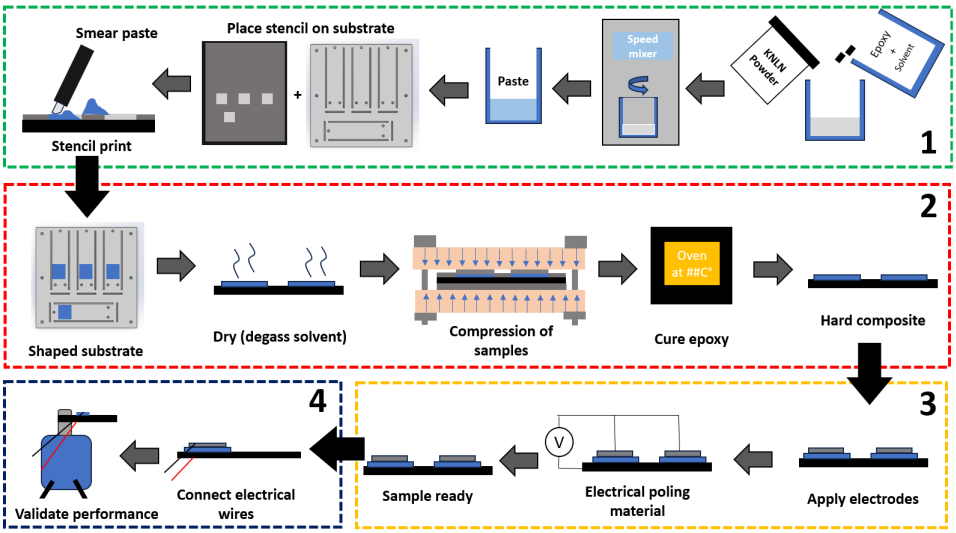


Figure 4.5: Schematic overview of the fabrication method.

stress in the piezoelectric layer limits the thickness. Being as close to this limit to harvest the most power, but stay under this limit to prevent failure of the material. Secondly, the input acceleration is a boundary condition; when this stays the same, the stress in the piezoelectric material scales with t^{-2}. This indicates that thicker layers will produce lower peak stresses with the same input.

With the mechanical stress converted into an electrical potential, the electrical circuit influences the maximum power. Piezoelectric capacitance and resistance do influence the impedance of this system. A model to simulate the optimal impedance load is used to estimate the required load resistance. Across this load resistance, the voltage is measured, and the peak and average power are calculated. The eigenfrequency of the design determines the frequency input. The electrical circuit helps determine the optimal resistance load (R_{load}) for the maximum power. [52]

The total electrical impedance of the internal piezoelectric system is stated in equation 4.8. With the effect of thickness on the resistance and capacitance, equations 4.9 and 4.10 are submitted in the total impedance seen in equation 4.11. Giving the correlation between impedance magnitude and the thickness of the piezoelectric layer. Seeing that a thicker sample needs a higher resistance load. For this study, parasitic losses of the piezoelectric material are not taken into account. And electrical impedance is just used to validate the power at optimal performance. A test will be performed to validate the modelled impedance resistance. This is further explained in the section 4.2.3.

$$|X| = R + j\left(\frac{1}{2\pi C\omega}\right) \tag{4.8}$$

$$C = \frac{\epsilon_r \epsilon_0 A}{t} \tag{4.9}$$

$$R = \frac{\rho_e t}{A} \tag{4.10}$$

$$|X| = \left(\frac{\rho_e}{A}\right) t + j\left(\frac{1}{2\pi \frac{\epsilon_r \epsilon_0 A}{t} \omega}\right) \tag{4.11}$$

R is the resistance (Ω), C the capacitance (F) and X the impedance magnitude (Ω). f the excitation frequency (Hz), ϵ_r and ϵ_0 relative permittivity (F/m) of the sample and air and ρ_e resistivity (Ωm). Dependent on dimensions A and t being area and the thickness(m).

4.2.2. Fabrication strategy

A method was designed and performed to fabricate stencil-printed layers onto a 0.2mm stainless steel substrate. By iteratively changing different parameters and encountering limitations of different substeps, the fabrication method is as follows and can be seen in figure 4.5.

The stencil print fabrication method begins with preparing the substrate, which involves cleaning with acetone and grinding horizontal, vertical, and diagonal passes using 80-grid grinding paper. This is followed by another round of cleaning with acetone to ensure a clean surface. Next, the materials, Epotek Epoxy A and B, are combined, with amounts precisely weighed; specifically, 2g of Part A is mixed with 0.2g of Part B. This mixture

is then subjected to a Speedmix process at 3000 RPM for 5 minutes. Subsequently, 2g of ethanol, representing 50% final volume, is added and mixed at 3000 RPM for 5 minutes. The next step involves adding KNLN3 powder to the mixture, making up 60% of the epoxy-powder volume, and mixing it at 1000 RPM for 5 minutes.

Following this, stencil printing equipment is assembled by placing the substrate, TPU98 seals [0.0; 0.15; 0.30mm], and stencil inside the printing clamp. Different thicknesses of the stencil [0.1; 0.25; 0.5; 0.75; 1.00mm] are used to vary the thickness of the sample. The epoxy paste is then generously applied to the stencil plate and carefully smeared into the desired shapes, after which the stencil is removed. The substrate is left to dry at room temperature for 1 hour, allowing solvents to evaporate. A visual inspection is done to make sure the samples are completely dried. Then, the assembly is done before the curing process of the composites is done. Anti-stick foil, compression shapes and additional side plates are then placed, and the system is compressed with beams and torqued with bolts. This assembly is then baked in an oven at 70°C for 1 to 2 hours, a period during which the epoxy is cured.

For electrode application, an aluminium electrode tape is applied in 20x20mm sections on the cured sample. Subsequent steps include cutting out the samples using steel cutters, cleaning the flexures by scraping off misplaced paste while using acetone and measuring the thickness of each sample. A set of 9 measurements of each sample is performed to get a better view of the fabrication precision, done with a micrometer Mahr 40ER

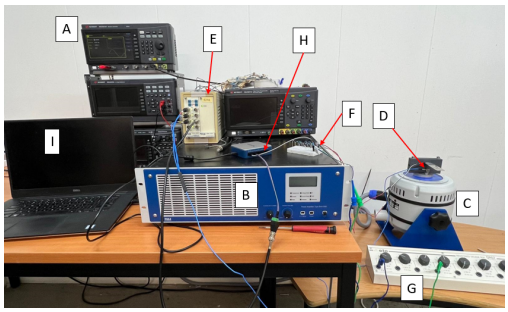
The poling process involves placing the samples in a poling device submerged in a silicone oil bath preheated to 130°C. After a 2-minute warm-up, the voltage slowly increases to 7.5 kV/mm and is maintained at this peak for 6 minutes. Following this, the heating is turned off, and after 15 minutes, the voltage supply is also discontinued. Samples are removed from the bath and cleaned of oil residues using acetone and paper towels.

Finally, each sample's D_{33} value is measured with a PiezoMeter System PM300 to ensure proper piezoelectric properties. Also, the capacitance and resistance are measured with an Agilent 4263B LCR meter. Eventually, wires are connected with aluminium tape to complete the fabrication process.

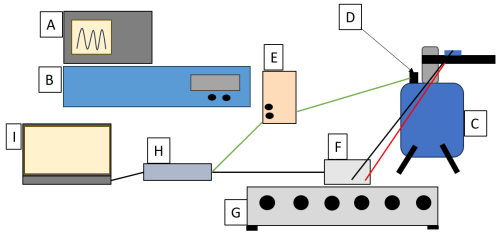
A cantilever embedded with a piezoelectric buzzer is made with the produced samples. Done by preparing the substrate, which involves cleaning with acetone, grinding in the again 4 directions. using 80-grid grinding paper, followed by another round of cleaning with acetone to ensure a clean surface. Epoxy (AP universal EP 2K epoxidharzklebstoff) is used to glue the substrate and buzzer together. The same area is used with stencil printing as the piezoelectric area of the buzzer.

4.2.3. Testing

An experimental setup is designed to evaluate the stencil-printed energy harvesters' power performances. The dynamic testing setup involves a Tira shaker TV51140 setup and an accelerometer PCB356B21 measuring the input acceleration. The voltages are measured with a NIDAQ-USB6002 and stored with NIDAQ software. The voltages U created by the energy harvester are measured across the load resistance R and are used to calculate the power [watt]. Figures 4.6a and 4.7 show the real and schematic test setup. Power is calculated as equations seen in equation 4.12.



(a) Test setup overview.



(b) Schematic test setup overview.

(c) Overview of the test setup. A) Signal generator, B) Amplifier, C) Shaker with cantilever mount, D)Accelerometer, E) Accelerometer voltage amplifier, F)Breadboard, G)Decade resistance box, H)NIDAQ express, I) Laptop.

$$P = \frac{U^2}{R} \tag{4.12}$$

For each sample, 3 tests will be performed to ensure all designs can be compared fairly. At first, an eigenfrequency evaluation is made. Then an analysis for the optimal load resistance is done,

a resistance where the harvested power is at a maximum. At last, an average power test is performed at eigenfrequency and optimal load. Using these steps, all measured power is at the optimal power of the sample, making it a fair comparison. Multiple-sized systems will be tested to compare their performance. Samples with piezoelectric layers between $[0.05 - 0.66mm]$ are evaluated and compared with a cantilever with a buzzer.

Eigenfrequency evaluation
The overall system eigenfrequency is caused by the cantilever resonance frequency and all electrical circuit influences and is the best-performing frequency at lower frequencies (0-100hz). A frequency sweep is performed around the eigenfrequency with a modelled optimal load, and the power is measured to determine the eigenfrequency.

Load resistance
The optimal load resistance is determined by iteratively changing the resistance value. An optimum is found between the measured voltage and current at the used resistance, resulting in the highest power.

Acceleration power correlation
The total power measured at different excitation accelerations allows us to compare input energy to generated electrical energy (power), which can be compared between all different samples.

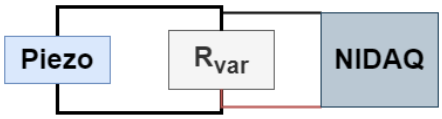


Figure 4.7: Electrical circuit to measure output voltage, across R_{var} the variable resistance of the decade box.

4.3. Results

This section gives the results of the theoretical models, fabricated systems and overall performance regarding measured properties, eigenfrequencies, optimised load resistance and power. The visualized results of the fabricated systems are shown.

4.3.1. Modelled results

With different printed heights, the stiffness of the piezoelectric layer increases. To match the mechanical impedance of the composite piezoelectric layer with the created substrate layer an optimization of the effective stiffness can be seen in Figure 4.8. To convert as much mechanical energy into the piezoelectric layer, a thickness of **0.19mm** is desired regarding the coupling factor.

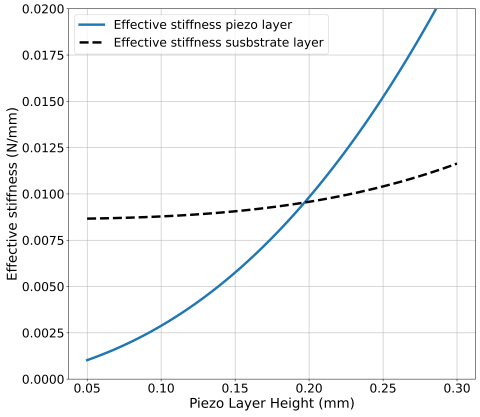


Figure 4.8: Effective stiffness optimization with variable piezoelectric layer thickness.

The electrical impedance modelling has been performed to find an initial optimal resistance load, and the optimization is compared with the tested systems at their eigenfrequency. The R_{load} values are shown in table 4.1

4.3.2. Fabricated samples

Equally sized stainless steel cantilevers (substrates) are made, with dimensions 110x25x0.2mm. With an eigenfrequency of 16.2hz. On one substrate, a buzzer (r=20mm) has been glued with 'type' epoxy. 9 substrate beams are made with a printed piezoelectric material squared area of 22x22mm. All properties and stats of the harvesters made are shown in the table 4.1 (two pages below). The samples are made with different thicknesses in the first batch, a wider range (0.21 - 0.67mm) is made. A second batch is made in the lower range (0.05 - 0.35mm).

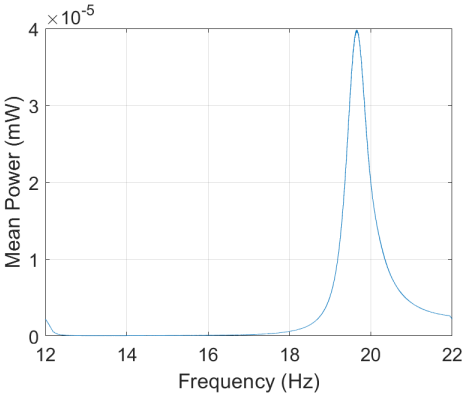


Figure 4.9: Power-frequency analysis for sample J01

The frequency–power analysis is done by deter-

mining eigenfrequencies of all samples, as seen in figure 4.9 for sample J01, this is done at their modelled resistance load at a $3m/s^2$ input acceleration.

4.3.3. Comparison fabricated samples

The max and average power of the fabricated samples measured at their eigenfrequency and optimised resistance for different acceleration inputs are shown in Figure 4.13 (one page below). At higher acceleration, the power of samples I-03, I-04, J-02 and J-03 decreases.

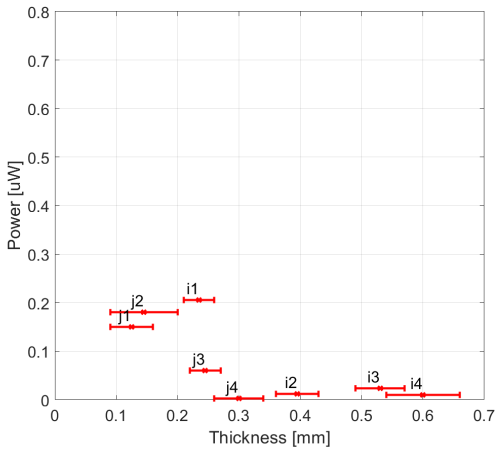


Figure 4.10: Average power of different sized samples, measured at 1G.

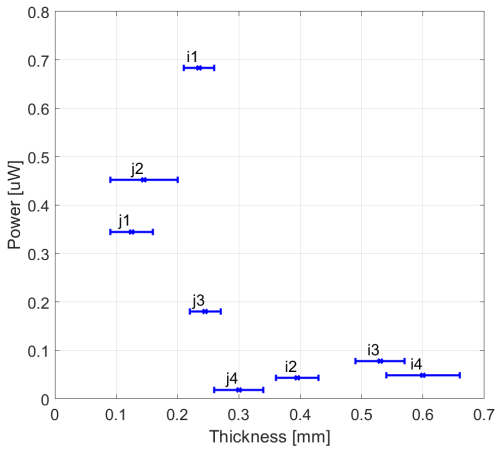
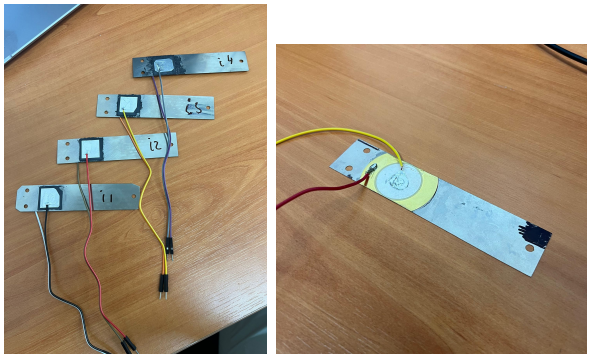


Figure 4.11: Average power of different sized samples, measured at 1G. **Scaled with optimal load ratio, for optimal power.**

The average power at $a = 1G$ of different sample thicknesses is shown in figure 4.10. Thicker samples generate approximately ten times less power than thinner ones. This disparity is largely due to fabrication limitations, such as increased cracking and porosity in thicker layers. Additionally, thicker samples may have poorer mechanical-to-electrical conversion efficiency. In figure 4.11 the average power results are shown with the ratio factor to analyse the power at optimal load resistance.

4.3.4. Visible results

During the fabrication process of the stencil-printed PEVH, the in-between sample status alters. The printing, drying and curing conditions have a great influence on the physical representation of the sample. The type and quantity of solvent especially influence the viscosity of the material during printing, the amount of time needed to dry, and the created cavities and cracks. Visual inspection between the steps is shown in the appendix. The thickness range of the samples can be seen in table 4.1. The fabricated buzzer cantilever design can be seen in figures 4.12a 4.12b



(a) Samples I after fabrication with connected wires.

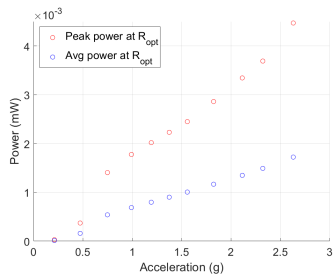
(b) Buzzer cantilever sample, glued together. (BU-01)

Figure 4.12: Fabricated samples

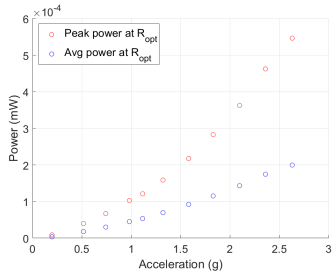
Sample ID	Thickness $[mm]$	*Avg Power $[\mu W]$	*Peak Power $[\mu W]$	D33 $[pC/N]$	C_p $[nF]$	R $[K\Omega]$	ω_n $[hz]$	Optimal load resistance $[M\Omega]$	Ratio
Solo1	-	-	-	-	-	-	16.2	-	-
Bu-01	-	880	1900	260	84	18	23.8	0.1	-
I-01	0.21-0.26	0.683	1.76	7	0.18	320	19.2	10	3.33
I-02	0.36-0.43	0.043	0.1	14	0.14	410	19.8	16.8	3.6
I-03	0.49-0.57	0.078	0.13	14	0.113	560	19.0	40	3.31
I-04	0.54-0.66	0.0485	0.165	7	0.105	670	19.0	40	5
J-01	0.09-0.16	0.348	0.633	5	0.17	222	19.6	42	2.3
J-02	0.09-0.21	0.452	1.0	5	0.18	200	19.0	29	2.51
J-03	0.22-0.27	0.18	0.42	8	0.1	320	20.7	43	3
J-04	0.26-0.34	0.0188	0.044	18	0.11	490	19.9	40	6.26
J-00	0.05-0.11	0	0	-	0.23	137	-	-	-

Table 4.1: Fabricated systems properties and test results.
*Peak and average power are measured with 1G input acceleration at eigenfrequency. And are multiplied with the power ratio to show power at optimal resistance.
The power ratio is shown in appendix G.3.

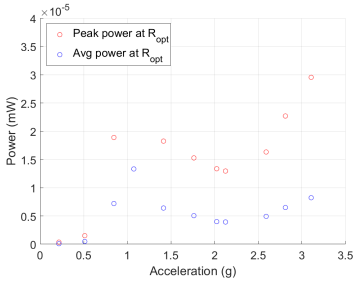
.



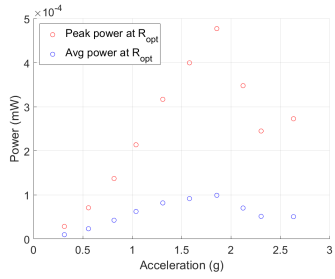
(a) Sample I-01 at R = 10 $M\Omega$, ratio = 3.33



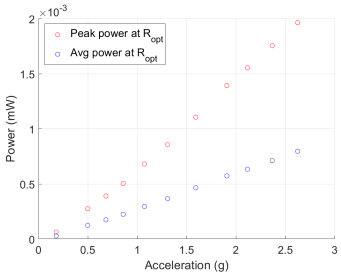
(b) Sample I-02 at R = 16.8 $M\Omega$, ratio = 3.6



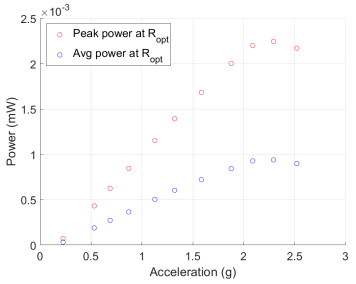
(c) Sample I-03 at R = 40 $M\Omega$, ratio = 3.31



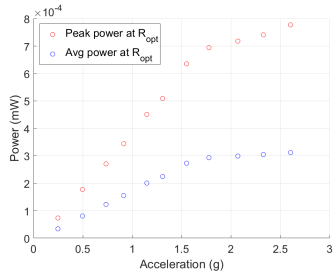
(d) Sample I-04 at R = 40 $M\Omega$, ratio = 5



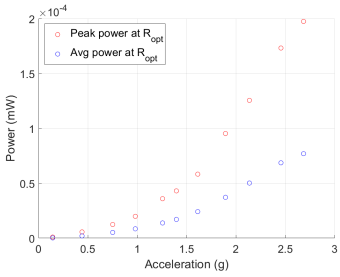
(e) Sample J-01 at R = 42 $M\Omega$, ratio = 2.3



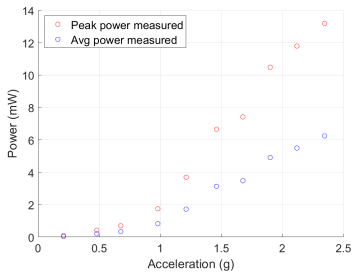
(f) Sample J-02 at R = 20 $M\Omega$, ratio = 2.51



(g) Sample J-03 at R = 43 $M\Omega$, ratio = 3.0



(h) Sample J-04 at R = 40 $M\Omega$, ratio = 6.26



(i) Buzzer (Bu-01) at R = 102$K\Omega$

Figure 4.13: Power measured at different accelerations for different samples, at their eigenfrequency. Measured and multiplied with optimal resistance factor (ratio). **NOTE: Y-axis magnitude may differ per figure.**

4.4. Discussion

This section will provide a detailed discussion based on the results, addressing the research question and analysing the effect of the thickness of a piezoelectric layer on the total harvestable power.

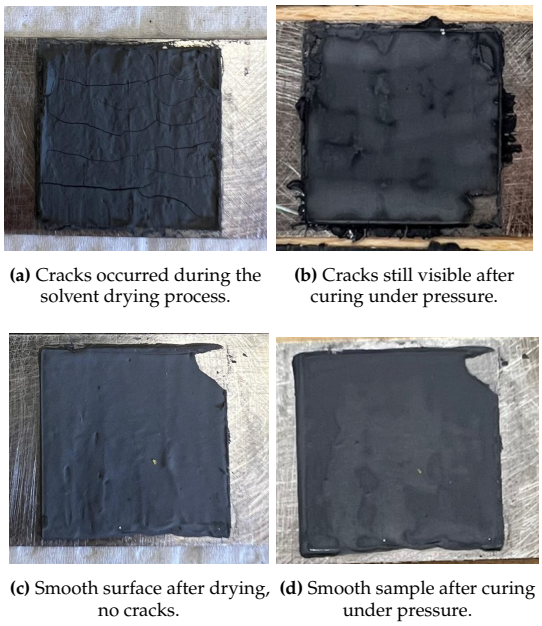
4.4.1. Feasibility stencil-printing

The feasibility of using stencil printing to fabricate piezoelectric materials (PEM) directly onto energy harvesters is demonstrated. Multiple samples were produced using this method, showing that stencil printing can be used for alternating thickness, shape or location. The main challenges arise in creating uniform samples free of cracks and with low porosity. Due to the need for a liquid paste for the stencil printing process, the amount of solvent was of great importance. The type and quantity of solvent influence the drying and curing process of the samples. In thicker samples, this resulted in more cracks due to longer evaporation time and bigger cavities. In figure 4.14a, cracks can be seen after the drying process. During compression, not all cracks could be restored. Especially underneath the surface, some cracks remained as seen in Figure 4.14b, creating air gaps inside the samples. In figures 4.14c and 4.14d, a thinner sample without cracks can be seen; however, this sample does have a nonuniform layer and is more porose in the middle. The variation of the thickness is large, indicating a shortcoming in the current fabrication method's precision [0.05 - 0.15mm]. During the poling process of the samples, cracks and porosity limit the magnitude of applied voltage. Preventing reaching high electric properties, especially the D_{33} value, which is of great importance. Despite these challenges, multiple samples have been created and tested. Indicating thinner samples are preferred regarding fabrication.

4.4.2. Thickness and power

Despite not all samples being uniform, without cracks or well poled to high piezoelectric properties. All samples except for one produced a charge output resulting in power, one failing due to failed fabrication (a short circuit during poling). The thinner samples produced up to a factor of 10 more power than the thicker ones. Samples around 0.19mm produced the highest power, which overlaps with the modelled mechanical impedance optimum. An optimum regarding the maximum amount of work converted from total mechanical input to mechanical energy in the piezoelectric layer. This result could indicate a better coupling factor is achieved, which causes a higher output. However, due to fabrication dissimilarities and failures, no hard conclusion can be drawn. The fabrication indicates an optimum around this same thickness because thinner and thicker samples are more difficult to fabricate to the same standard.

The optimal load of the fabricated systems is very high due to the low capacitance; this is opted not to be a problem in measuring the power. However, its use as a real-world power source needs to be looked into further.



(a) Cracks occurred during the solvent drying process.

(b) Cracks still visible after curing under pressure.

(c) Smooth surface after drying, no cracks.

(d) Smooth sample after curing under pressure.

Figure 4.14: Produced samples with or without cracks, before and after curing.

The dissipated energy in the piezoelectric energy is mostly influenced by viscoelastic and electrical damping. It is difficult to say what the total influence of this damping is relative to the total damping. If everything is held the same, it can be discussed that viscoelastic and electrical damping increases with more piezoelectric material. However, it is important to say that this doesn't directly correlate to higher power. Damping is one of the main drivers of how much energy is eventually converted from input mechanical energy in the piezoelectric material towards electrical energy and depends on many parameters. The environment of operation is especially important, as this changes between accelerations, frequencies, types of inputs, and other mechanical influences like clamping of the beam.

Delamination of the piezoelectric layer from the substrate was problematic in most thick samples, as seen in figures 4.13c and 4.13d, a reduction in power after certain acceleration. Despite cleaning the substrate and increasing its surface roughness,

the adhesion still lacked the strength to hold the two layers together. With smaller input accelerations, this wasn't a problem; exceeding 1G's, this started to occur. After delamination, voltages were measured again at a lower acceleration, giving lower power than earlier tests at the same acceleration. The delamination of the sample I-04 is shown in figure 4.15. In figure 4.16, cracks under the surface can be seen, causing worse properties and possible earlier delamination. Compared to other literature regarding composites, delamination is often stated as a problem regarding matching certain properties to prevent high stresses at the boundary layers. [53] However, no research was found that explains how to improve this for piezoelectric material integration onto an energy harvester.

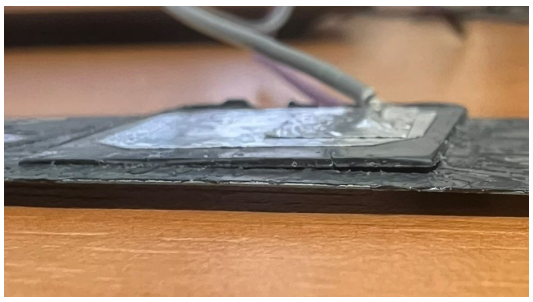


Figure 4.15: Delamination of the piezoelectric layer and the substrate.

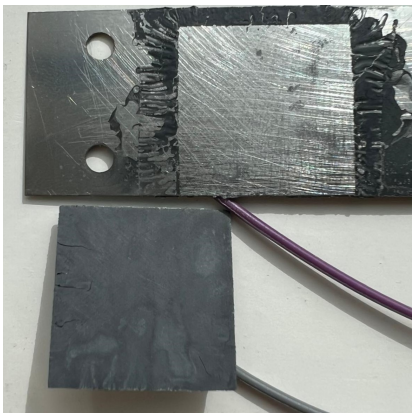


Figure 4.16: After complete delamination, below surface cracks can be seen.

In samples J02 and J03 in figures 4.13f and 4.13g, a plateau can be seen at higher acceleration, possibly the cause of a smaller defect not visible with the eye. However, these samples didn't produce significantly less power with remeasurements at lower accelerations.

Compared with the buzzer transducer, the produced KNLN3 - epoxy samples produced significantly lower power. The average power of the best sample harvesting is 69 μW, 1000 times lower than the sample with the buzzer. The produced samples did not exceed the desired D_{33} values of the created samples. of its proven and modelled values.[1] [54] (shown in appendix G.3.1) Achieving these optimal properties for the current measured samples would already produce a factor 36 more power, presumed a factor 6 increase in D_{33} values would exponentially increase the power output. Accurate measurement or improved fabrication could better compare the produced samples with buzzers.

Because of non-uniform layers, the D_{33} values obtained in the measurements are inaccurate. Thicker parts of the sample are less poled because the electrical field is weaker in the thicker regions. During measurement with the piezometer, the sample is compressed, finding support on the thicker parts, creating a lower charge output and resulting in a lower overall charge per unit force. A visualisation of this problem is shown in figure 4.17.

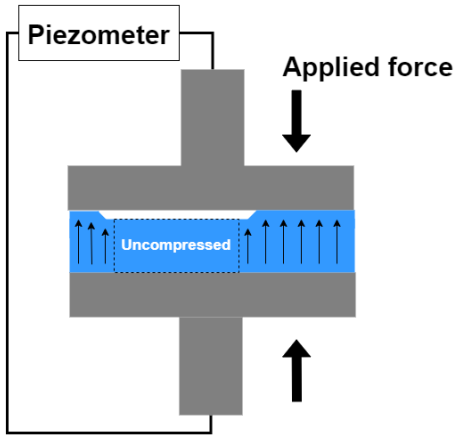


Figure 4.17: D_{33} measurement of non-uniform layer causing lower and inaccurate values. Only the less poled area is compressed during the measurement.

With the current fabrication method, the samples do not produce enough power to be competitive with the buzzers. However, based on the theory of the coupling factor and the voltage output of piezoelectric material, a higher output can be expected. With the use of equation 4.4 and 4.13. The potential of composite samples with PZT buzzer can be made. After keeping all dimensions the same, achieving a higher k^2 for the composites. This is, however, purely based on the relation between charge constant D, the PEM k_m stiffness, and the capacitance C_p. Additionally, the mechanical impedance is easier to optimise with the stencil printed material; thus, the factor α could be closer to 0.5 with this tuned impedance. Solely looking

at the coupling factor doesn't allow us to see the full aspect of piezoelectric energy harvesting, but it gives theoretical potential. In application, other limitations, such as maximum stresses allowed in the material, need to be taken into account. This paper shows the basis for the potential of using stencil printing of piezoelectric composites. When the quality of produced samples is at the same level as that of PZT fabrication methods, denser and uniform samples could be produced, contributing significantly to a better output. [55]

$$\alpha \cdot k^2_{composite} > \alpha \cdot k^2_{PZT} \tag{4.13}$$

Printing piezoelectric directly onto a substrate prevents the use of extra electrodes and epoxy to stick a piezoelectric patch together with a resonator. This has more impact on the stiffness of the harvester and thus its eigenfrequency coming back in the coupling factor α and reducing the effective coupling factor k'. Differences in the printed layer thickness do influence the eigenfrequency, but all stiffness added is in the piezoelectric material itself. Comparison of the eigenfrequencies can be seen in table 4.1.

4.4.3. Limitations and further research

Composite piezoelectric material is commonly used in other literature to integrate material or modify its structure or location. The fabrication methods used to accomplish this require a more user-friendly material because ceramics are usually hard to work with. The poling of these non-regular systems is well researched; however, it has always been difficult to receive the wanted piezoelectric properties. [30] [32]

The overall approach of this paper focuses on fabricating different thicknesses of piezoelectric energy harvesters, validating the power output and trying to find a theoretical and practical optimum. Theoretically, the coupling coefficient depends on the stiffness of the piezoelectric layer and substrate. However, due to the limitations of the fabrication method, no hard conclusion can be given. It only shows a potential optimum. Furthermore, the accuracy of the measured D_{33} value is low. A non-uniform layer prevents proper sample measurements. The variation in the fabrication of the different-sized samples causes cracks and prevents the use of the same poling conditions. Smooth and non-cracked samples are required to validate the thickness study. For a fair comparison, the samples must be poled under the same conditions, resulting in uniform piezoelectric properties.

With the test performed in a certain order, it was not possible to determine the optimal resistance load beforehand. So, first, acceleration tests were done on a set resistance and later multiplied with a power scaling ratio to compensate for the optimal resistance value. Some samples did break down during the acceleration test, preventing the remeasurement of the optimal resistance load value. Therefore, in the next studies, the power measurements should be performed at optimal load.

The fabrication method needs improvements in terms of creating uniform, non-cracked, and high-density layers. This is to improve the piezoelectric properties and mechanical strength of the samples, which would result in a higher power output and be more comparable with each other. This would allow further research to focus on parameter optimisations like thickness optimisation.

4.5. Conclusion

We have found that it is possible to use stencil printing to fabricate piezoelectric energy harvesters and we are able to harvest up to 0.68 μW. It allows for direct integration of the piezoelectric material into the design. And can provide a solution for shape, thickness or location optimisations. The reliability and total performance of the created harvesters are minimal. Being more reliably fabricated for only the thinner layers up to 0.25mm, after which delamination and cracks become major problems. For all samples, porosity and non-uniform thickness are issues, mostly limiting the poling of the PEM.

Fabrication is the major limitation of optimising the layer thickness, and no conclusions regarding the optimised coupling coefficient can be drawn from the results.

For now, the working thinner samples produce only a small fraction of the average power buzzers could produce. Identifying a huge gap to bridge to make stencil printing a KNLN3-epoxy composite competitive. Mainly due to non-uniform created layers with low piezoelectric properties. With theory supporting the potential of applying this method to create PVEHs, **Further research regarding the influence of better properties, smooth surfaces and optimal thickness is needed to start using stencil printing for competitive energy harvesters.**

5

Discussion, conclusion and recommendations

This chapter presents an overview of the research, detailing the processes, findings, and discussions that emerged throughout the study. It begins with a reflection on the initial project objectives, examining how they guided the research and evaluating the extent to which they were achieved stated as successes and critical points. The chapter also includes a personal reflection on the project, offering insights into the challenges faced and the lessons learned. The main conclusions are highlighted, providing a concise summary of the key outcomes. Finally, recommendations for follow-up studies are proposed, suggesting directions for future research to build upon the findings of this work.

5.1. Overview and discussion of research activities

An overview of all the research activities and achievements is shown in Figure 5.1. This project started on the 11th of September 2023 till the 19th of July 2024, a total of 10 months. Fabrication of a total of 45 different samples in a total of 10 different batches resulted in a fabrication strategy. Used to validate the power harvesting capabilities of stencil-printed piezoelectric energy harvesters. Finalising a fabrication manual as a basis for further development, an experimental paper showing a method to validate and potentially optimise the thickness of the printed layer and examine the power output. Comparing the power output to an off-the-shelf-fabricated sample. It also indicates limitations of the fabrication method of the produced designs.

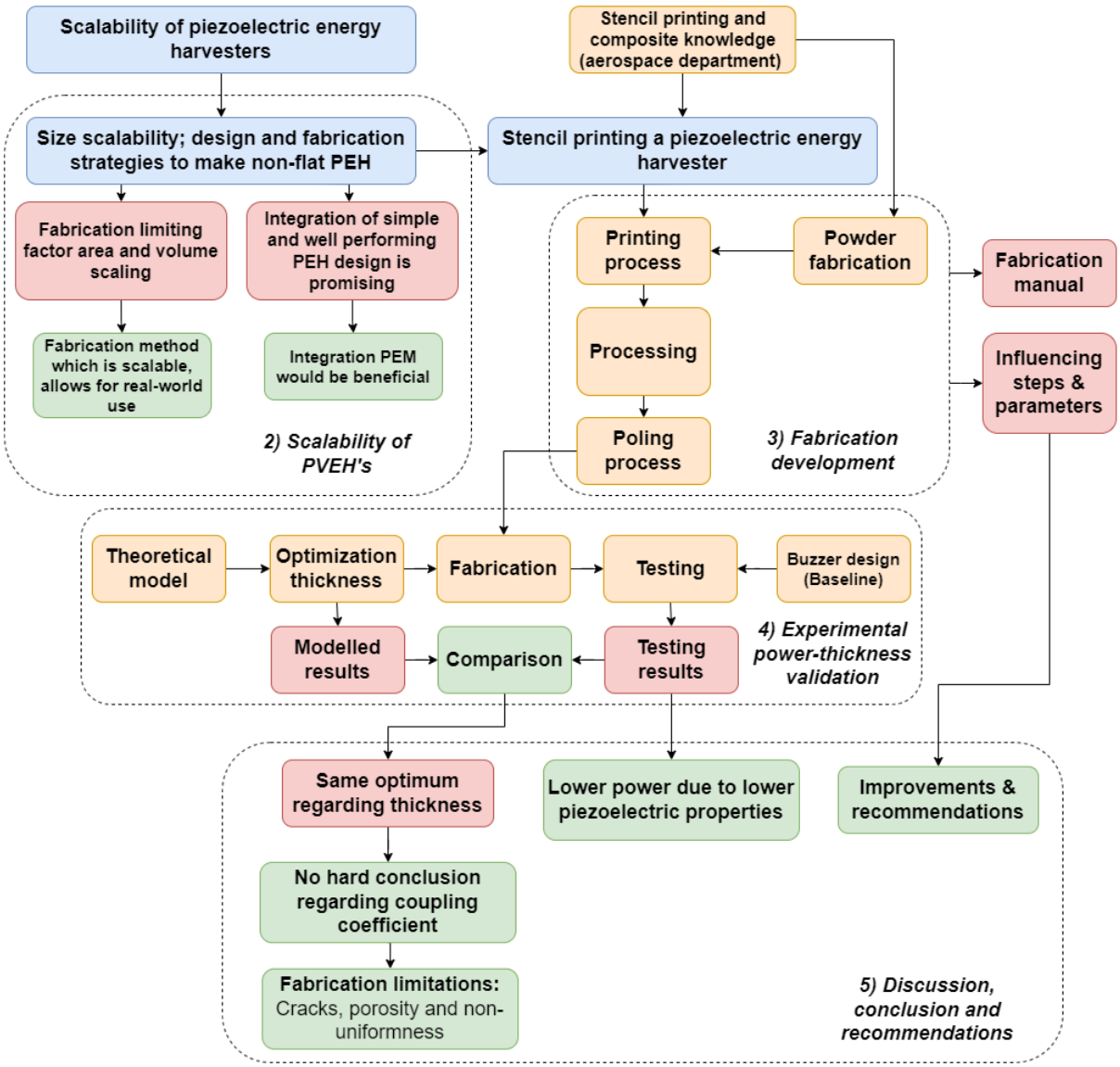


Figure 5.1: A schematic overview of all the research activities and achievements. In blue, the objectives or research direction is shown. The yellow fields contain the knowledge used, methods made or gathered. The red fields are the findings displayed as results. The green fields highlight the main discussion and conclusion findings.

Looking back to the initial objectives of this thesis and to answer the research questions, we can divide the activities into successes and critical points.

***Objective*: Develop, fabricate and test a piezoelectric thick-layer stencil printed composite for energy harvesters.**

Research (sub)questions:

- How does introducing a stencil-printed thick-layer piezoelectric energy harvester affect the total harvested power?
  - What are the limitations of stencil printing?
  - What are potential process optimisations?
  - What is the effect on power by changing the layer thickness?

5.1.1. Successes

The objective to develop, fabricate and test a piezoelectric thick-layer stencil printed composite for energy harvesters was met with significant achievements. Firstly, power was harvested using stencil-printed designs by further developing a stencil-printing method to apply a piezoelectric composite directly onto an energy harvester. The method of fabricating 5 systems manually at once already shows some scalability. However, further optimisation and automation will allow for better scalability. Through systematic experimentation, the research identified key variables that improved the quality of the printed layers, such as drying time, curing pressure and poling conditions. Many fabrication limitations were identified, especially in the use of solvent and the influence on cracks and uniformness. These are identified as the main failure points regarding achieving high piezoelectric properties. A whole experimental study has been dedicated to the effect of layer thickness on power output, using a reproducible method for validating certain systems in the future. This experimental validation highlights the effect of the fabrication shortcomings but provides insight into where the stencil-printed energy harvesters stand regarding other simple designs and their total power. This provides a good basis for further research and easy-to-use fabrication manuals.

5.1.2. Critical points

Despite these successes, several critical points emerged and need further consideration. One of the primary challenges was the complexity of achieving consistent uniform thickness or samples without cracks. Mainly to get higher piezoelectric properties and, thus, potentially receive higher power output. Multiple studies regarding the fabrication of piezoelectric composite face similar problems. Mostly regarding porosity, low piezoelectric properties and breakdown during poling. Porosity was shown as the main cause of reaching lower poling voltages.[30] [32] In other studies, more is worked with prefabricated PZT or prefabricated MFC patches, which are made with high-end industrial machines and have high piezoelectric properties. [56] [57] Looking at theory, piezoelectric composites could be comparable to using these pre-made systems. However, further development is needed to improve fabrication.

A more systemic approach would allow us to draw harder conclusions regarding the fabrication development. Now, the parameters influencing the fabrication outcome are found, but how they correlate and how much they influence are not to be said. A better structured parametric study would benefit further development of this method.

Also, smaller inconsistencies during the final fabrication influence the end product, making the validated systems less comparable due to small differences. More consistent fabrication is required to analyse the optimal thickness of a piezoelectric layer. Also, more possible influences must be considered instead of only looking at the mechanical coupling coefficient and electrical impedance.

Regarding improving scalability, the optimisation of the whole process is a major improvement point. Creating samples manually shows the feasibility and potential, but further research in optimisation is needed to be more scalable.

5.2. Reflection

"It's relatively easy to make a prototype but extremely difficult to mass manufacture (vehicles) reliably at scale."

Elon Musk

The journey of my thesis project started with a discussion about manufacturing piezoelectric energy harvesters. I wanted to focus more on this side of the field because fabrication could often be seen as a limitation for upscaling, meeting design requirements or is generally hard to reproduce. In other words, a lot could be discovered here, and it would definitely be a challenge. Starting with a more in-depth search into literature, a better understanding of what was done, what worked and what didn't was created. However, beginning to develop or improve a fabrication method from nothing felt like looking for a needle in a haystack. Luckily, I came in contact with some amazing people in the Aerospace faculty. Who had experience making and applying piezoelectric materials. This really boosted my motivation and, thereby, knowledge of the fabrication of PEM by giving me the tools, spaces to work, and fundamentals in terms of methods or nice discussions.

The fabrication process was a hands-on learning experience, often taking the most time and requiring repeating the same steps to alter other small things. Sometimes, riding back and forth between the Aerospace, YesDelft, and ME buildings multiple times daily. And quite often figuring out that, again, another batch had failed, often in only 1 specific thing: Cracks! The long hours in the lab really provided me with a lot of knowledge about stencil printing and the fabrication of piezoelectric composites. It reminded me that doing things is often the best way to learn but definitely not always the most fun way. Using this development style, it was important to strictly keep track of all changes and different things I tried. I also continually had to look back and reflect on what went wrong and how it could be improved. With the danger of losing sense of time, it was necessary to plan hours or be reminded that the theoretical background was also important.

The way of validating started with understanding piezoelectric materials and how they convert kinetic energy into electrical output. A more mechanical focus has been chosen here to look at the influences of different parameters. A possible way of finding an optimum regarding the layer thickness. Seeing enormous amounts of fundamental literature made me conclude one thing: the piezoelectric energy harvester field is far from completely known. This makes it more attractive to validate different steps and produce samples experimentally. Because theory never explains everything before it really happened.

Making stuff requires more planning than anticipated. Especially when ordering special materials or custom designs, with delivery times up to 10 weeks. Time management allowed me to keep track of the things that did matter at a certain point. It was also a whole new experience to manage such a big project all by myself.

In the end, more than 40 samples are fabricated, and 10 samples are experimentally tested on a shaker. It does not provide the hoped power outputs but provides an amazing learning experience with a fundamental contribution to the use of the stencil printing method. With definitely some great recommendations for further research, seen in section 5.4.

5.3. Conclusions

This thesis has demonstrated the feasibility of using stencil printing to fabricate piezoelectric vibrational energy harvesters capable of harvesting up to 0.68 µW. The developed and improved fabrication steps allow the application of piezoelectric composite material directly onto a stainless steel substrate, providing opportunities for multiple design parameter changes and potential optimisations. This study spans fabrication techniques to theoretical analysis and experimental validation, offering a full-circle perspective on the energy harvester's power output.

Despite the promising results, the power output remains low compared to commercial buzzer samples. The primary challenges identified include porosity and cracks in the piezoelectric layers, which hinder high-density samples and result in non-uniform and low piezoelectric properties. These defects significantly impact the device's performance, limiting its power output. While other studies on piezoelectric composites have encountered similar issues, few have directly compared them with alternative methods.

The exploration of the coupling factor of the mechanical impedance of the layers showed potential for optimising energy transfer. However, due to fabrication limitations, no definitive conclusions could be drawn. We have seen that samples around this optimum perform better, but this is probably mostly due to cracks and non-uniformity in the piezoelectric layers, thereby reducing the overall efficiency of the energy harvesters.

The findings highlight the importance of surface treatment and precise control over the deposition and curing processes to minimise defects. The provided fabrication manual and identified improvements form the basis for a set of recommendations to enhance the performance of stencil-printed piezoelectric energy harvesters. Key recommendations include optimising solvent selection and drying conditions, implementing controlled curing protocols, and ensuring uniform poling conditions to achieve consistent piezoelectric properties.

While the current stencil-printed piezoelectric energy harvesters show potential, significant challenges need to be addressed to improve their performance. Future research should focus on refining fabrication techniques to reduce defects, exploring alternative materials and designs, and conducting comparative studies with other fabrication methods. Addressing these challenges will pave the way for more efficient and reliable piezoelectric energy harvester fabrication, contributing to advancing sustainable and portable power sources for various applications.

5.4. Recommendations

During and after this research, the main results concluded in many findings. The major findings show promise for further research and better validation of the potential of using stencil printing to create piezoelectric energy harvesters. Also, some tips and tricks are stated, which I wanted to know before starting.

5.4.1. Future research objectives

As shown in previous chapters as discussion and conclusions, the quality and precision of created piezoelectric layers could be improved. Mainly, the porosity, cracks and uniform thickness prevented the use of high poling voltages and resulted in lower piezoelectric properties. Some improvement research directions are listed below:

- **Creating high-density, uniform piezoelectric layers:** To really show the potential of using stencil printing to create high-performing piezoelectric energy harvesters, it is required to have smooth, high-density samples to test. This can be done by looking at the effect of solvent and porosity and using a vacuum or higher and better-controlled pressure during curing, with the overall precision of the samples in mind.
- **Improving piezoelectric properties:** Looking at fabrication steps or material used to enhance the total piezoelectric properties. Consider using high-temperature epoxy to pole at higher temperatures (near piezoelectric curing temperature). Or combining different methods to increase max voltage output or maximum allowable stresses.
- **Discover the effect of different materials:** A lot of other epoxies or piezoelectric fillers are

available, with the theoretical effect of each material property assumed as known. It is interesting to see the effect of different properties on the power output.

When the major issues regarding uniform, non-cracked, and dense samples are solved, the power output is indeed closer to the theoretically possible value. Multiple interesting follow-up researches are:

- **Optimisation of piezoelectric layer; position, thickness and/or shape:** When fabrication isn't the limiting factor anymore or when uniform, smooth samples can be fabricated consistently, stencil printing allows for modifying shape, thickness and location. This gives the opportunity to discover optimisations of the application of the piezoelectric material onto a piezoelectric energy harvester.
- **Stencil-printing piezoelectric layer on a 3D-shaped surface:** Cantilever beams work only at a small frequency bandwidth; however, bistable mechanisms show more promise in the range of their operations. These systems' surfaces are shaped outside the 2D plain and, therefore, would benefit from an applied layer in this state to get maximal deformation out of the piezoelectric material.
- **What is the long-term effect on the performance of piezoelectric composites:** Aging and mechanical fatigue are 2 effects limiting the performance of piezoelectric material after multiple cycles or amounts of time. A better understanding of the effect of these two on piezoelectric composites would highlight the preference for using piezoelectric composites instead of ceramics.

5.4.2. Tips and tricks

Some tips regarding the development of a fabrication method and the process of doing a project like this:

- Make use of a fabrication design loop, like using a morphological chart and a more structured design approach
- Fabrication never goes as planned, but always report what you are doing differently than initially was the plan.
- Validate power or voltage outputs as soon as possible. To better know if your fabrication influences this result. Not everything is seen visually or with property measurements.
- Focus on understanding the theory first. Starting directly with fabrication is good and keeps the tempo high. However, changing things without knowing the basics could allow focus on the wrong problem
- Think early on about what materials and equipment are needed. This can take a long time to arrange, resulting in delays.
- Keep the mood high; fabrication can fail often, or results can be disappointing. But remember, bad results can sometimes explain even more than good results.

Acknowledgements

I want to express my deepest gratitude to my supervisor, Andres Hunt from the TU Delft, for his invaluable guidance and support throughout my thesis project. His insights and encouragement have been instrumental in the successful completion of this work. I am also immensely grateful to Thijs Blad, the founder and supervisor at MEMSYS, for his mentorship and for providing me with the opportunity to work on this fascinating project. His expertise and vision have greatly supported my research experience.

A special thanks goes to Dion Hogervorst from MEMSYS for the numerous discussions and insightful advice. His contributions, along with the camaraderie of the other interns, made my time during the project enjoyable. With the highs of the year, the Friday drinks and intensive pool table sessions, and the lows to sometimes fight for the use of the shaker. Thank you, Joost Bankras, Kiet Foeken, Alfonso Lizza, and Jasper Verduijn, for making the past ten months memorable.

I would also like to acknowledge Kunal Masania, who responded in 10 minutes to my email, and promptly redirected me to his team working on piezoelectric composite fabrication and stencil printing. A very big thank you to Satya Ammu and Saurav Sharma for helping me get started and providing a foundation of knowledge that was crucial to my research.

On a personal note, I want to thank my roommate and best friend, Chris, for always being there to listen when I came home after a long day. And, of course, all my other friends who took me away from work and provided me with the needed breaks and fun. I am also deeply grateful to my parents and little sister for their unwavering support and for always being open to discussions and providing motivation. Lastly, I want to express my heartfelt appreciation to my girlfriend, Lisa, who especially motivated and encouraged me throughout this journey.

Thank you all for your support and contributions.

References

[1] Takeshi Yamada, Toshinobu Ueda, and Toyoki Kitayama. "Piezoelectricity of a high-content lead zirconate titanate/polymer composite". In: *Journal of Applied Physics* 53 (6 1982), pp. 4328–4332. ISSN: 00218979. DOI: 10.1063/1.331211.

[2] Yasuyoshi Saito and Hisaaki Takao. "High performance lead-free piezoelectric ceramics in the (K,Na)NbO 3-LiTaO3 solid solution system". In: vol. 338. Aug. 2006, pp. 17–32. DOI: 10.1080/00150190600732512.

[3] CORDIS News. "Up to 78 million batteries will be discarded daily by 2025, researchers warn". In: *CORDIS: EU research results* (2021). URL: https://cordis.europa.eu/article/id/430457-up-to-78-million-batteries-will-be-discarded-daily-by-2025-researchers-warn.

[4] Nurettin Sezer and Muammer Koç. "A comprehensive review on the state-of-the-art of piezoelectric energy harvesting". In: *Nano Energy* 80 (2021), p. 105567. ISSN: 2211-2855. DOI: https://doi.org/10.1016/j.nanoen.2020.105567. URL: https://www.sciencedirect.com/science/article/pii/S2211285520311411.

[5] Shashank Priya and Daniel J. Inman. *Energy harvesting technologies*. Springer US, 2009, pp. 1–517. ISBN: 9780387764634. DOI: 10.1007/978-0-387-76464-1.

[6] Shashank Priya et al. *A Review on Piezoelectric Energy Harvesting: Materials, Methods, and Circuits*. 2019. DOI: 10.1515/ehs-2016-0028.

[7] Huicong Liu et al. *A comprehensive review on piezoelectric energy harvesting technology: Materials, mechanisms, and applications*. Dec. 2018. DOI: 10.1063/1.5074184.

[8] R. Salazar, M. Serrano, and A. Abdelkefi. "Fatigue in piezoelectric ceramic vibrational energy harvesting: A review". In: *Applied Energy* 270 (July 2020). ISSN: 03062619. DOI: 10.1016/j.apenergy.2020.115161.

[9] "Fabrication of bulk piezoelectric and dielectric BaTiO 3 ceramics using paste extrusion 3D printing technique". In: *Journal of the American Ceramic Society* 102 (6 June 2019), pp. 3685–3694. ISSN: 15512916. DOI: 10.1111/jace.16242.

[10] Yimin Fan et al. "Design, development, and theoretical and experimental tests of a nonlinear energy harvester via piezoelectric arrays and motion limiters". In: *International Journal of Non-Linear Mechanics* 142 (June 2022). ISSN: 00207462. DOI: 10.1016/j.ijnonlinmec.2022.103974.

[11] Chabum Lee and Joshua A. Tarbutton. "Electric Poling-assisted Additive Manufacturing Process for Lead-free Piezoelectric Device Fabrication". In: vol. 1. Elsevier B.V., 2015, pp. 320–326. DOI: 10.1016/j.promfg.2015.09.035.

[12] Haitong Liang et al. "Ultra-low wide bandwidth vibrational energy harvesting using a statically balanced compliant mechanism". In: *International Journal of Mechanical Sciences* 219 (Apr. 2022). ISSN: 00207403. DOI: 10.1016/j.ijmecsci.2022.107130.

[13] Daniel A. Porter and Thomas A. Berfield. "A bi-stable buckled energy harvesting device actuated via torque arms". In: *Smart Materials and Structures* 23 (7 2014). ISSN: 1361665X. DOI: 10.1088/0964-1726/23/7/075003.

[14] Lucas Q. Machado et al. "Multi-dimensional constrained energy optimization of a piezoelectric harvester for E-gadgets". In: *iScience* 24 (7 July 2021). ISSN: 25890042. DOI: 10.1016/j.isci.2021.102749.

[15] Shaofan Qi et al. "Design of a multiresonant beam for broadband piezoelectric energy harvesting". In: *Smart Materials and Structures* 19 (9 Sept. 2010). ISSN: 09641726. DOI: 10.1088/0964-1726/19/9/094009.

[16] Guansong Shan, Yang Kuang, and Meiling Zhu. "Design, modelling and testing of a compact piezoelectric transducer for railway track vibration energy harvesting". In: *Sensors and Actuators A: Physical* 347 (Nov. 2022). ISSN: 09244247. DOI: 10.1016/j.sna.2022.113980.

[17] Zbigniew Kulesza et al. *15th International Conference Mechatronic Systems and Materials : MSM'2020 : the book of selected, peer reviewed papers presented at the 15th International Conference Mechatronic Systems and Materials MSM'2020, July 1-3, 2020, Białystok, Poland*. 2020. ISBN: 9781728169569.

[18] Iman Fattahi and Hamid Reza Mirdamadi. "A novel multimodal and multidirectional energy harvester by asymmetric 3D skeletal frame structures". In: *Journal of the Brazilian Society of Mechanical Sciences and Engineering* 42 (6 June 2020). ISSN: 18063691. DOI: 10.1007/s40430-020-02369-4.

[19] Xiaoxiang Wei et al. "A Tower-Shaped Three-Dimensional Piezoelectric Energy Harvester for Low-Level and Low-Frequency Vibration". In: *International Journal of Precision Engineering and Manufacturing - Green Technology* 8 (5 Sept. 2021), pp. 1537–1550. ISSN: 21980810. DOI: 10.1007/s40684-020-00281-9.

[20] Tianbing Ma et al. "Investigation on the design and application of 3-dimensional wide-band piezoelectric energy harvester for low amplitude vibration sources". In: *Smart Materials and Structures* 28 (10 Aug. 2019). ISSN: 1361665X. DOI: 10.1088/1361-665X/ab377a.

[21] Iresha Erangani Piyarathna et al. "Linear Segmented Arc-Shaped Piezoelectric Branch Beam Energy Harvester for Ultra-Low Frequency Vibrations". In: *Sensors* 23 (11 June 2023). ISSN: 14248220. DOI: 10.3390/s23115257.

[22] "Three-dimensional piezoelectric polymer microsystems for vibrational energy harvesting, robotic interfaces and biomedical implants". In: *Nature Electronics* 2 (1 Jan. 2019), pp. 26–35. ISSN: 25201131. DOI: 10.1038/s41928-018-0189-7.

[23] Tien Hoang Ngo et al. "An Energy Harvester Based on a Bistable Origami Mechanism". In: *International Journal of Precision Engineering and Manufacturing* 23 (2 Feb. 2022), pp. 213–226. ISSN: 20054602. DOI: 10.1007/s12541-021-00614-x.

[24] Ryo Ichige et al. "Size optimization of metamaterial structure for elastic layer of a piezoelectric vibration energy harvester". In: *Sensors and Actuators, A: Physical* 318 (Feb. 2021). ISSN: 09244247. DOI: 10.1016/j.sna.2020.112488.

[25] Dilpreet Bath and Armaghan Salehian. "A novel 3D folded zigzag piezoelectric energy harvester; Modeling and experiments". In: *Smart Materials and Structures* 28 (2 Feb. 2019). ISSN: 1361665X. DOI: 10.1088/1361-665X/aaf15b.

[26] "Curved flexoelectric and piezoelectric micro-beams for nonlinear vibration analysis of energy harvesting". In: *International Journal of Solids and Structures* 264 (Mar. 2023). ISSN: 00207683. DOI: 10.1016/j.ijsolstr.2022.112096.

[27] Yingchun Su et al. "3D spring-based piezoelectric energy generator". In: *Nano Energy* 90 (Dec. 2021). ISSN: 22112855. DOI: 10.1016/j.nanoen.2021.106578.

[28] Mohammadsadegh Saadatzi et al. "Modeling and Fabrication of a Multi-Axial Piezoelectric Energy Harvester Based on a Metamaterial-Inspired Structure". In: *IEEE Sensors Journal* 18 (22 Nov. 2018), pp. 9410–9419. ISSN: 1530437X. DOI: 10.1109/JSEN.2018.2870993.

[29] Guangzu Zhang et al. "Flexible three-dimensional interconnected piezoelectric ceramic foam based composites for highly efficient concurrent mechanical and thermal energy harvesting". In: *Energy and Environmental Science* 11 (8 Aug. 2018), pp. 2046–2056. ISSN: 17545706. DOI: 10.1039/c8ee00595h.

[30] Mingyang Yan et al. "Flexible pillar-base structured piezocomposite with aligned porosity for piezoelectric energy harvesting". In: *Nano Energy* 88 (Oct. 2021), p. 106278. ISSN: 22112855. DOI: 10.1016/j.nanoen.2021.106278.

[31] Lin Dong et al. "In vivo cardiac power generation enabled by an integrated helical piezoelectric pacemaker lead". In: *Nano Energy* 66 (Dec. 2019). ISSN: 22112855. DOI: 10.1016/j.nanoen.2019.104085.

[32] Rui Tao et al. "Multi-material fused filament fabrication of flexible 3D piezoelectric nanocomposite lattices for pressure sensing and energy harvesting applications". In: *Applied Materials Today* 29 (Dec. 2022). ISSN: 23529407. DOI: 10.1016/j.apmt.2022.101596.

[33] Gang Jian et al. "3D BaTiO3 Flower Based Polymer Composites Exhibiting Excellent Piezoelectric Energy Harvesting Properties". In: *Advanced Materials Interfaces* 7 (16 Aug. 2020). ISSN: 21967350. DOI: 10.1002/admi.202000484.

[34] Marc A. Meyers and Krishan Kumar Chawla. *Mechanical behavior of materials*. Cambridge University Press, 2009, p. 856. ISBN: 9780521866750.

[35] *CES EduPack*. 2023rd ed. Material selection and education software. Granta Design. 2023.

[36] Amitabha Ghosh. "Scaling Laws". In: Springer New York, 2011, pp. 61–94. DOI: 10.1007/978-1-4419-9601-5_2.

[37] Rammohan Sriramdas and Rudra Pratap. "Scaling and Performance Analysis of MEMS Piezoelectric Energy Harvesters". In: *Journal of Microelectromechanical Systems* 26 (3 June 2017), pp. 679–690. ISSN: 10577157. DOI: 10.1109/JMEMS.2017.2689326.

[38] Hamideh Khanbareh. "Expanding the Functionality of Piezo-Particulate Composites". PhD thesis, approved by Prof. Dr. Ir. S. van der Zwaag and Prof. Dr. W.A. Groen. PhD thesis. Delft, the Netherlands: Delft University of Technology, 2016.

[39] Daniella Deutz. "Flexible piezoelectric composites Bridging the gap between materials and applications". In: (2017). DOI: 10.4233/uuid:3ed1b44e-44f4-4b84-abd1-34722d106c22. URL: https://doi.org/10.4233/uuid:3ed1b44e-44f4-4b84-.

[40] S.K. Ammu et al. "Lead-free piezoelectric ceramic-polymer composites for flexible, large-area ultrasound applications". In: (not yet published).

[41] FIBERMAX. *SR1700-SD280x & 7820 Epoxy Systems*. Accessed: 2024-07-02. 2024. URL: https://www.fibermax.eu/image/catalog/MDS/Epoxy%20systems/SR1700-SD280x%20&%207820.pdf.

[42] Epoxy Technology. *320NC-2*. Accessed: 2024-07-02. 2024. URL: https://www.epotek.com/product/320nc-2/.

[43] Epoxy Technology. *H77 Epoxy System Datasheet*. Accessed: 2024-07-02. 2024. URL: https://www.epotek.com/docs/en/Datasheet/H77.pdf.

[44] P. Atkins and J. de Paula. *Physical Chemistry*. 9th. Oxford University Press, 2010.

[45] COMSOL Blog. *Piezoelectric Materials: Crystal Orientation and Poling Direction*. https://www.comsol.com/blogs/piezoelectric-materials-crystal-orientation-poling-direction. Accessed: 2024-07-09. n.d.

[46] Demeke Girma Wakshume and Marek Łukasz Płaczek. *Optimizing Piezoelectric Energy Harvesting from Mechanical Vibration for Electrical Efficiency: A Comprehensive Review*. Mar. 2024. DOI: 10.3390/electronics13050987.

[47] TUSA Inc. *Piezoelectric Transducers*. Accessed: 2024-06-21. 2024. URL: https://www.tusainc.com/products/piezoelectrictransducers/.

[48] NSW Automation. *Stencil Printing vs Dispensing*. Accessed: 2024-06-21. 2021. URL: https://nswautomation.com/NSW/stencil-printing-vs-dispensing/.

[49] Jan Holterman and Pim Groen. *An Introduction to Piezoelectric Materials and Applications*. Apeldoorn, The Netherlands: Applied Piezo, 2013.

[50] R. C. Hibbeler. *Mechanics of Materials*. Tenth. Authorized adaptation from the United States edition. Harlow, United Kingdom: Pearson Education Limited, 2018. ISBN: 978-1-292-17820-2.

[51] T. H. Hsieh et al. "The mechanisms and mechanics of the toughening of epoxy polymers modified with silica nanoparticles". In: *Polymer* 51 (26 Dec. 2010), pp. 6284–6294. ISSN: 00323861. DOI: 10.1016/j.polymer.2010.10.048.

[52] "Model of a single mode energy harvester and properties for optimal power generation". In: *Smart Materials and Structures* 17 (6 Dec. 2008). ISSN: 09641726. DOI: 10.1088/0964-1726/17/6/065026.

[53] Jalal Mohammed Zayan et al. "A Systematic Review of Piezoelectric Materials and Energy Harvesters for Industrial Applications". In: *Sensors* 21.12 (2021), p. 4145. DOI: 10.3390/s21124145. URL: https://www.mdpi.com/1424-8220/21/12/4145.

[54] Satya K. Ammu. *Unpublished Data on [KNLN3-320NC-2 epoxy]*. Data provided by Satya Ammu through personal communication. The data was collected as part of the research on stencil printing piezoelectric composites. 2024.

[55] American Piezo. *PZT: Piezoelectric Ceramics - PZT Properties Applications*. https://www.americanpiezo.com/piezo-theory/pzt.html. Accessed: 2024-07-04. 2024.

[56] Zhengbao Yang et al. *High-Performance Piezoelectric Energy Harvesters and Their Applications*. Apr. 2018. DOI: 10.1016/j.joule.2018.03.011.

[57] Xiaobiao Shan et al. "Novel energy harvesting: A macro fiber composite piezoelectric energy harvester in the water vortex". In: vol. 41. Elsevier Ltd, July 2015, S763–S767. DOI: 10.1016/j.ceramint.2015.03.219.

[58] Anonymous. *Piezo Material Properties Data Sheet*. 2020. URL: https://info.piezo.com/hubfs/Data-Sheets/piezo-material-properties-data-sheet-20201112.pdf.

A

Scalability of Piezoelectric vibrational energy harvesters; Literature review

A.1. Search query

Search Query
(3d OR 3-dimensional OR three-dimensional) AND design AND piezoelectric AND energy AND (harvester OR harvesters OR generator)
PEH OR (piezoelectric AND energy-harvester) AND (systems OR structures) AND (3D OR 3-dimensional) AND vibrations
piezoelectric AND energy AND vibration AND harvest AND design
Kinetic AND energy AND harvesting AND (three OR 3) AND dimensions
Multidimensional AND piezoelectric AND energy AND conversion
Spacial AND piezoelectric AND energy AND harvesters
Piezoelectric AND energy AND harvester AND design
vibration AND piezoelectric AND energy AND harvester AND design + design in title
fabrication AND piezoelectric AND energy AND harvester
3d AND piezoelectric AND generator | fabrication OR design (title)
Vibration AND energy AND harvester AND design
Vibration AND energy AND harvester AND fabrication
Vibration AND piezoelectric AND energy AND harvester AND fabrication
Vibration AND piezoelectric AND energy AND harvester AND design

Table A.1: Search Queries for creating initial data set.

A.2. Design score rubrics

Rubrics for the given design scores can be seen in tables: A.2, A.3, A.4, A.5.

Simplicity score	**Score 1**	**Score 2**	**Score 3**	**Score 4**	**Score 5**
Number of components *(Weight = 3)*	Above average	X	+/−30% average	X	Below Average
Size order of system *(Weight = 2)*	Nano range (1-100nm)	Micro range (100nm-1mm)	Milli range (1mm-1cm)	Macro range (1cm – 1m)	Large scale (>1m)
Degrees of freedom *(Weight = 1)*	5 or 6	X	3 or 4	X	5 or 6
Integration of PEM *(Weight = 4)*	Completely integrated	X	2 sub-systems integrated	X	2 sub-systems added onto eachother

Table A.2: Simplicity score rubric.

Performance score	**Score 1**	**Score 2**	**Score 3**	**Score 4**	**Score 5**
Operating range (bandwidth) *(Weight = 5)*	1-5 Hz	X	6 – 20 Hz	X	20+ Hz
Real life application use *(Weight = 2)*	Doesn't cover application frequency	X	Covers part of application frequency	X	Couples with application frequency
Number of eigenmodes *(Weight = 2)*	1 mode	X	2-3 modes	X	3+ modes
Operating mode *(Weight = 1)*	D31	X	D33	X	Both modes
PEM coverage *(Weight = 4)*	0-20% of deformed area	21-40% of deformed area	41-60% of deformed area	61-80% of deformed area	81-100% of deformed area

Table A.3: Performance score rubric

Production time score	Score 1	Score 2	Score 3	Score 4	Score 5
Number of steps *(weight = 5)*	Above average	X	+25% around average	X	Below average
Post processing *(weight = 1)*	yes, multiple	X	1 Step	X	no
Fabrication procedure automation *(weight = 2)*	Not done	X	Semi	X	Automatable
Assembly complexity *(weight = 2)*	No repeatable steps **AND** step for step	X	Repeatable steps **OR** multiple steps at once	X	Repeatable steps **AND** multiple steps at once

Table A.4: Production time score rubric

Scaling score	Score 1	Score 2	Score 3	Score 4	Score 5
Space occupancy change *(weight = 5)*	Exponential	X	Linear	X	Sublinear
Number of components change *(weight = 1)*	Exponential	X	Linear	X	Sublinear
Number of DOF's change *(weight = 2)*	Decrease	X	No change	X	Increase
Yield effectiveness change *(weight = 2)*	Decrease	X	No change	X	Increase
Operating range change *(weight = 2)*	Decrease	X	No change	X	Increase
Number of production steps change *(weight = 2)*	Linear increase	Sublinear increase	Same	X	Decrease
Assembly complexity change *(weight = 2)*	Increase	X	No change	X	Decrease

Table A.5: Scaling score rubric

B

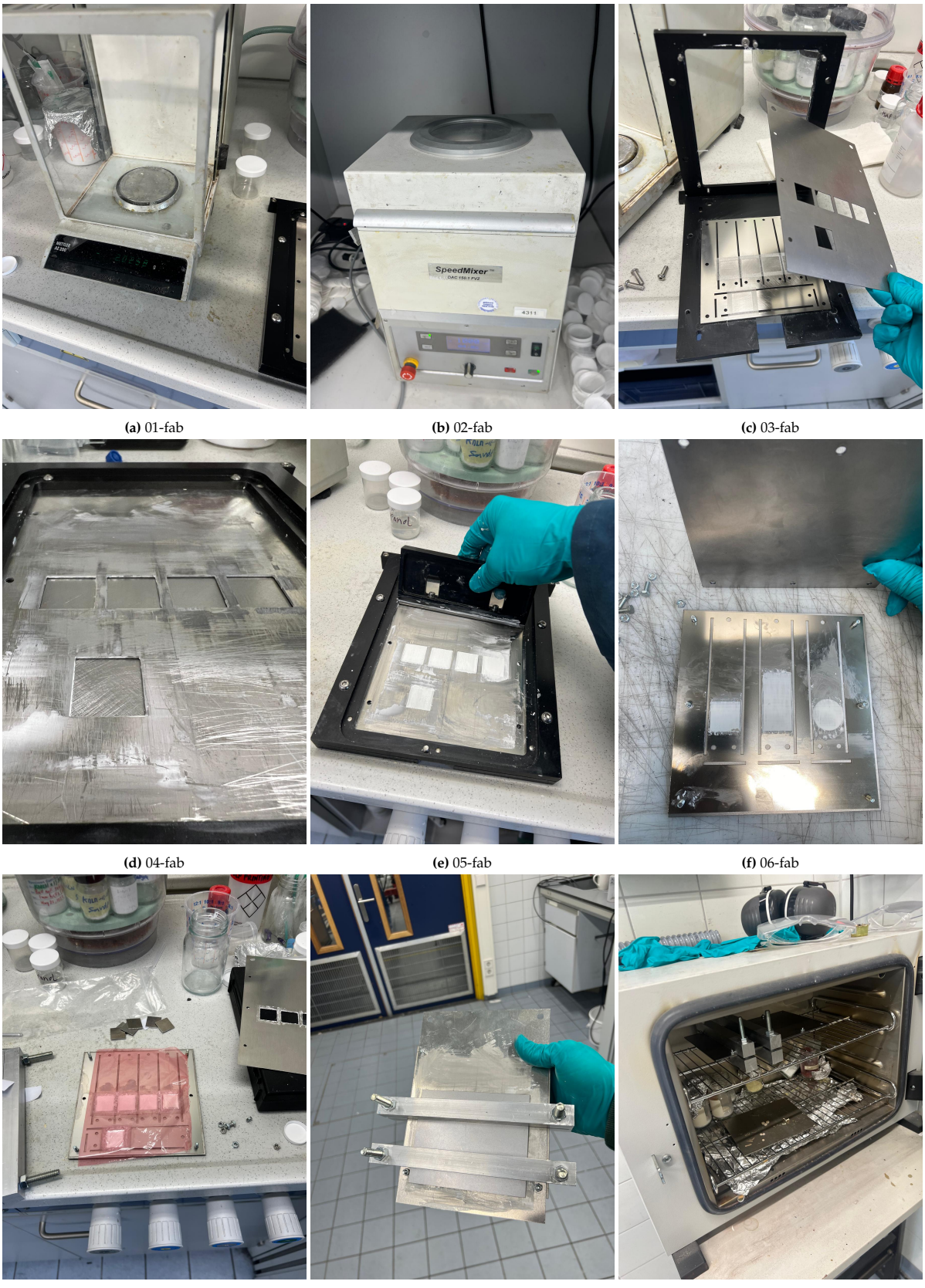
Overview fabrication development

Fabrication Steps	Batch 1 (A)	Batch 2 (B)	Batch 3 (C)	Batch 4 (D)	Batch 5 (E)
Goal of Batch	Check feasibility, and find limitations	Thicker samples see feasibility and limitations thick layer	Smoother samples without leakage	Increased adhesion, Flat samples Faster drying in vacuum	Be careful with drying, change vacuum Low temp poling
Cleaning	x	x	x	Aceton 2 times	Aceton 2 times
Grinding	x	x	x	4 directions	4 directions
Epoxy Material	Simicon SR1700 + SD2801 (1g + 0.39g)	Simicon SR1700 + SD2801 (0.5g + 0.185g)	Simicon SR1700 + SD2801 (1g + 0.39g)	Simicon SR1700 + SD2801 (1g + 0.39g)	Simicon SR1700 + SD2801 (1g + 0.39g)
Mixing epoxy & solvent or KNLN	5 min at 3000RPM or 600RPM	5 min at 3000RPM or 600RPM	5 min at 3000RPM or 600RPM	5 min at 3000RPM or 600RPM	5 min at 3000RPM or 600RPM
Add solvent	3g isopropanol	1.5g isopropanol	2.5g isopropanol	2.5g isopropanol	2.5g isopropanol
Add KNLN3	8.62g	4.31g	8.62g	8.62g	8.62g
Stencil thickness	0.1mm	2.0mm	1.0mm	1.0mm	0.5mm
Seal thickness	x	x	0.30mm	0.30mm	0.30mm
Stencil Printing Setup	3 samples; circle, square, rectangular	3 samples; square	3 samples; square	5 samples; square	5 samples; square
Printing Epoxy Paste	1 strike	Multiple strikes, samples filled extra	Multiple strikes	Multiple strikes	Multiple strikes
Drying	Air dried for 1h	Air dried 2hours	Air dried 12 hours	0 bar dried 2.5h + 0.5h open air	0.4 bar dried 2h + 0.5h open air
Curing	Pressure plates 3h at 130C	Pressure plates 40h at 130C	Pressure beams 4h at 130C	Pressure constraint 4h at 130C	Pressure constraint 4h at 130C
Electrode Application	Carbon painted	Carbon painted	3/5 carbon painted 2/5 alu tape	Aluminium tape	Aluminium tape (more from the sides)
Poling condition	12kV/mm 130°C, 6min	0.5kV/mm 130°C, 6min	2.0kV/mm 130°C, 6min	3-3.5kV/mm 130°C, 6min	0.8kV/mm 70-110°C, 6min + teflon
Poling result	2 of 3 samples breakdown	2 of 2 samples breakdown	3 of 5 samples poled [1-4pC/N]	3 of 5 samples poled [7.5-14pC/N]	2 of 5 samples poled [1-4pC/N]
Learnings	Thin layer difficult	Calculate material needed	Remove stencil while drying	Not complete vacuum	Too quick drying causes extra cracks
	Need high-pressure curing	Make sure samples are dried	Adhesion is not sufficient (seal and surface)	Cracks and short circuit poling setup	Poling voltage dependent on cracks
	Stencil/substrate seal	Side compression needed	Faster dielectric breakdown (porosity) with carbon paste	Kinematic constraint doesn't resolve cracks	Electrode doesn't cause a short, Low temp no poling

Table B.2: Fabrication steps for Batch 1 to Batch 5

Fabrication Steps	Batch 6 (F)	Batch 7 (G)	Batch 8 (H)	Batch 9 (I)*	Batch 10 (J)*
Goal of Batch	Try restoring cracks with pressure	Try restoring cracks before curing + 1 strike (more uniform)	Different solvent air drying, more pressure	New epoxy different thickness range for power study	Lower thickness range for power study
Cleaning	Aceton 2 times	Aceton 2 times	Aceton 2 times	Aceton 2 times	Aceton 2 times
Grinding	4 directions	4 directions	4 directions	4 directions	4 directions
Epoxy Material	Simicon SR1700 + SD2801 (1g + 0.39g)	Simicon SR1700 + SD2801 (1g + 0.39g)	Simicon SR1700 + SD2801 (1g + 0.39g)	**Epotek 320NC-2 (2g + 0.2g)**	Epotek 320NC-2 (2g + 0.2g)
Mixing epoxy & solvent or KNLN	5 min at 3000RPM or 600RPM	5 min at 3000RPM or 600RPM	5 min at 3000RPM or 600RPM	5 min at 3000RPM or 600RPM	5 min at 3000RPM or 600RPM
Add solvent	**2.2g isopropanol**	2.2g isopropanol	**2g Ethanol**	**1.9g Ethanol**	1.9g Ethanol
Add KNLN3	8.62g	8.62g	8.62g	**7.12g**	7.12g
Stencil thickness	**0.25mm**	**0.75mm**	**0.25mm**	**[0.25 ; 0.50 ; 0.75 ; 1mm]**	**[0.1 ; 0.1 ; 0.25 ; 0.25 ; 0.25mm]**
Seal thickness	0.30mm	0.30mm	**0.15mm**	0.15mm	**[0 ; 0.15 ; 0 ; 0.15 ; 0.30mm]**
Stencil Printing Setup	5 samples; square	5 samples; square	5 samples; square	**4 individual samples; square**	5 individual samples; square
Printing Epoxy Paste	Multiple strikes	**1 strike, square**	1 strike, square	1 strike, square	1 strike, square
Drying	0.4 bar dried 2h + 0.5h open air	0.4 bar dried 2h + 0.5h open air	**1h open air**	1h open air	1h open air
Curing	High pressure 4 hours at 130C	High pressure 4 hours at 130C	**Extra high pressure 4 hours at 130C**	**Single, high pressure 1.5h at 75C**	Single, high pressure 1.5h at 75C
Electrode Application	Aluminium tape	Aluminium tape	Aluminium tape	Aluminium tape	Aluminium tape
Poling condition	3.6kV/mm 130°C, 6min	4-5.1kV/mm 130°C, 6min	4.4-9kV/mm 130°C, 6min	3.7 - 7.6kV/mm 130°C, 6min	6.5 - 10kV/mm 130°C, 6min
Poling result	2 of 5 samples poled [9pC/N]	2 of 5 samples poled [9-20pC/N]	3 of 5 samples poled [2-12pC/N]	4 of 4 samples poled [7 -14pC/N]	4 of 5 samples poled [3 -18pC/N]
Learnings	Fabrication without cracks a must	Striking direction causes nonuniform/oblique layer	No cracks allow way higher voltages	Thick layer with ethanol solvent cause cracks	0.1mm stencil requires more solvent
	Higher pressure helps a bit	Poling bath without dust improves voltage	Slow striking allow more uniform sample	Different epoxy more viscous (more solvent)	
		High pressure restores surface cracks			

Table B.4: Batch 6-10 fabrication steps, *batch I and J fabrication manual is shown in appendix D



(a) 01-fab **(b)** 02-fab **(c)** 03-fab

(d) 04-fab **(e)** 05-fab **(f)** 06-fab

(g) 07-fab **(h)** 08-fab **(i)** 09-fab

Figure B.1: First set of fabrication figures in chronological order 1 - 9



(a) 10-fab **(b)** 11-fab **(c)** 12-fab

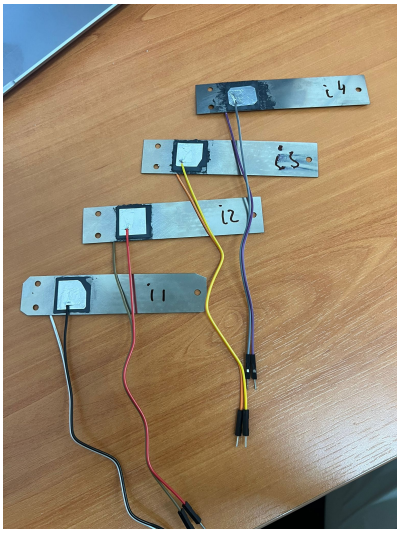
(d) 13-fab **(e)** 13-fab **(f)** 14-fab

(g) 15-fab **(h)** 16-fab **(i)** 17-fab

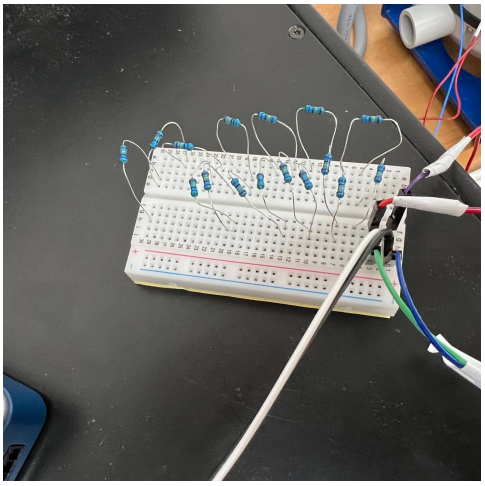
Figure B.2: Second set of fabrication figures in chronological order 10 - 17



(a) 18-fab



(b) 19-fab



(c) 20 - fab detail of resistance connetction

Figure B.3: Third set of fabrication figures in chronological order 18-20

C

KNLN fabrication manual

Material	Quantity
$NaCO_3$	20.56 g
K_2CO_3	26.812 g
Li_2CO_3	106.324 g
Nb_2O_5	0.866 g
Cyclohexane	50 ml
Isopropanol	50 ml + 50 ml
Glass jar	2x (store the powder)

Table C.1: Needed Materials and Their Quantities

Equipment	Description
5mm yttria-stabilized balls 300g	Small ball for the milling process
Chemical scale	
Milling jar	To add powder and solvents to mill in the milling machine
Sieve (general)	To sieve the balls out of the powder/solvent substance
Metal plate	To drop the powder/solvents substance and let it dry
Heat bed	To increase the temperature to dry the powder from its solvent
Oven	Be able to set programs of up-ramp and max temperature of 1050 ° C
Mortar and pestle	To grind the bigger pieces into a smaller powder
Spatula	To move the powders between storage or jars
Non-sticky paper	Put the powder on top and guide it into a jar
$63\mu m$ sieve	The sieve is used to sieve out the currently useful powder
Shaker machine	To do automatic sieving
Milling/mixing machine	Which moves at a certain RPM to mill the powder

Table C.2: Equipment and Their Descriptions

Property	Value
Curie Temperature (T_c)	460°C
Dielectric Constant (ϵ_r	750
Crystal Phase	Orthorhombic
Sintering Temperature (°C)	1050°C
Grain Size Distribution	Uniform
Resistivity ($\Omega \cdot$ cm)	$1 \times 10^{11}\ \Omega \cdot$ cm
Piezoelectric Constant (d_{33})	130 pC/N
Piezoelectric Coupling (K_p)	0.35
Young's Modulus (Y_{11}^E)	90 GPa
Poisson's Ratio (σ)	0.33

Table C.3: Properties of KNLN with 0.05 Lithium and 0.00 Ta Content [2]

1. Dry materials; $NaCO_3$ and K_2CO_3
   - at 200 °C for 8h.
2. Combine materials, $NaCO_3$, K_2CO_3, Li_2CO_3 and Nb_2O_5
   - from Sigma Aldrich
     a. Weigh the materials in the fumehood at a chemical scale.
     b. In an aluminium cup → towards the milling jar.
     c. Make sure no powder is left behind.
3. Mill the ball, such that it is ready for the first calcination round

- Add cyclohexane into milling jar
  - 50ml
- Add 5mm yttria-stabilized balls
  - 300g
    - @200 RPM for 3hrs
    - Dry in fumehood 150 ° C for 1h on heated bed

4. First calcination
   - Add the dried and milled powder into 2 crucibles (ceramic container).
   - Put into the oven
     - 3h at 1050°C (5°C/min) (total_time = 10hrs)
5. Grinding and milling
   - Break block pieces into small pieces with mortar and pestle.
   - Add IPA (isopropanol)
     - 50ml
   - Add balls and mill
     - @200RPM for 8hrs
     - @300RPM for 3hrs
   - Dry in fumehood 150°C for 1h on heated bed
6. Second calcination
   - Add the dried and milled powder into 1 crucible (ceramic container).
   - Put into the oven
     - 20h at 925°C (1°C/min) (total_time = 50hrs)
7. Grinding and milling
   - Break block pieces into small pieces with mortar and pestle.
   - Add IPA (isopropanol)
     - 50ml
   - Add 5mm yttria-stabilized balls
     - 300g
       - @200RPM for 3hrs
       - Dry in fumehood 150°C for 1h on heated bed
8. Sieved with 63 μm mesh
   - Sieve on a shaker for 3hrs
   - All bigger powder/pieces need better milling
     i. Manually
     ii. @300RPM for 3hrs
9. Store the powder
   - Vacuum
   - Room temperature

D

Stencil printing process manual

Material	Quantity
KNLN	8.62 g
Ethanol	2 g
Simicon SR1700, Part A	1 g
Simicon SD2801, part B	0.39 g

Table D.1: Needed Materials and Their Quantities; Simicon SR1700 and SD2801

Material	Quantity
KNLN	7.12 g
Ethanol	2g
Epotek 320NC-2; part A	2 g
Epotek 320NC-2; part B	0.2 g
Acetone	50 ml

Table D.2: Needed Materials and Their Quantities; Epotek 320NC-2

Equipment	Description	Quantity
Chemical weigh scale	To measure the amount of material	1
Plastic jar	To put the materials in and mix	1
Planetary speedmixer (DAC 150.1FVZ)	For mixing the different substances at high speed	1
Pipets	To dose the amount of liquid materials	4
Small spatula	To dose the powder	1
Stencil print substrate	Stainless steel substrate, to get the lower electrode and cantilever beam. Clean this first.	1
Stencil holder and squeegee	Parts already available to use for stencil printing	1
Stencils	Stencil of different thicknesses	1
Clamb parts bottom and top plate	To put the paste under pressure during curing	2
Stencil clamb bolts (m4)	To clamb the stencil plate on the substrate	4
Compression (squares, top plate, compression beams) + M8 x 80	To put the samples under high pressure	5, 1, 4, 2
Foil	Between compression and paste to prevent sticking	1
Micrometer (Mahr 40ER)	To measure the thickness of the layers	1
Aluminium tape	For the electrodes and wire connection	1
Poling device (Heinzinger PNC 30000)	To pole the samples at high voltage, give composite its properties	1
Heater Heidolph M8 Hei-standard + thermometer	To heat the poling bath	1
Silicon oil	to pole the samples	100-200ml
Steel scissors	To cut out the cantilevers from the general substrate	1
Cleaning paper towels	To clean oil of substrate	25

Table D.3: Equipment, Descriptions, and Quantities

The manual below takes the final fabrication method of samples I and J, with Epotek 320NC-2 epoxy.

1. Prepare substrate
    a. Clean with acetone.
    b. Grind 2x diagonally, horizontal and vertically with grinding paper (80).

c. Clean again with acetone.

2. Combine materials of Epotek A and B
   - Amount calculated in Excel
     a. Part A with Part B - 2g 0.2g
     b. Speedmix at 3000 RPM for 5 min
3. Add Ethanol
   a. +-40 vol% (total volume) - 2g.
   b. Speedmix at 3000 RPM for 5 min.
4. Add the KNLN powder
   a. 60 vol% KNLN powder (epoxy-powder). - 7.12g
   b. Speedmix at 600 RPM for 5 min.
5. Assemble the stencil printing equipment
   a. Place substrate, TPU98 seals, and stencil inside the printing clamp.
6. Apply paste
   a. Put more than required paste on stencil plate.
   b. Smear in shapes.
   c. Remove stencil.
   d. Let dry for 1h at room temperature (evaporate all solvents and initial start of curing).
7. Compression curing of the composite
   a. Check if the samples are dry (visual and physical).
   b. Compress system
      i. Put foil in between.
      ii. Side support
      iii. Beams, pressure plates, and shape pressure.
   c. Put in the oven at 75°C for 1-2h.
      i. Curing of material → epoxy is leading for time.
8. Cut out samples
   a. With steel cutters, cut out the flexures.
9. Cut out samples
   a. Clean the flexures → scraping and acetone.
   b. Measure the thickness of the sample with piezo and flexure.
      i. Report in Excel document.
      ii. Subtract thickness flexure.
   c. Apply aluminium electrode tape 20x20mm.
10. Poling
    a. Put in poling device.
    b. In silicon oil bath at 130°C, wait 2 min to heat up.
    c. Slowly increase voltage to +-7.5kV/mm, keep at max for 6 min. Make sure no high leakage current occurs.
    d. Turn off heating → 10 min.
    e. Turn off voltage provider.

f. Remove from bath.

g. Clean the samples of oil → acetone and towels.

11. Measure properties
    - Check D33 value
    - Check capacitance
    - Chek resitance
12. Connect wires with aluminium tape.

Main Task	Sub Tasks	Total of minutes
0. Preparing	Gather all materials, Gather all gear, Prepare planning	30
1. Prepare substrate	Clean with acetone, Grind 2x diagonal, horizontal and vertical, Clean again with acetone	15
2. Combine materials	epoxy parts, Speedmix	21
3. Add Ethanol	50 vol% (total volume), Speedmix	4
4. Add KNLN powder	60 vol% KNLN powder (epoxy-powder), Speedmix	10
5. Assembly the stencil printing equipment	Place substrate, TPU98 seals and stencil inside the printing clamp	10
6. Apply paste	Put more than the required paste on the stencil plate, Smear in shapes, Remove stencil, Let dry	80
7. Compression curing	Check if the system is dry, Compress the system, Put in the oven	275
8. Apply electrodes	Cut out aluminium tape electrode, Stick electrode on sample	25
9. Cut out samples	With steel cutters cut out the flexures, Clean the flexures, Measure thickness of sample, Report in Excel document, Subtract thickness flexure	45
10. Poling	Put in poling device, In silicon oil bath at 130°C wait 2 min to heat up, Slowly increase voltage to 7.5kV/mm, Turn off heating, Turn off voltage provider, Remove from bath, Clean the samples of oil	155
11. Check properties value	D33, capacitance, resistance	25
12. Connect wire	Wire, aluminium tape	25
Total		**706**

Table D.4: Needed minutes per fabrication task. For 1 substrate of 5 beams.

E

Derived and used equations

E.1. Derived stress equation

$$\sigma = \frac{My}{I} \tag{E.1}$$

$$\sigma_{\max} = \frac{M_{\max} \cdot \frac{t}{2}}{\frac{bt^3}{12}} = \frac{-F \cdot L \cdot \frac{t}{2}}{\frac{bt^3}{12}} = \frac{-6FL}{bt^2} \tag{E.2}$$

$$\sigma_{\max} = -\frac{6FL}{bt^2} \tag{E.3}$$

$$\sigma_{\max} \propto \frac{1}{t^2} \tag{E.4}$$

- F: Applied force at the free end (Newtons, N)
- L: Length of the beam from the fixed end to the point of force application (meters, m)
- b: Width of the beam (meters, m)
- t: Thickness of the beam (meters, m)
- M: Bending moment (Newton-meters, Nm)
- y: Distance from the neutral axis to the outermost fiber (meters, m)
- I: Moment of inertia (meters to the fourth power, m^4)
- σ: Stress (Pascals, Pa)
- $\sigma_{\max}$: Maximum stress (Pascals, Pa)

E.2. Coupling equations

The coupling factor is one of the driving parameters for the amount of power to produce. And is affected by the material and configuration. Equations E.5 and E.6 result in the inequality shown in E.7. This could say something about the coupling coefficient of both PZT and the created composite. With table E.1 the values used. This is normalized with holding all dimensions the same, allowing the k_m to be dependent only on the Youngs modulus E. With the other factor being the piezoelectric charge constant D and the capacitance which is only dependent on the relative permittivity ε_r. Giving a normalized factor k^2, which shows some theoretical potential.

$$k^2_{composite} = \frac{k_m}{k_m + k_{st}} \cdot \frac{D^2 k_m}{C_{el}} \tag{E.5}$$

$$k^2_{PZT} = \frac{k_m}{k_m + k_{st}} \cdot \frac{D^2 k_m}{C_{el}} \tag{E.6}$$

$$\alpha \cdot \frac{60^2 \cdot 21}{0.43} > \alpha \cdot \frac{260^2 \cdot 54}{85} \tag{E.7}$$

$$C = \frac{\varepsilon_0 \varepsilon_r A}{t} \tag{E.8}$$

-	Composite	PZT	*unit*
D_{33}	60	260	pC/N
E	21	54	GPa
ε_r	80	1600	nF/m
C_{el}	0.43	85	nF
k^2_{factor}	176000	42000	-

Table E.1: Used input for coupling factor calculation [58]

F

Details of fabricated samples

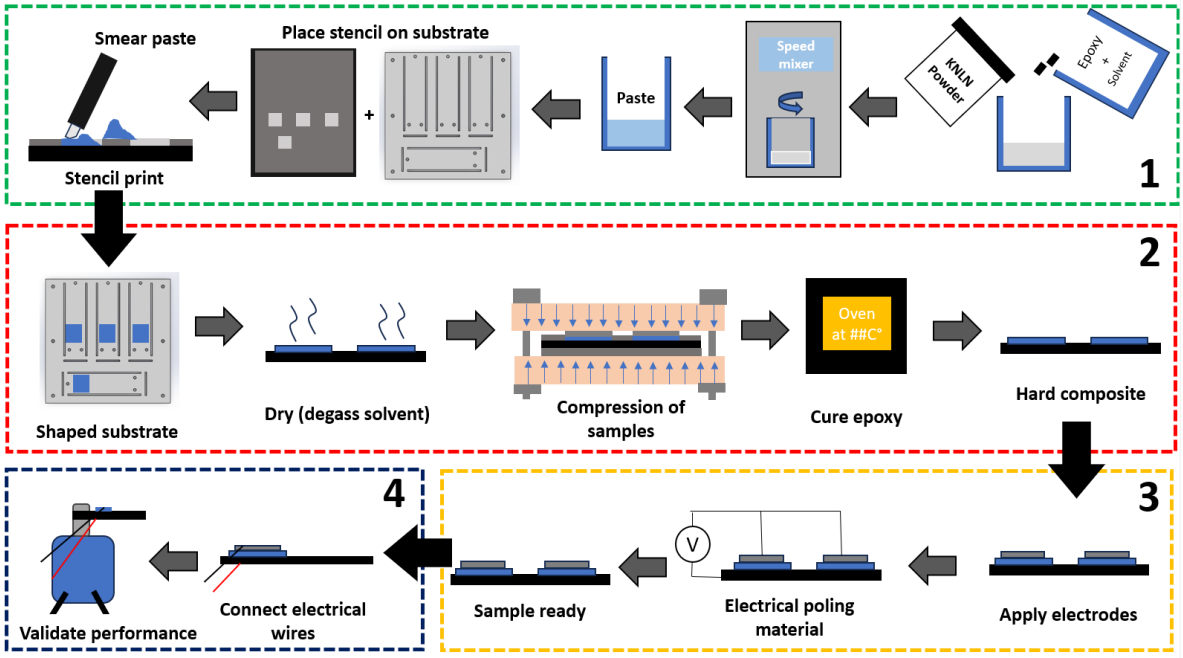
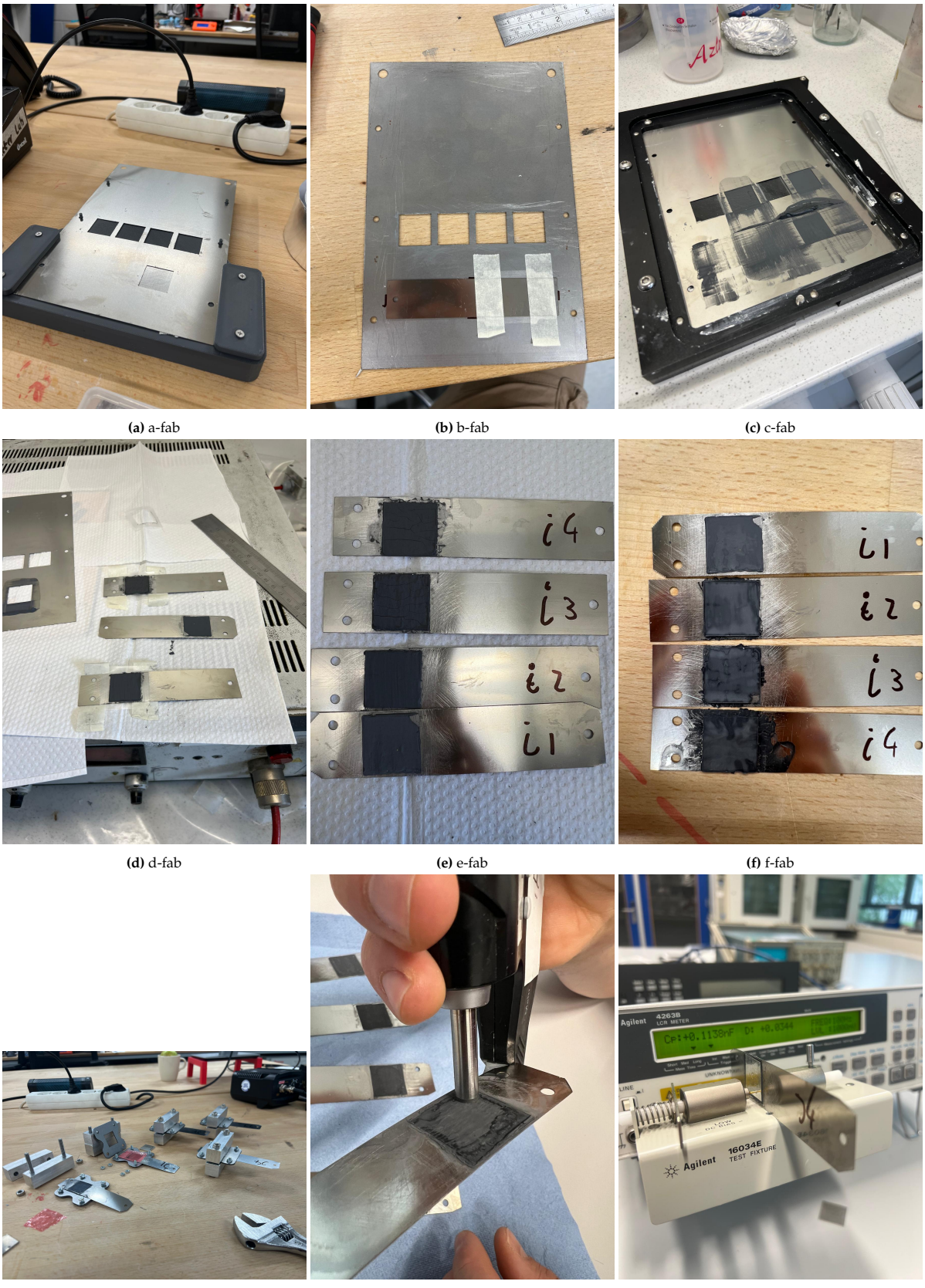


Figure F.3: Fabrication schematic overview enlarged.

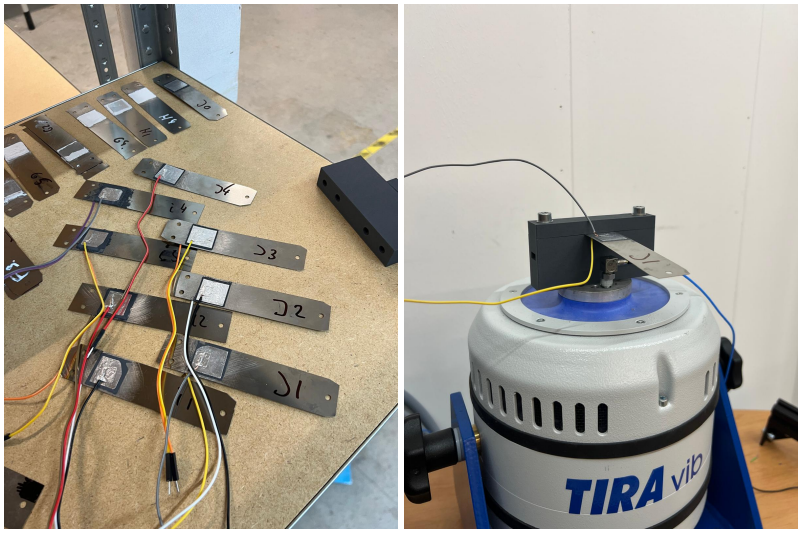


(a) a-fab **(b)** b-fab **(c)** c-fab

(d) d-fab **(e)** e-fab **(f)** f-fab

(g) g-fab **(h)** h-fab **(i)** i-fab

Figure F.1: Overview of fabrication pictures in chronological order from a - i



(a) j-fab **(b)** k-fab

Figure F.2: Overview of fabrication pictures in order from j - k

F.1. Thickness measurements

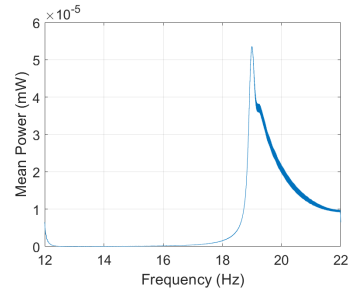


Figure F.4: Thickness measurements in [mm] for each fabricated sample. The arrows indicates the paste's striking direction.

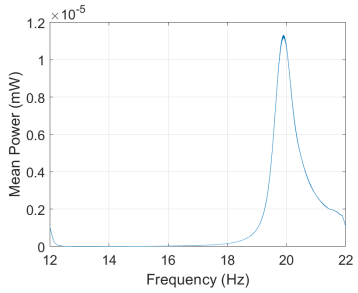
G

Performance (sub)results per sample

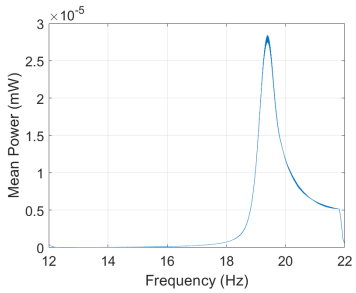
G.1. Sample eigenfrequency analysis



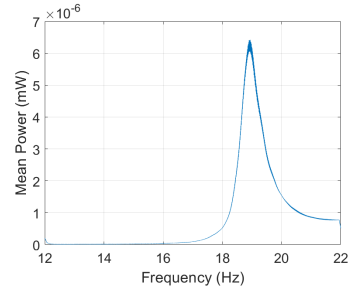
(a) Sample I01 (0.21-0.26mm) eigenfrequency test, $\omega = 19.2Hz$



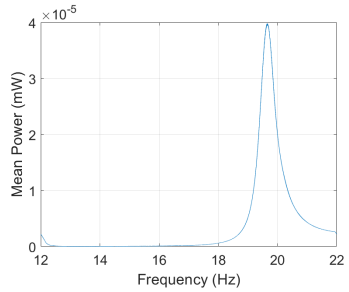
(b) Sample I02 eigenfrequency test, $\omega = 19.8Hz$



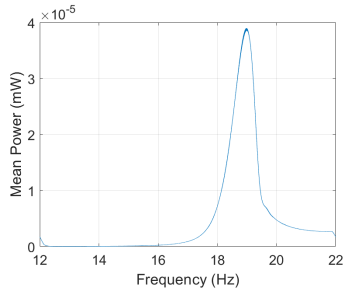
(c) Sample I03 eigenfrequency test, $\omega = 19.0Hz$



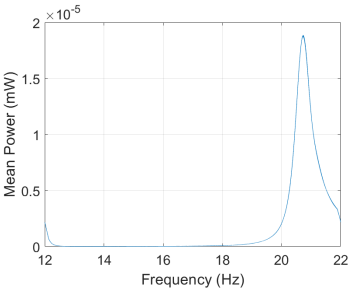
(d) Sample I04 eigenfrequency test, $\omega = 19.0Hz$



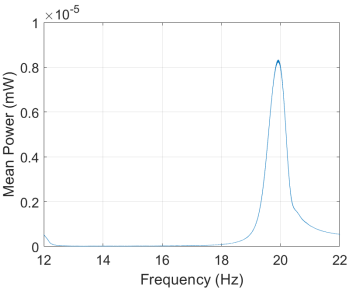
(e) Sample J01 eigenfrequency test, $\omega = 19.6Hz$



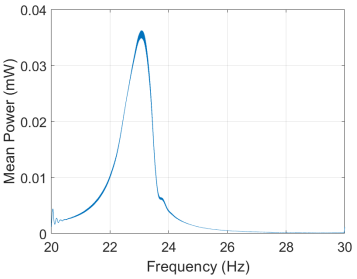
(f) Sample J02 eigenfrequency test, $\omega = 19.0Hz$



(g) Sample J03 eigenfrequency test, $\omega = 20.7Hz$



(h) Sample J04 eigenfrequency test, $\omega = 19.9Hz$

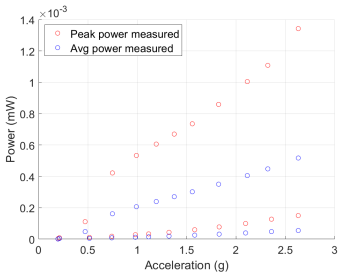


(i) Buzzer eigenfrequency test, $\omega = 23.8Hz$

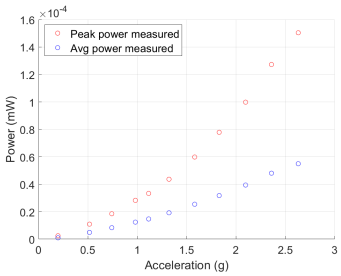
Figure G.1: Eigenfrequency analysis of different samples.

G.2. Meausred acceleration data

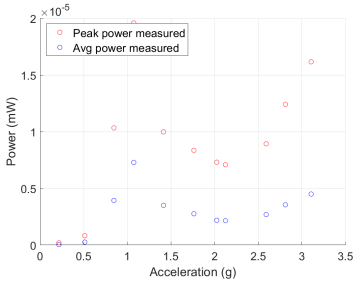
To make the power-to-acceleration test more precise each measurement is done at an initial easy-to-set resistance. With the determined power ratio in appendix G.3 the optimal power can be calculated.



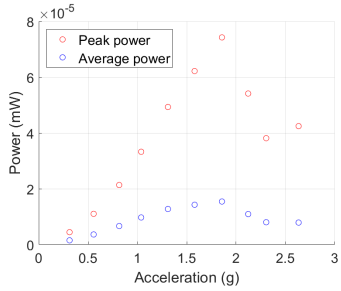
(a) Sample I-01 at R = 2.2 $M\Omega$



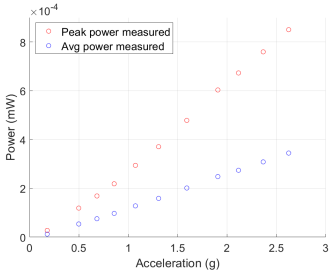
(b) Sample I-02 at R = 3.2$M\Omega$



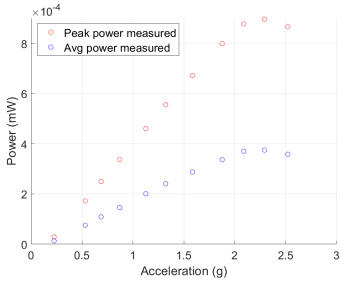
(c) Sample I-03 at R = 5$M\Omega$



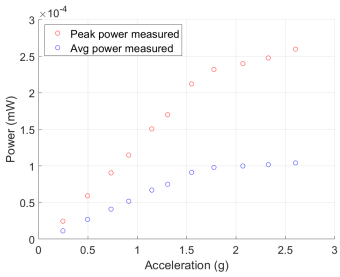
(d) Sample I-04 at R = 5$M\Omega$



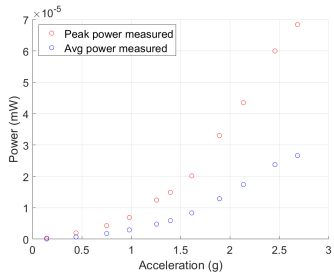
(e) Sample J-01 at R = 5$M\Omega$



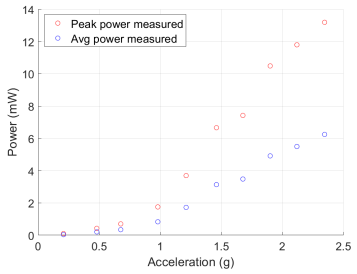
(f) Sample J-02 at R = 5$M\Omega$



(g) Sample J-03 at R = 5$M\Omega$



(h) Sample J-04 at R = 5$M\Omega$

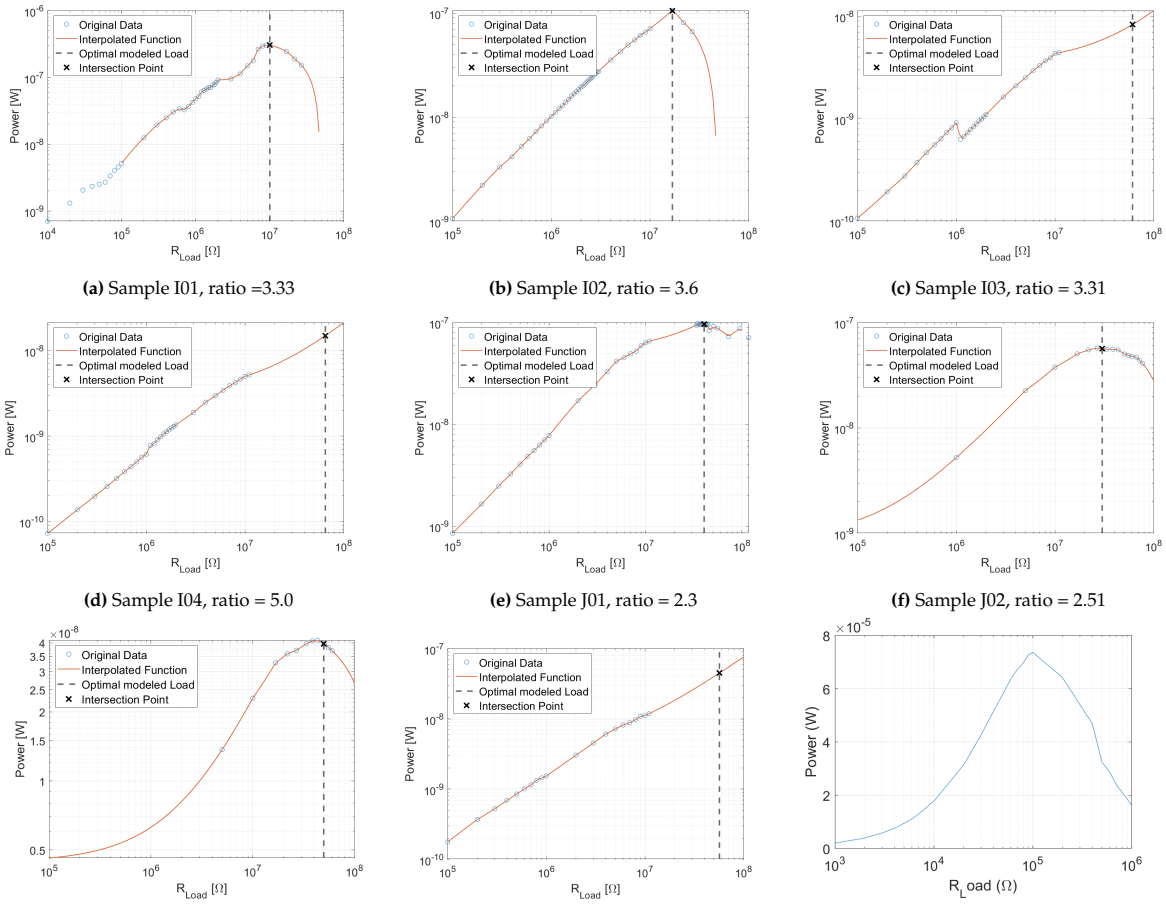


(i) Sample J-00 at R = 5$M\Omega$

Figure G.2: Power measured at different accelerations for different samples. Not measured at optimal resistance.

G.3. Interpolation resistance load

Due to the extremely high impedance, the voltage measurements are not suitable for the decade box. Therefore wider measurements of additional resistances in series are done. In the figures G.3, for all samples the resistance optimisation is shown. The derived power ratio is compared to the resistance used to measure the power at different accelerations. With the first resistance sweep from $10K\Omega$ to $11M\Omega$ not indicating a top. Taking the extrapolation of the power-resistance test results towards a different modelled optimum results in the optimal load resistance. To validate these values a discrete test has been performed with higher resistances in series. Resulting in multiplier ratios for the results from the acceleration tests, to cover the different resistance loads.



(a) Sample I01, ratio =3.33 **(b)** Sample I02, ratio = 3.6 **(c)** Sample I03, ratio = 3.31

(d) Sample I04, ratio = 5.0 **(e)** Sample J01, ratio = 2.3 **(f)** Sample J02, ratio = 2.51

(g) Sample J03, ratio = 3 **(h)** Sample J04, ratio = 6.26 **(i)** Buzzer optimal load sweep

Figure G.3: Optimal resistance measurements, interpolated to modelled optimal resistance load. Used to determine the optimal power ratio.

G.3.1. Apendix F: KNLN3-epoxy D33 (earlier) measurement

These are fabricated samples pressed in malls with 10% solvents, and measurements are done with a piezometer. Data provided by [54].

Sample	t [mm]	m [mg]	rho	relative	C before	C after	ϵ_r before	ϵ_r after	d33
1	1,3	406,2	2,764168	0,764004	44,4	40	72,53533	65,34714	44
2	0,99	336	3,002423	0,829857	54,9	45	68,30159	55,98491	46
3	1,08	368	3,014338	0,833150	47,6	44	64,60319	59,71724	40
4	1,126	332,2	2,609931	0,721374	48,4	41	68,48682	58,01570	46
5	1,147	328,1	2,530525	0,699427	44,9	40	64,71918	57,65629	46
6	1,134	304,6	2,376209	0,656774	41,3	44	58,85541	62,70310	45
7	1,199	356,6	2,631055	0,727213	49,1	38	73,98164	57,25667	45

Table G.1: Sample data 320NC-2 with 60% KNLN3 particles, poled at 3V/mm.

H

Technical drawings

H.1. Technical drawings substrate, stencils and seals

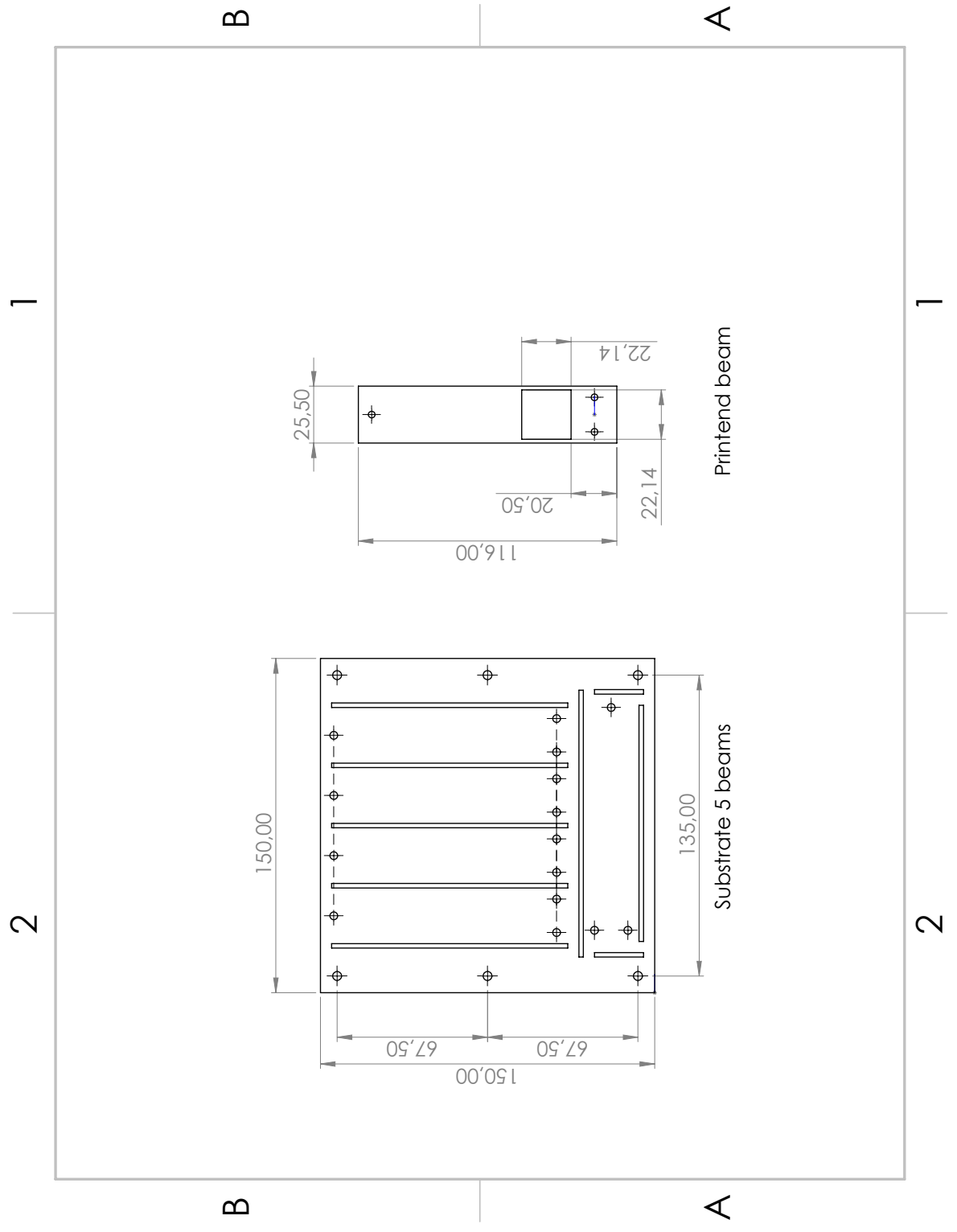


Figure H.1: Substrate and printed cantilever drawing.

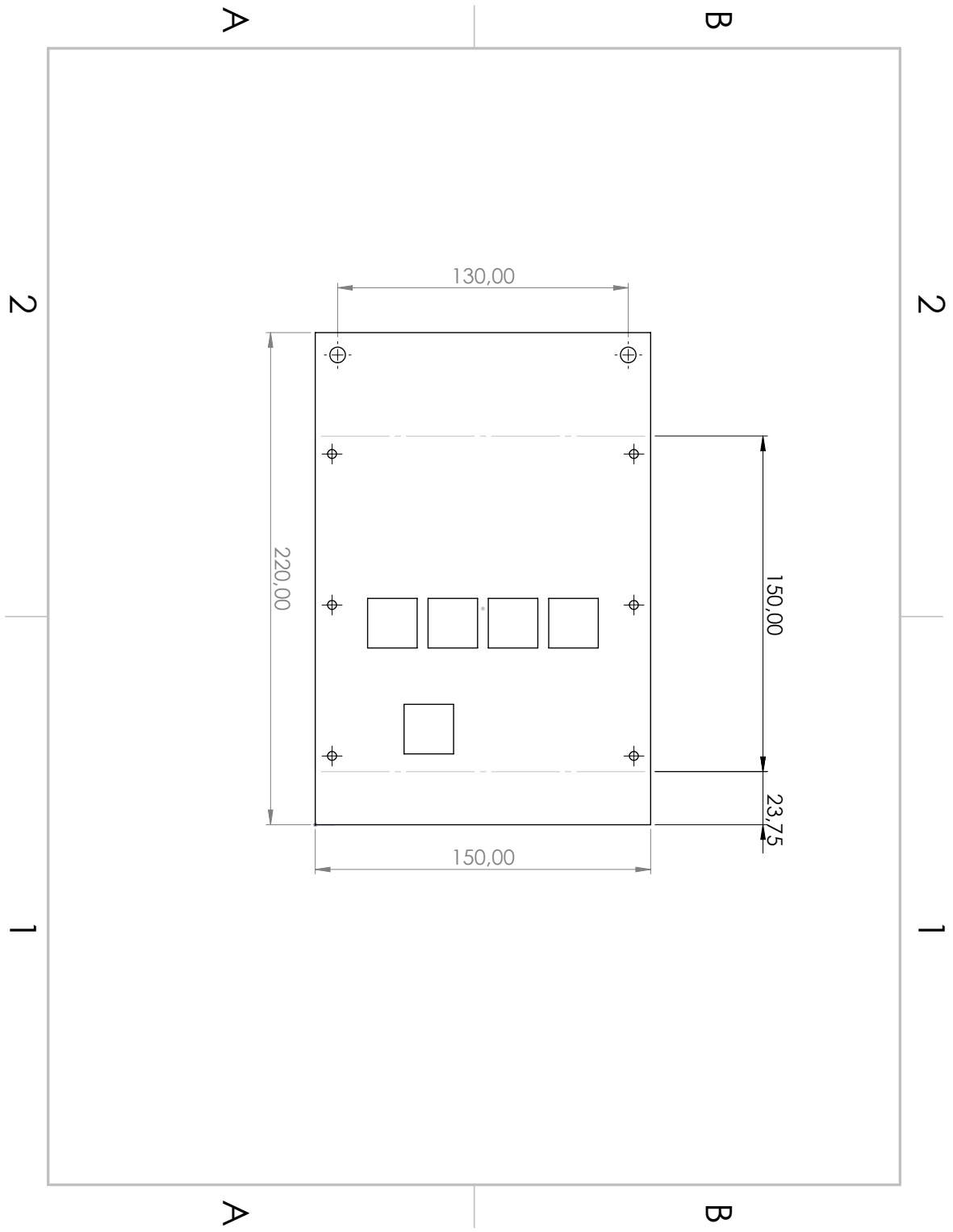


Figure H.2: Stencil drawing, 150x150mm printing area.

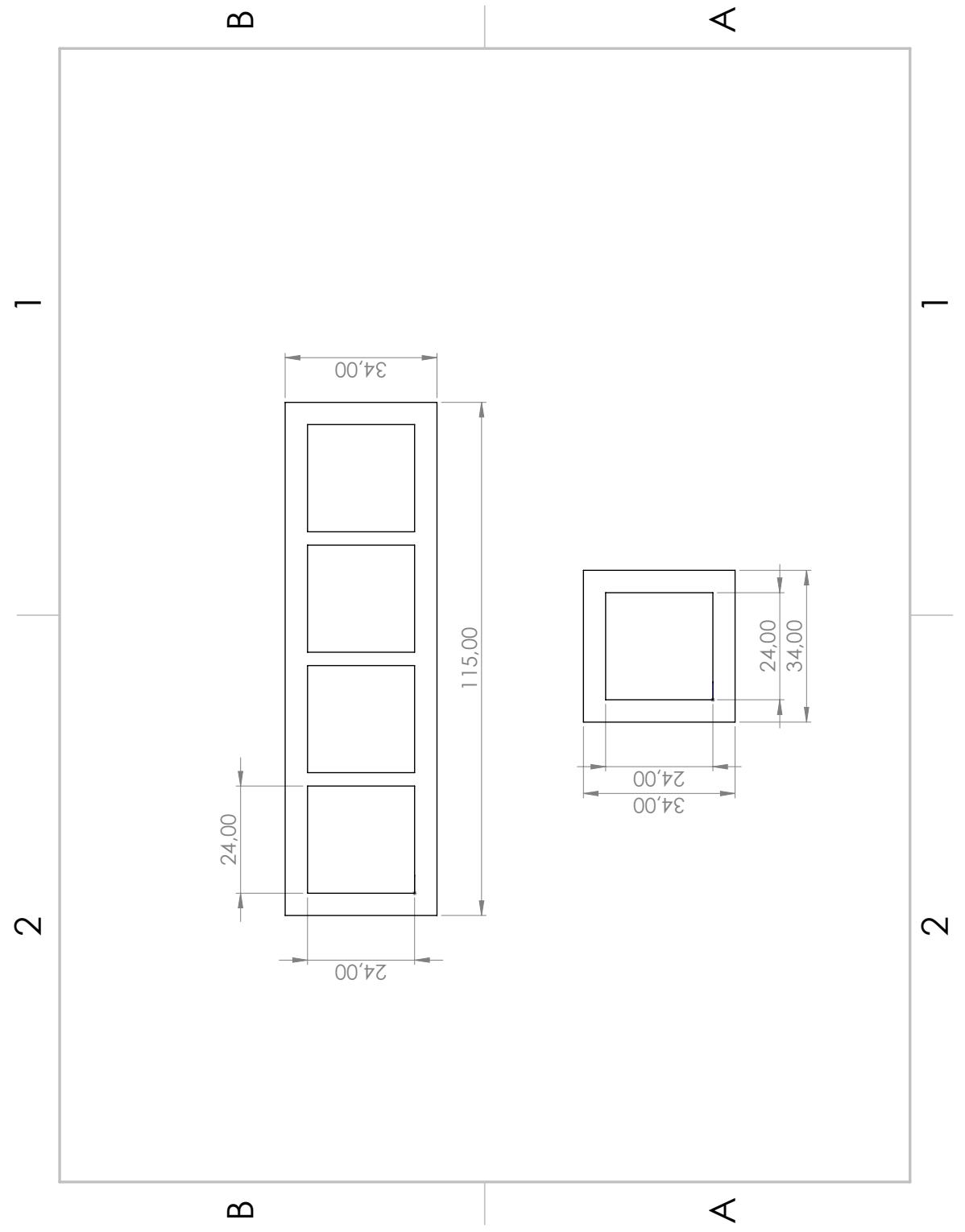


Figure H.3: Seal drawings, TPU seal for during printing.

H.2. Technical drawings compression units

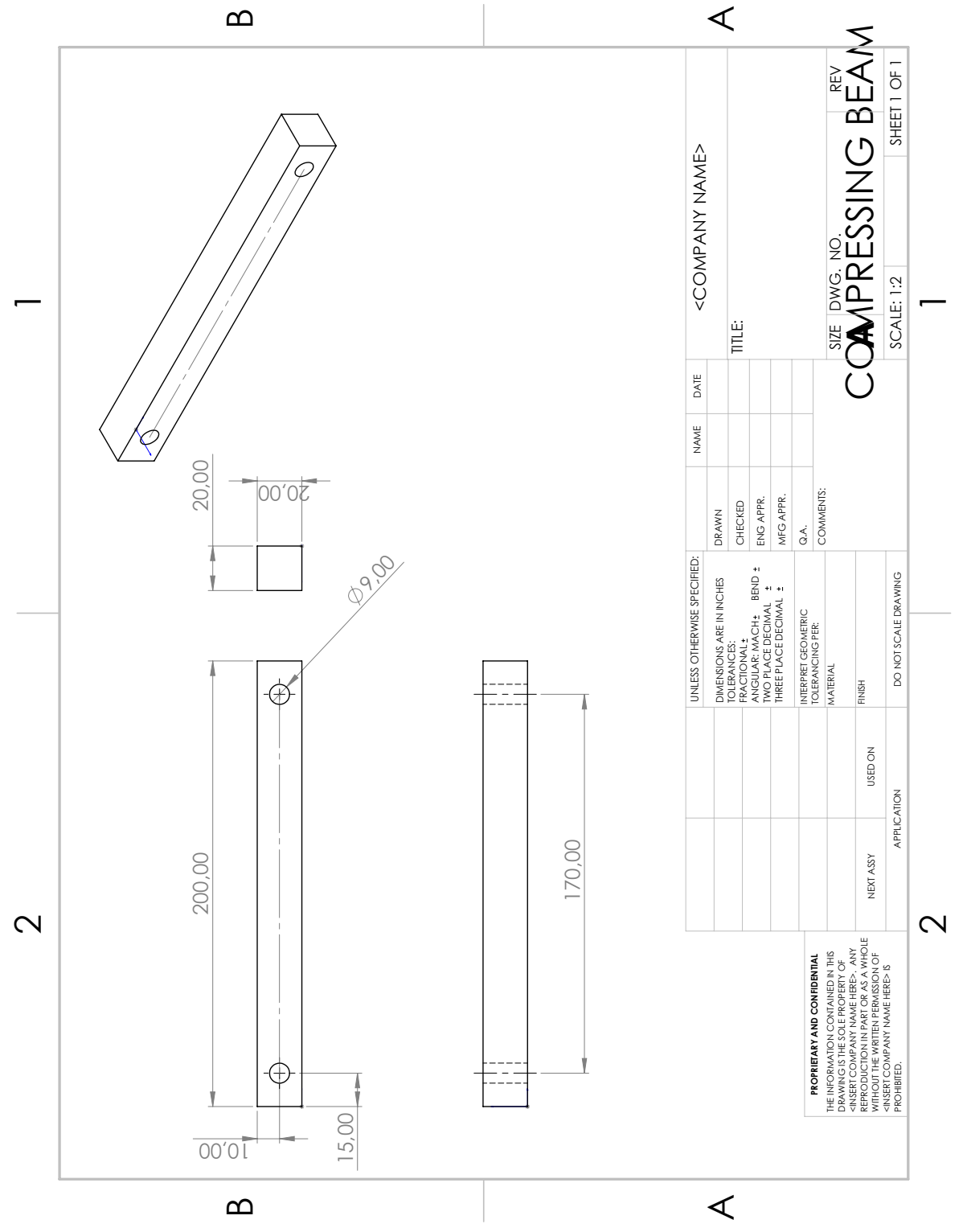


Figure H.4: Compression beams for 5 sample press.

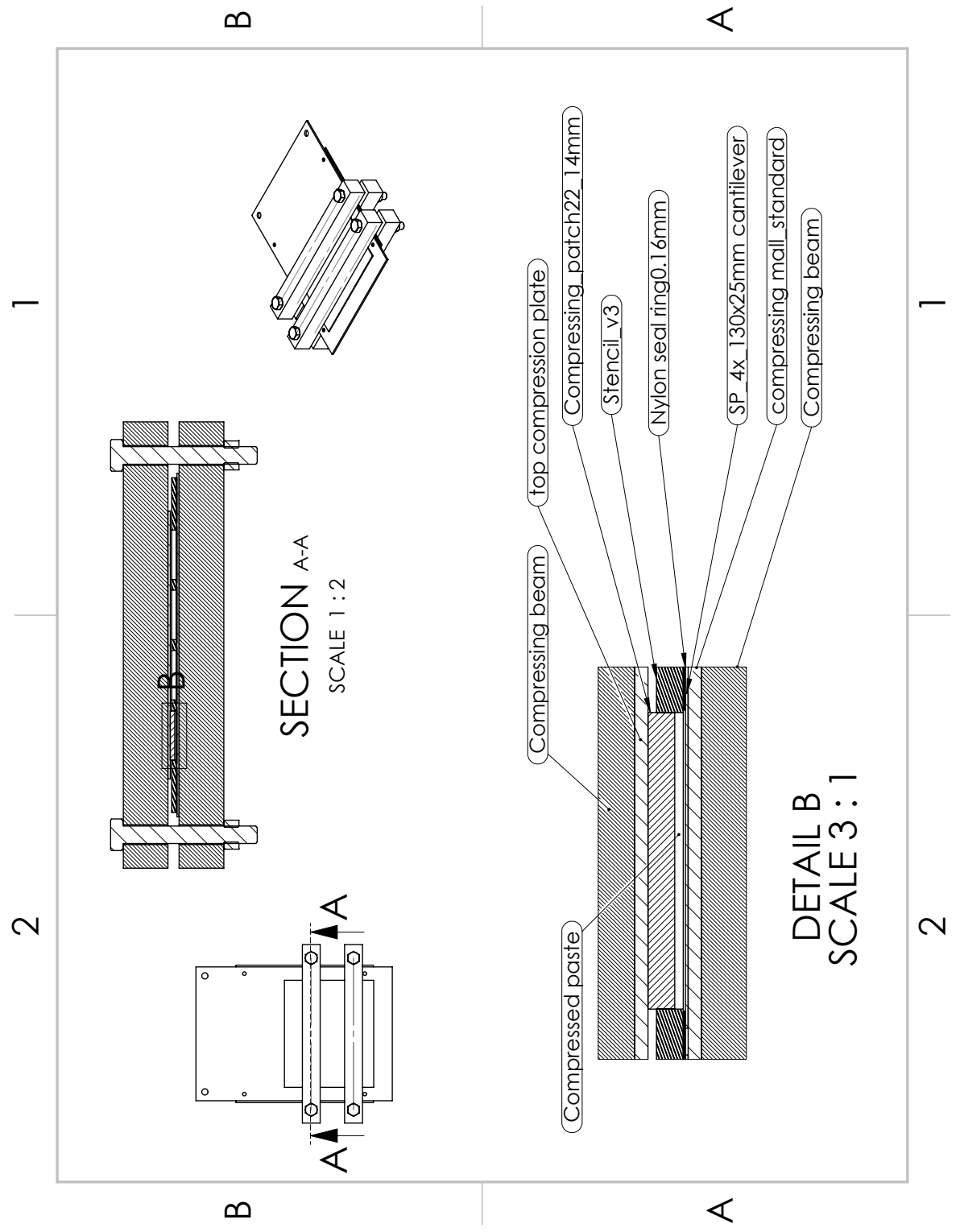


Figure H.5: Overview of compression setup for 5 sample press.

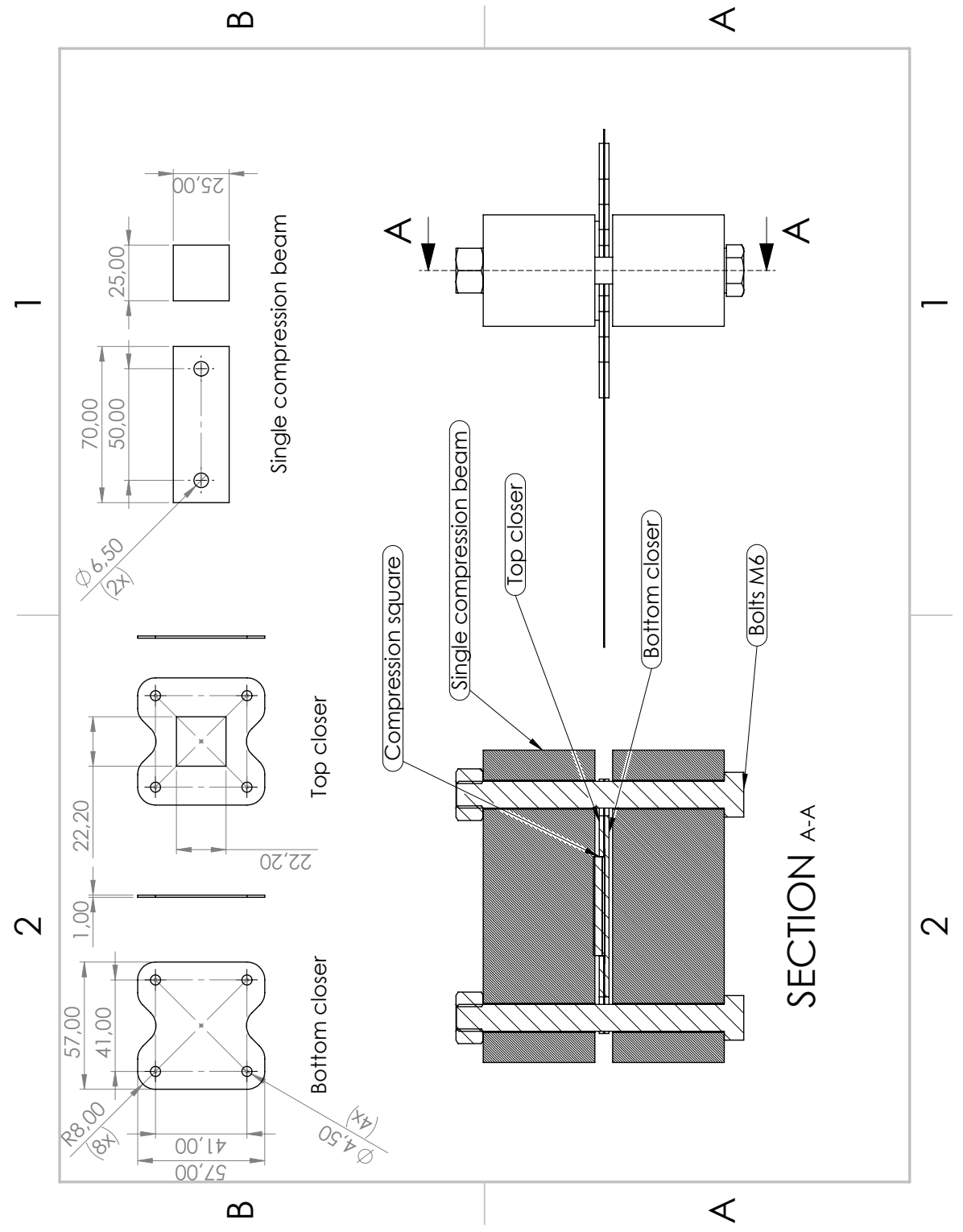


Figure H.6: Overview of compression setup for 1 sample press.

I

Models and code

I.1. Comsol frequency model

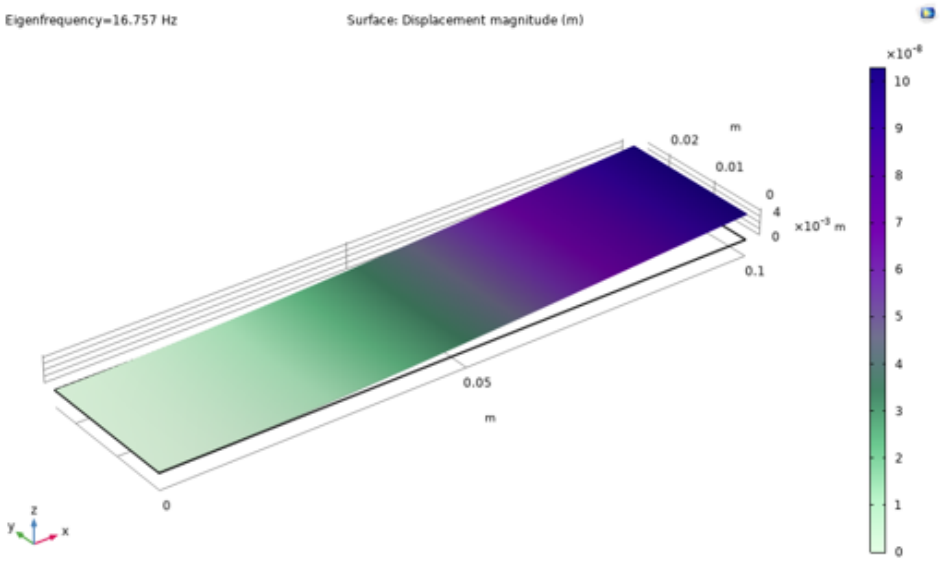


Figure I.1: Comsol eigenfrequency analysis cantilever without piezoelectric layer, $\omega = 16.75Hz$

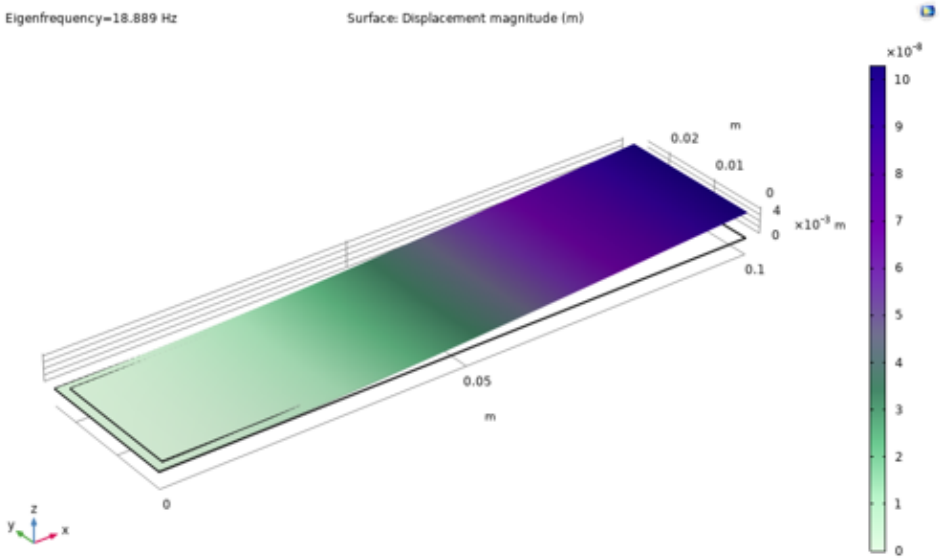


Figure I.2: Comsol eigenfrequency analysis cantilever **with** piezoelectric layer of 0.2mm $\omega = 18.9Hz$

I.2. Effective stiffness model code

```
# -*- coding: utf-8 -*-
"""
Created on Fri May 17 15:07:26 2024

@author: sande
"""
import numpy as np
import matplotlib.pyplot as plt

```

```
def calculate_neutral_axis(E1, A1, y1, E2, A2, y2):
    Q_weighted = (E1 * A1 * y1) + (E2 * A2 * y2)
    A_weighted = (E1 * A1) + (E2 * A2)
    y_NA = Q_weighted / A_weighted
    return y_NA

def calculate_moment_of_inertia(b, h, y_c, y_NA, A):
    I_c = (b * h**3) / 12
    d = abs(y_c - y_NA)
    I_NA = I_c + A * d**2
    return I_NA

def calculate_stiffness(E, I, L):
    return (3*(E * I)) / (L**3)

def plot_stiffness_vs_height(h_range, E1, b1, h1, E2_values, b2, A1, y1, L):
    heights = np.linspace(h_range[0], h_range[1], 500)

    plt.figure(figsize=(12,11))

    for E2 in E2_values:
        stiffness1_values = []
        stiffness2_values = []

        for h2 in heights:
            A2 = b2 * h2
            y2 = h1 + h2 / 2
            y_NA = calculate_neutral_axis(E1, A1, y1, E2, A2, y2)

            I_NA1 = calculate_moment_of_inertia(b1, h1, y1, y_NA, A1)
            I_NA2 = calculate_moment_of_inertia(b2, h2, y2, y_NA, A2)
            I_total = I_NA1 + I_NA2

            stiffness1 = calculate_stiffness(E1, I_NA1, L)
            stiffness2 = calculate_stiffness(E2, I_NA2, L)
            stiffness1_values.append(stiffness1)
            stiffness2_values.append(stiffness2)

            if np.isclose(stiffness1, stiffness2, atol=1e-7):
                intersection_height = h2
                print(f'For E2 = {E2}, the optimal thickness where both stiffnesses are equal
                    is: {intersection_height} mm')

        plt.plot(heights, stiffness2_values, label=f'Effective stiffness piezo layer',
            linewidth = 4)
    plt.plot(heights, stiffness1_values, 'k--', label='Effective stiffness susbstrate layer',
         linewidth = 4)
    plt.xlabel('Piezo Layer Height (mm)', fontsize = 22)
    plt.ylabel('Effective stiffness (N/mm)', fontsize = 22)
    #plt.title('Stiffness Variation with Top Layer Height')
    plt.ylim(0, 0.02)
    plt.grid(True)
    plt.legend(fontsize = 20)
    plt.tick_params(axis='both', which='major', labelsize=20)
    plt.show()


# Example parameters
E1 = 200000 # MPa for material 1
b1 = 25      # mm
h1 = 0.2     # mm
A1 = b1 * h1 # mm^2
y1 = h1 / 2  # mm
b2 = 25      # mm
ee = 1700
e_0 = 0
e_r = 0
d33 = 300*(10**(-12))
L = 105     # mm (beam length)

# E2 values to test
```

```
78 E2_values = [21000] #np.arange(15000, 21001, 6000) # from 10000 to 100000 with steps of 10000
79
80 # Plot stiffness variation for top layer height from 0.05 mm to 2 mm
81 plot_stiffness_vs_height((0.05, 0.3), E1, b1, h1, E2_values, b2, A1, y1, L)
82
83 #plt.savefig('Stiffness_optimization', dpi=600)
```